

Chemistry of Trisdecacyclic Pyrazine Antineoplastics: The Cephalostatins and Ritterazines

Seongmin Lee,[‡] Thomas G. LaCour,[§] and Philip L. Fuchs^{*,§}

Department of Chemistry and Chemical Biology, Harvard University, Cambridge, Massachusetts 02138, and Department of Chemistry, Purdue University, West Lafayette, Indiana 47907

Received July 1, 2008

Contents

1. Introduction	2275	8.4. An Aromatic Moiety Is Not Necessary	2308
2. Isolation and Biological Activity	2276	8.5. Hydrogen-Bonding: Sugars and Spiroketal	2308
2.1. Cephalostatin Family	2276	8.6. Two or More Pro-(stabilized)carbenium Ion Moieties	2308
2.2. Ritterazine Family	2279	8.7. Discussion	2308
2.3. OSW-1 and Natural Analogues	2281	9. Conclusions and Medicinal Prospects	2311
2.4. Solamargine	2282	10. Abbreviations	2312
2.5. Simple Analogues	2282	11. Acknowledgments	2312
3. Pyrazine Synthesis	2283	12. References	2312
3.1. Symmetrical Pyrazine Synthesis	2284		
3.2. Biomimetic Random Coupling of α -Aminoketones	2284		
3.3. Unsymmetrical Pyrazine Synthesis	2285		
3.3.1. Heathcock Method	2285		
3.3.2. Winterfeldt Method	2285		
3.3.3. Guo's Unsymmetrical Pyrazine Synthesis	2287		
4. Classical First-Generation Syntheses	2289		
4.1. Synthesis of the C17-Deoxy-C14,15-Dihydro North Cephalostatin 1	2290		
4.2. Cephalostatin 7, Cephalostatin 12, and Ritterazine K	2291		
4.2.1. Construction of the North Hemisphere of Cephalostatin 1	2291		
4.2.2. South Unit of Cephalostatin 7	2293		
4.3. Cephalostatin 1 and C14',15'-Dihydrocephalostatin 1	2293		
4.3.1. South Unit of Cephalostatin 1	2293		
4.3.2. Cephalostatin 1 and C14',15'-Dihydrocephalostatin 1	2295		
5. Second-Generation Synthesis	2296		
5.1. Ritterazine North Hemispheres B, F, G, and H	2296		
5.2. North M and Ritterazine M	2298		
5.3. North 1 Analogues	2298		
5.4. Interphylal Hybrid Ritterostatsins G _N 1 _N and G _N 1 _S	2300		
6. Third-Generation Biomimetic Synthesis	2300		
6.1. C23'-Deoxy South Unit of Cephalostatin 1	2302		
6.2. South Hemisphere of Cephalostatin 7	2304		
7. Related Syntheses	2305		
8. Structure–Activity Relationships	2306		
8.1. Appropriate Pairing of Polar/Nonpolar Subunits	2306		
8.2. Homoallylic Oxygen	2307		
8.3. 17-OH Function Is Beneficial	2308		

1. Introduction

The search for natural products of medicinal significance led the Pettit group to isolate the cephalostatins¹ (from the hemichordate worm *Cephalodiscus gilchristi*,² e.g., cephalostatin 1 (**1**)) and the Fusetani team to isolate the ritterazines³ (from the tunicate *Ritterella tokioka*, e.g., ritterazine B (**2**)), respectively. The cephalostatins and ritterazines are a family of 45 trisdecacyclic bissteroidal pyrazines that display striking cytotoxicity against human tumors (~1 nM in the 2-day NCI 60 cell panel,⁴ and in some cases, ~10 fM 6-day in the Purdue mini panel⁵), thereby ranking them among the most potent anticancer agents tested by the NCI.

Computer matching at the NCI using the COMPARE program has revealed several additional compounds exhibiting similar profiles to the cephalostatin/ritterazine family. These compounds include OSW-1⁶ (**3**), a monosteroidal saponin glycoside from the garden perennial *Ornithogalum saundersiae* (GI₅₀ of 0.8 nM in the NCI 60 cancer cell line), and solamargine⁷ (**4**) (from *Solanum* species) as additional possible candidates for cancer therapy. OSW-1 (**3**) shows low toxicity to normal human pulmonary cells but encouraging activity against malignant solid tumor cells. Solamargine (**4**) is an active ingredient of crème Curaderm, claimed to be 100% effective against melanomas in preliminary clinical trials without significant side effects or recurrence of cancer 10 years after treatment (Figure 1).⁸

Following Pettit's seminal report on cephalostatin 1 (**1**) in 1988,¹ several articles⁹ have reviewed the structure elucidation, biological activities, and syntheses of cephalostatins. This account will focus on the advances in the syntheses of cephalostatins and ritterazines over the past 15 years (up to ~July 2008), emphasizing the different strategies adopted, key transformations, and methods for achieving the late construction of the dissymmetric bissteroidal pyrazine framework.

Classical steroid numbering (carbons 1–27) and ring designations (A–F) are used throughout the text, supplemented by a “prime” designator for the second steroidal

* Corresponding author. E-mail: pfuchs@purdue.edu.

[‡] Harvard University.

[§] Purdue University.



P. L. Fuchs' grade school education took place in a four-room elementary school in Nashotah, Wisconsin (pop. 237). In 1959, eighth-grade graduation saw the stage decorated in a scientific theme complete with a Fuchs-built *Boron atom*, foreshadowing both his interest in chemistry and his ultimate university. Fuchs' secondary education took place in Hartland, Wisconsin. At the end of his sophomore year, Fuchs and another student renovated an old one-room building. At the end of that summer, Willow Brook Laboratory, WBL, complete with epoxy-top laboratory benches and a homemade fume hood, was in place. During the next two years, the neophyte chemists performed reactions from the literature of organic and inorganic synthesis. Fuchs then attended the University of Wisconsin at Madison and continued summer projects at WBL. WBL sold reagents to Aldrich Chemical Co. in Milwaukee and eventually advertised its chemicals on the back page of the *Journal of the American Chemical Society*. After graduation, Fuchs stayed at UW, beginning graduate studies with Edwin Vedejs in 1968. In the summer of 1971, he received his degree as Vedejs' first Ph.D. and moved to Harvard for a two-year postdoctoral fellowship at with E. J. Corey. Fuchs has been on the Purdue faculty since 1973 and is the current R. B. Wetherill Professor of Chemistry, with 230 papers published and 62 Ph.D.'s granted. His awards and honors include an Eli Lilly young faculty fellowship (1975), an Alfred P. Sloan fellowship (1977), a Pioneer in Laboratory Robotics award (1986), a Martin teaching award (1991), and being voted by the students as one of Top 10 Teachers in School of Science at Purdue (1991, 1993, 1995, 1996). He earned Purdue's highest scientific award, the McCoy Research award, in 2003. Fuchs has consulted for Pfizer and Eli Lilly and has served on the editorial board of the *Journal of Organic Chemistry*. Since 2003 Fuchs has been an executive editor for the John Wiley Encyclopedia of Organic Reagents (EROS).

hemisphere (e.g., C21' = 21'Me of the South hemisphere of cephalostatin 1 (**1**). Steroidal subunit nomenclature follows published practice, e.g., "North 1" indicates the North¹⁰ unit of cephalostatin 1 (**1**), abbreviated to "1_N" especially in analogue names or tables (Figure 2). Known stereochemistry is always shown. The somewhat controversial use of solid circles and short dashes to indicate β (up, as drawn) and α (down) hydrogens, respectively, will be retained in the absence of a superior alternative.

2. Isolation and Biological Activity

2.1. Cephalostatin Family

In 1972, Pettit and co-workers first collected a sample of the marine tubeworm *Cephalodiscus gilchristi*. Two years later, methanol and water extracts proved active in vivo in the National Cancer Institute's PS system (murine lymphocytic leukemia) with a significant lifespan increase in mice.^{1a} In 1988, they were "pleased to report that 15 years of relentless research" had culminated in the structure elucidation of the cephalostatins.

Currently, 19 cephalostatins have been reported (Figure 3). All cephalostatins possess two highly oxygenated steroidal



Seongmin Lee was born in Pohang, South Korea, in 1969. He received his B.S. and M.S. degrees in Chemistry from Seoul National University in 1992 and 1994, respectively. After working for LG Chemical Institute as a medicinal chemist, in 1999 he began his graduate studies at Purdue University under the supervision of Professor Philip Fuchs. During his Ph.D. program, he developed various C—H oxidation protocols and applied them to the synthesis of an anticancer steroidal pyrazine, ritterazine M. In 2004, he joined the group of Professor Gregory Verdine at Harvard University as a postdoctoral researcher, where he has been combining tools of synthetic organic chemistry and X-ray crystallography to elucidate molecular mechanisms by which DNA glycosylases, key enzymes in base-excision DNA repair, recognize and repair damaged bases in DNA. Beginning in the fall of 2009, he will undertake independent research on DNA damage and repair in the College of Pharmacy at the University of Texas at Austin.



Thomas G. LaCour was born and raised in Dallas, Texas. After wandering Europe, North Africa, and North America, he completed degrees in English (B.A., University of Dallas) and Chemistry (B.A., M.A., University of Texas at Austin). He performed patented Process Research at Pfizer (Groton) for several years. Fortune led to the laboratory of Professor Philip Fuchs, who mentored his Ph.D. studies on Steroidal Anticancer Agents. Advances included completion of natural (Cephalostatin 1, several Ritterazines) and potent hybrid (Ritterostatins) bis-steroidal pyrazines. A semiempirical calculation method precisely relating structure to cytoplasmic activity for the entire family was discovered to correct published structures (Cephalostatins 8 & 16, Ritterazine M) and accurately predict new extremely potent analogues. Postdoctoral labors with Professor Larry Overman (UC Irvine), followed by sojourns with Professors J.R. Falck and Patrick Harran at the University of Texas Southwestern Medical Center, rounded out his medicinal chemistry research. Dr. LaCour currently endeavours to enlighten high school (and younger) minds in Dallas and explores history, psychology, and predictive statistics of the markets.

spiroketal units linked by a central pyrazine ring. Cephalostatin 1 (**1**) is among the most powerful anticancer agents ever tested, displaying subnanomolar-to-picomolar cytotoxicity against much of the National Cancer Institute's (NCI) 60-cell line panel,³ with femtomolar activity against the P388 cell line and in the Purdue Cell Culture Laboratory (PCCL) human tumor panel.⁴ Four cephalostatins, 3, 4, 8, and 9, were

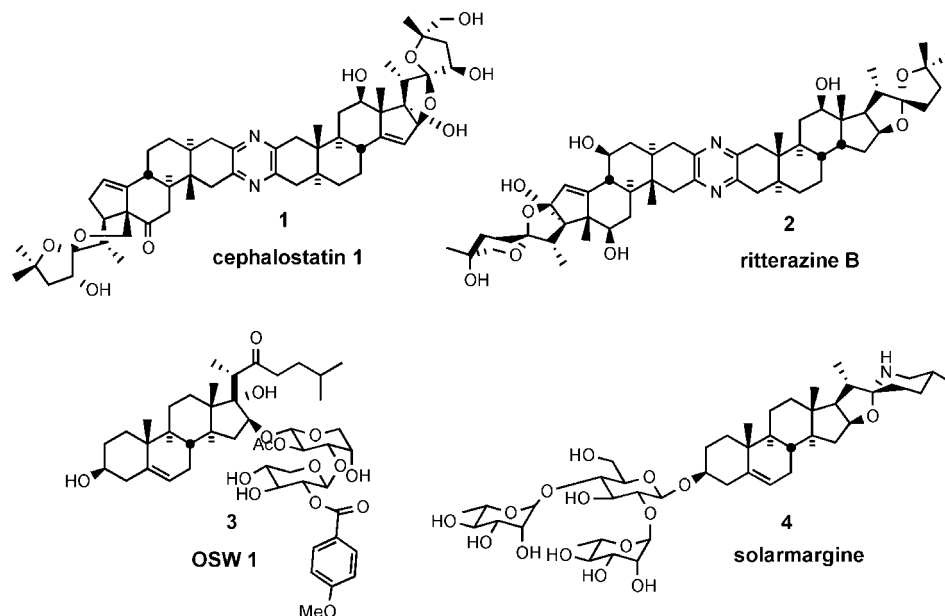


Figure 1. Steroidal anticancer agents.

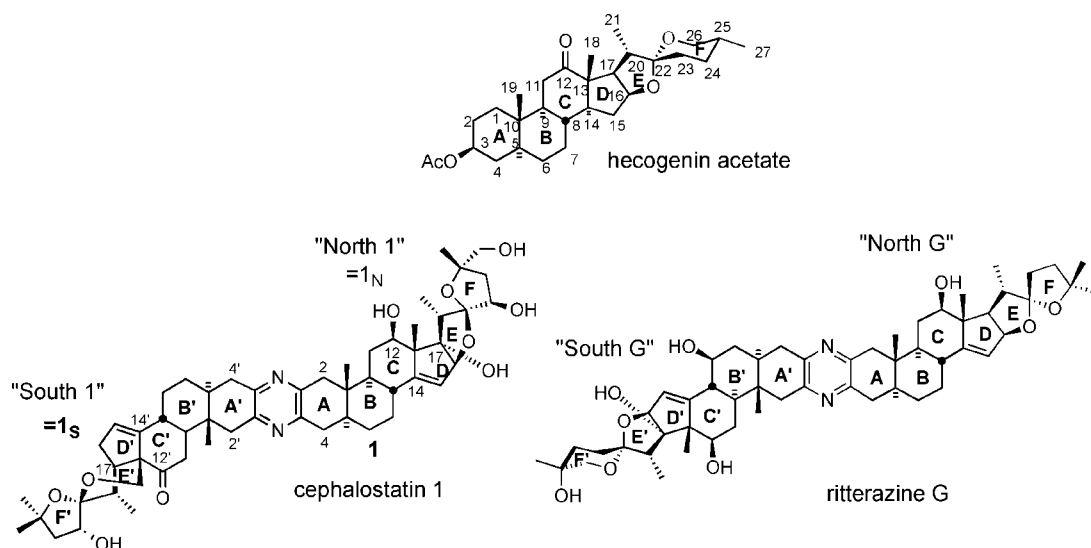


Figure 2. Steroid and bissteroid nomenclature and numbering.

as potent versus P388 (10^{-4} – 10^{-6} nM) but 4–30-fold weaker in the NCI human tumor panel, while three more cephalostatins, 10, 11, and 17, displayed 3–10 nM GI_{50} 's in both tests. Cephalostatin 16 displayed a mean GI_{50} (1 nM, NCI) similar to that for cephalostatin 1 but a 10^4 – 10^6 weaker ED_{50} (P388). Cephalostatin 7 was assumed to have activity comparable to cephalostatin 1 based on the fact that it was championed along with cephalostatin 1 for clinical trials and was reported to display a comparable \sim femtomolar ED_{50} (P388) as well as “remarkable potency. . . against a number of cell lines; the mean graphs of cephalostatin 1 (**1**) and cephalostatin 7 (**5**) were remarkably similar, if not indistinguishable” in the NCI panel. The cephalostatin's complex, unprecedented structure and promise as an anticancer lead compound inspired attention by several groups.

Clinical trials of a cephalostatin (or analogue) will require several grams of material. Pettit's fourth and most prodigious collection afforded only ~ 0.1 g of cephalostatin 1 (**1**) from half a ton (450 kg) of this tiny (<5 mm) worm, which hides

as colonies in small calcium carbonate sheaths. The harvest involved repeated SCUBA operations at ~ 25 m depth in waters off East Africa patrolled by the great white shark. The bioassay-guided isolation followed a complex, evolving protocol of extraction (whole worm, several months with aq. MeOH), multiple large-scale solvent partitionings, and protracted chromatographic separations. Clearly, chemical synthesis is the only solution to the availability problem (see Table 1).

Early speculation on the mode of action of the cephalostatins centered around (i) the likelihood of cell membrane penetration due to the steroidal nature and dimensions (~ 30 Å \times 9 Å \times 5 Å) of cephalostatin 1 (**1**),¹¹ (ii) the possibility that the compounds serve as a spatially defined set of hydrogen-bond donors/acceptors for enzyme binding,¹² and (iii) the importance of the Δ^{14} moiety,¹³ perhaps due to a chemical role of a derived β -epoxide and the C-ring ketone in the South half of cephalostatin 1 or 7 (Scheme 1).¹⁴

The Purdue group initially speculated that reaction of the C/D homoallylic alcohol array of South 7 generated similar potential

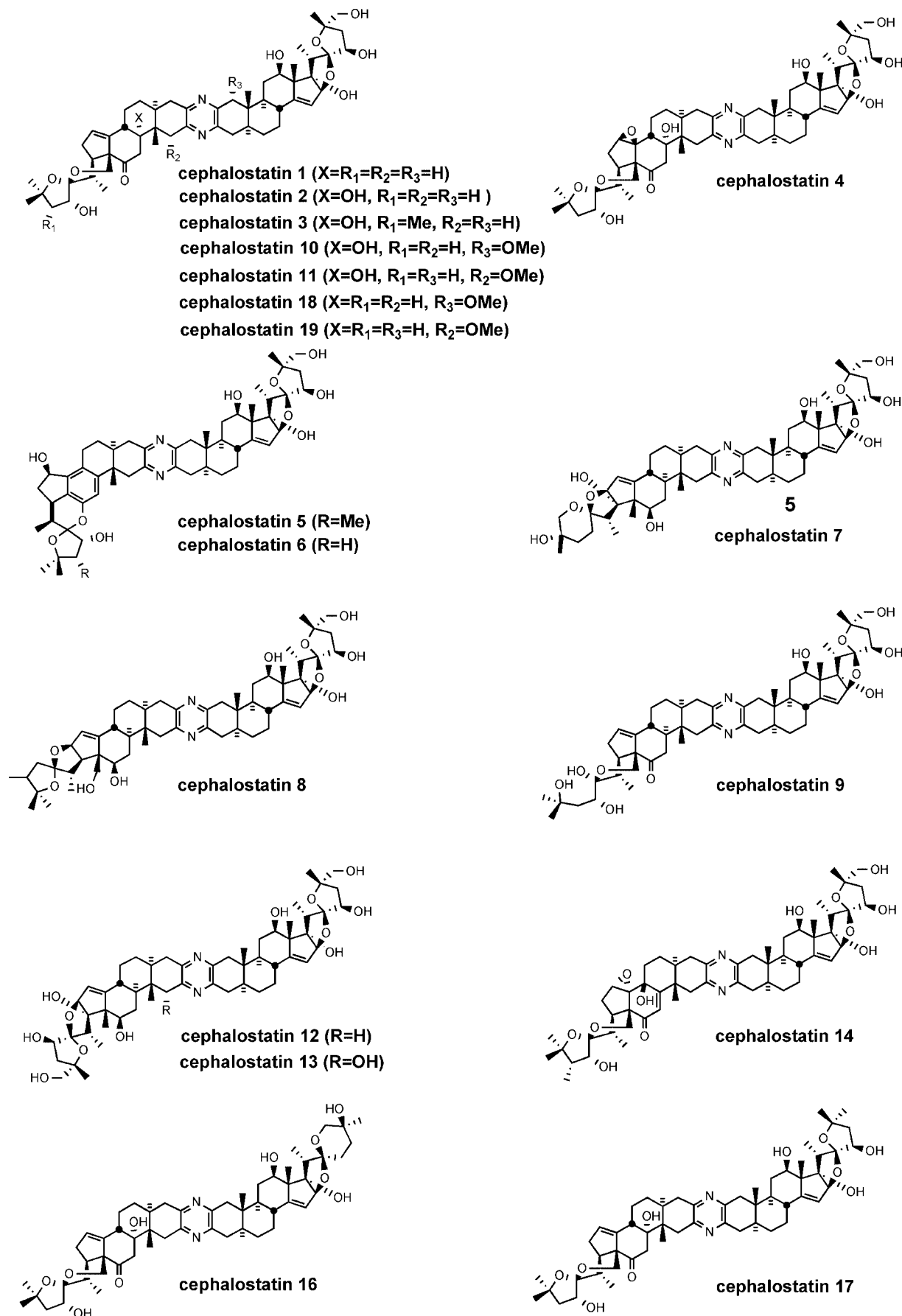


Figure 3. Cephalostatin family.

alkylating centers. However, the 1997 revelation¹⁵ that OSW-1 (**3**), a monosteroidal glycoside lacking a South unit, displayed

a profile and potency similar to cephalostatin 1 against human tumor lines prompted consideration of an equilibrium

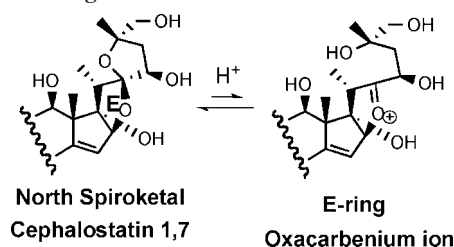
Table 1. Biological Activity of Cephalostatins

pyrazines	P388 (nM, IC ₅₀ , ED ₅₀)	NCI-60 ^a (nM, GI ₅₀)	NCI-10 ^b (nM, GI ₅₀)	PCCL ^b (nM, ED ₅₀)
Cstat 1	10 ⁻⁴ –10 ⁻⁶	1.2 (4.1)	0.14–0.77	2.4 × 10 ⁻⁵
Cstat 2	10 ⁻⁴ –10 ⁻⁶	0.78 (6.5)	0.12	
Cstat 3	10 ⁻⁴ –10 ⁻⁶	(4.0)	0.4	
Cstat 4	10 ⁻⁴ –10 ⁻⁶	(36)	4.0	
Cstat 5	4.2	(130)	35.5	
Cstat 6	22	(320)	104	
Cstat 7	10 ⁻⁴ –10 ⁻⁶	76 (6.5)	16.3–34.4	0.052
Cstat 8	10 ⁻⁴ –10 ⁻⁶	29 (9.7)	3.1	
Cstat 9	10 ⁻⁴ –10 ⁻⁶	(6.3)	0.85	
Cstat 10	3.2	4.1		
Cstat 11	2.7	11		
Cstat 12	76	400		
Cstat 13	48	>1000		
Cstat 14	4.4	100		
Cstat 15	27	68		
Cstat 16	<1	1		
Cstat 17	4.6	4		
Cstat 18	4.6	22		
Cstat 19	7.9	17		

^a GI₅₀ values of cephalostatins at dosages of 1 μM max. Values in parentheses were obtained at dosages of 3–10 μM max. ^b Activity in a 10-line panel of leukemia, brain, renal and breast cancers particularly responsive to this class of cytotoxins.³ ^b Activity in 6-line panel of generally less susceptible breast, renal, lung, prostate, and colon cancers.⁴

between the North spiroketal and its E-ring oxacarbenium ion as a potential alkylating agent (Scheme 2).

The antineoplastic mechanism of the cephalostatins is presently largely unknown. The fingerprint of cephalostatin activity in the NCI 60-tumor panel is quite different from known anticancer agents, likely indicating a new mechanism of action. The cephalostatin pattern was most similar to the topoisomerase II inhibitors, but Pettit relates that cephalostatins 1 (**1**) and 7 (**5**) are neither topoisomerase inhibitors nor serve as antimicrotubule agents like taxol.¹⁶ Studies using synthetic cephalostatin 7 (**5**) indicate that this compound is not an inhibitor of protein Kinase C nor does it inhibit the tyrosine phosphatase cdc25. A recent biological study¹⁷ revealed that cephalostatin 1 affects cells by disrupting the mitochondrial transmembrane potential. Dirsch et al., in collaboration with Pettit, documented¹⁸ that cephalostatin 1 triggers the release of Smac/DIABLO, a pro-apoptotic mitochondrial signaling factor that induces receptor-inde-

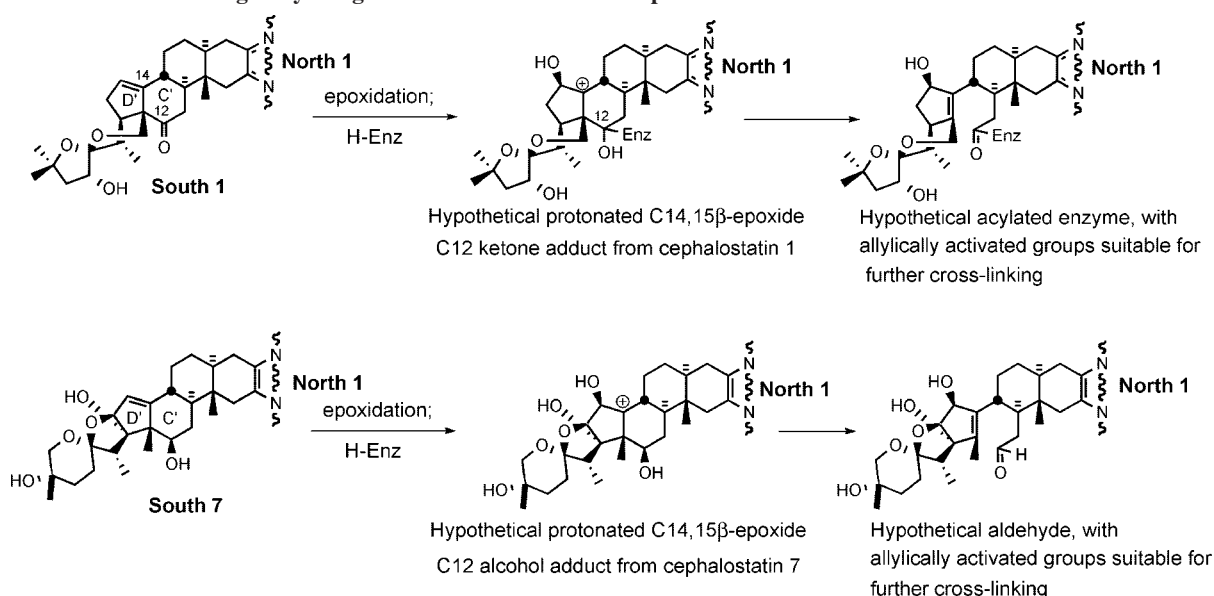
Scheme 2. E-ring Oxacarbenium Ion

pendent apoptosis. Müller and co-workers demonstrated¹⁶ that cephalostatin 1 inactivates Bcl-2, an antiapoptotic protein, by activating JNK (c-Jun N-terminal Kinase). In 2006, Vollmar et al. reported^{19a} that cephalostatin 1 utilizes the endoplasmic reticulum stress pathway rather than the intrinsic mitochondrial pathway. Cephalostatin 1 (**1**) not only induces classical apoptosis parameters (e.g., cell shrinkage, increased cellular granularity, DNA fragmentation, and caspase activation) but also shows very unusual apoptosis signaling events (e.g., selective Smac/DIABLO release, no cytochrome c release from mitochondria, and apoptosome-independent activation of caspase-9).^{19b} This unique apoptotic pathway triggered by cephalostatins implies that they could be used to treat drug-resistant cancers.

2.2. Ritterazine Family

During the 1990s, Fusetani's group completed the structure determination of 26 ritterazines³ from extracts of the tunicate *Ritterella tokioka* collected off the coast of Japan (Figure 4). The ritterazines, found 7000 miles from where the cephalostatins were discovered, are surprisingly similar to the cephalostatins both in structure and bioactivity, again unifying two highly oxygenated steroidal spiroketals by a central pyrazine.

Isolation of closely related cephalostatins and ritterazines from different phyla raises questions as to the true origin of bissteroidal pyrazines.³ Pettit originally observed that the *Cephalodiscus* worm is not confined to its conecium (worm tube) but is independent, able to move in or out of the tube using a sucker-like proboscis, and he speculated that exposure to predators during food harvesting may have necessitated development of the cephalostatins for biological defense.

Scheme 1. Possible C/D Ring Alkylating Sites Generated from a Cephalostatin

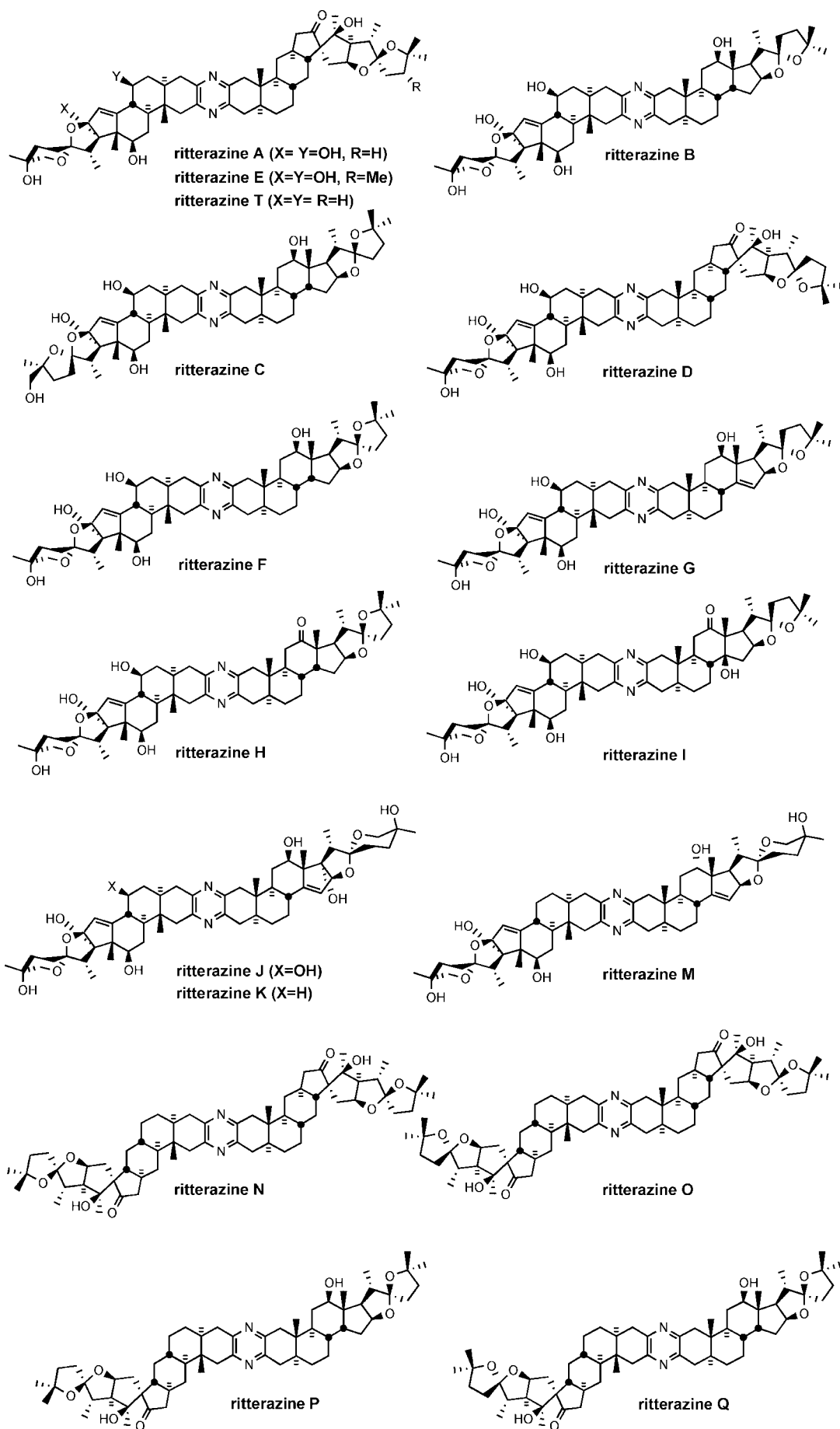


Figure 4. Ritterazine family.

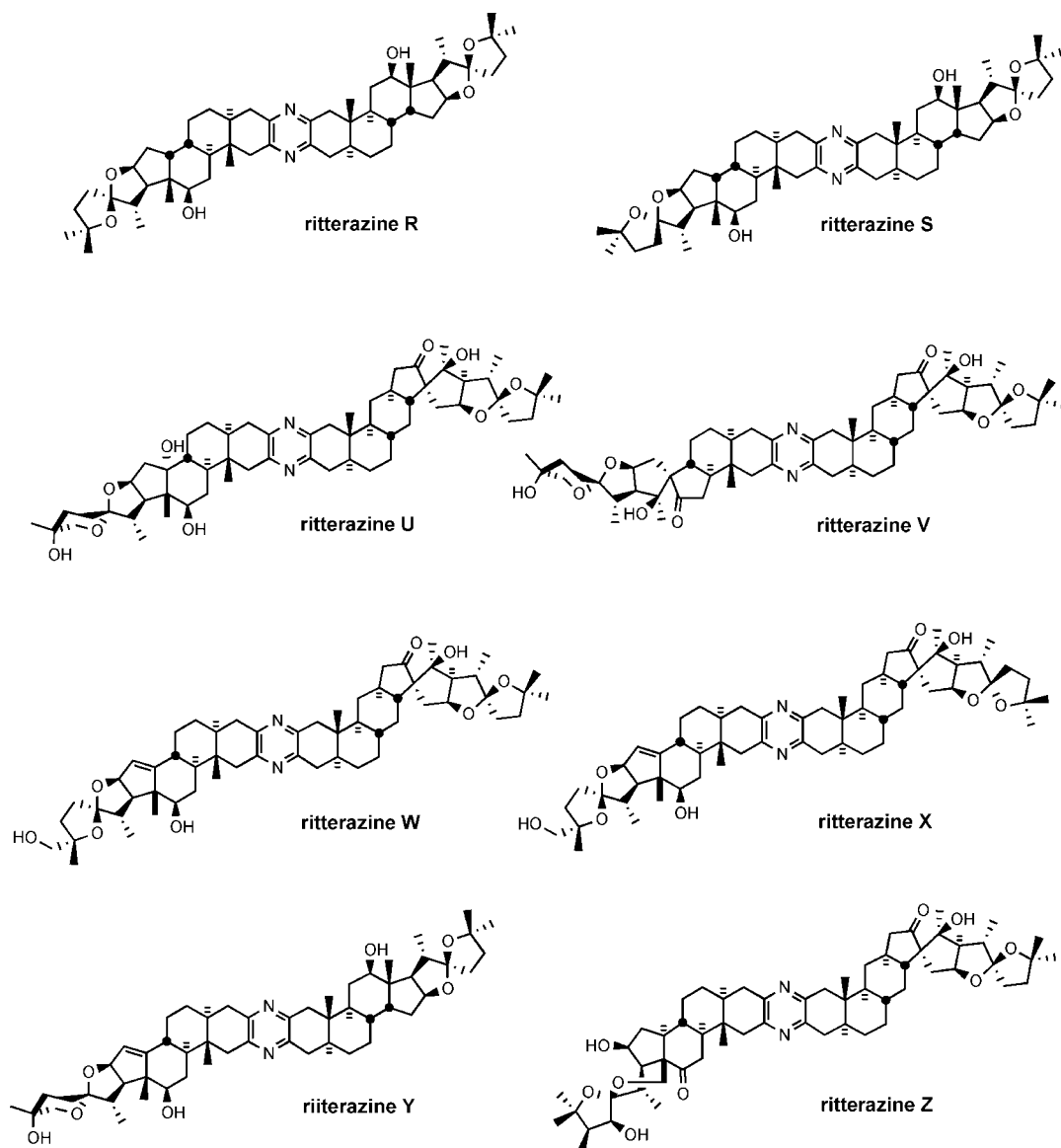


Figure 4. Continued.

While the isolation yields of the ritterazines are slightly better than the cephalostatins, they also are too low to supply clinical trials. Ganesan outlined an exciting prospect that has not yet been realized. If the compounds derive from a shared symbiotic microorganism that could be grown in the laboratory, large-scale fermentation might provide much greater quantities of these highly potent agents.^{9d}

This scarcity has been nontrivial to alleviate via synthesis because of the complexity of the steroid substructures, as evidenced by the preparation of cephalostatin 7 (**5**),²⁰ wherein the 3-ketosteroid South 7 and North 1 precursors required 32 and 33 steps from hecogenin acetate (2 and 3% yields, respectively). Interestingly, several ritterazines, although far less oxygenated, exhibited P388 cytotoxicities approaching the same nanomolar range as those of some cephalostatins. A COMPARE pattern-recognition analysis gave correlation coefficients of ~ 0.9 between cephalostatins and ritterazines in NCI-10 cell lines, suggesting they share the same mechanism.²¹ The relative simplicity of ritterazines promises greater synthetic accessibility with probable retention of significant bioactivity (see Table 2).

2.3. OSW-1 and Natural Analogues

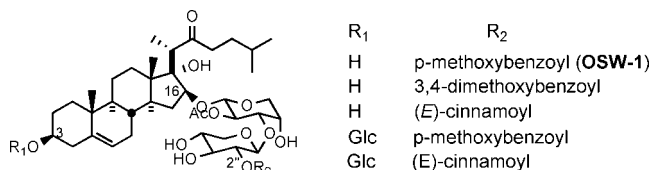
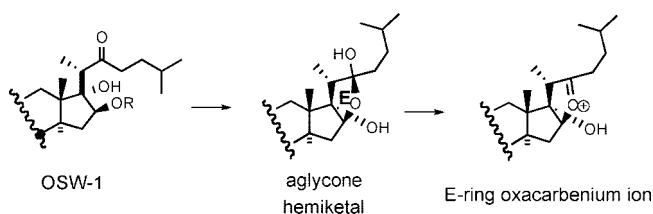
The steroidal saponin OSW-1 (**3**) and its four natural analogues (Figure 5) were isolated by Sashida and his co-workers at Tokyo University from *Ornithogalum saundersiae*, a perennial cultivated in southern Africa as a cut flower and garden plant.²² These natural products belong to a family of cholestane glycosides. OSW-1 (**3**) and its analogues (i) share the same steroidal unit, namely, $3\beta,16\beta,17\alpha$ -trihydroxycholest-5-en-22-one, (ii) have the attachment of a disaccharide to the C-16 position of the steroid aglycone, and (iii) have structural variation at the 2'' position of the disaccharide moiety and the C3 alcohol position of the steroid.

All five saponins exhibit strong cytotoxicity against leukemia HL-60 cells with IC_{50} values ranging between 0.1 and 0.3 nM. An in vivo study showed that OSW-1 (**3**) prolonged the life span of P388 leukemia infected mice by 59% with a single administration at 10 mg/kg. While OSW-1, the major component from the extraction, is exceptionally cytotoxic against various human tumors, it has surprisingly lower toxicity (IC_{50} 1500 nM) to normal human pulmonary cells. The compound was tested in the NCI 60 cancer cell

Table 2. Biological Activity of Ritterazines

pyrazines	P388 (nM, IC ₅₀ , ED ₅₀)	NCI-60 (nM, GI ₅₀)	NCI-10 ^a (nM, GI ₅₀)	PCCL ^b (nM, ED ₅₀)
Ritt A	3.8	24	12.7	7×10^{-3}
Ritt B	0.17	3.2	1.0	2.6×10^{-5}
Ritt C	102	115	178	18
Ritt D	18	102	76.8	0.012
Ritt E	3.8	37	15.9	1.9×10^{-3}
Ritt F	0.81			8.3×10^{-5}
Ritt G	0.81			5.7×10^{-5}
Ritt H	18			
Ritt I	15	88	47.3	0.010
Ritt J	14			
Ritt K	10	70	4.5	5.8×10^{-3}
Ritt L	11	20	20.5	9.5×10^{-3}
Ritt M	17			
Ritt N	522			
Ritt O	2380	inactive	>625	570
Ritt P	819			
Ritt Q	657			
Ritt R	2462			
Ritt S	539			
Ritt T	522	>590	>650	>1500
Ritt U	2340	>243	272	480
Ritt V	513			
Ritt W	3632			
Ritt X	3405			
Ritt Y	4	27	13.9	4.5×10^{-3}
Ritt Z	2200	>722	inactive	560

^a Activity in a 10-line panel of leukemia, brain, renal and breast cancers particularly responsive to this class of cytotoxins.³ ^b Activity in 6-line panel of generally less susceptible breast, renal, lung, prostate, and colon cancers.⁴

**Figure 5.** OSW-1 and its natural congeners.**Scheme 3. Hypothetical Access to an E-Ring Oxocarbenium Ion from OSW-1**

line and showed an average GI₅₀ of 0.78 nM. Intriguingly, the cytotoxicity profile of OSW-1, a plant-derived monosteroidal glycoside, is similar to that of cephalostatins, the marine animal-derived bissteroidal pyrazines. COMPARE analysis shows a correlation with cephalostatin 1 (**1**) of 0.83 for OSW-1,^{22b} suggesting that these two classes might share the same mechanism of action. The Purdue group hypoth-

esized that the C22-oxocarbenium ion, which could be generated from both OSW-1 and cephalostatins, may function as an alkylating agent.²³ Loss of the disaccharide, which may be serving as a recognition element or a polarity modifier, from OSW-1 might generate aglycone hemiketal and thence an oxocarbenium ion (Scheme 3).

2.4. Solamargine

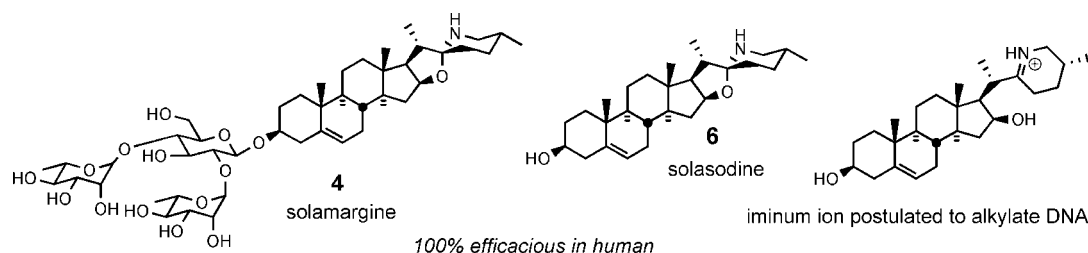
The solanum alkaloids (Figure 6) have been used for centuries in traditional anticancer folk medicine in China. Cham et al. disclosed²⁴ that solamargine **4** was extraordinarily effective against melanomas in vivo. A crme (called BEC and later Curaderm) containing solasodine and its dirham-noglucoside solamargine has been demonstrated to be highly efficacious both in mice in the terminal state of murine leukemia and in humans with advanced melanomas,²⁵ with complete remission of the cancers in all human tests (56/56 patients, 181/181 lesions in initial clinical trials). The crme is now being widely tested, especially in Australia.

More recently, it has been shown²⁶ that solamargine causes membrane lysis and mitochondria damage and exhibits antiproliferative activity in several cell lines at about 19 μ M. Solamargine is now known to trigger apoptosis by up-regulating the expression of external death receptors, such as tumor necrosis factor receptor I and the Fas receptor.²⁷ The rhamnose portion of solamargine has been shown to be a critical recognition element. The susceptible (especially melanoma) cancer cells apparently express a unique endogenous endocytic lectin (EEL) that binds the solamargine molecule prior to membrane penetration. The differential cytotoxicity of solamargine (nontoxic to normal cells both in in vitro tests and when applied to healthy subjects in animal and human trials) may thus be rationalized, since normal mammalian cells do not incorporate rhamnose in glycoconjugates nor express a receptor for such glycals.

In 1996, Kingston et al. reported that steroidal alkaloid solasodine **6**, aglycone of solamargine, displayed considerable activity against DNA-repair-deficient yeast, and *N*-acetylation destroyed its DNA-alkylating ability.⁷ Kingston postulated that solasodine acts in a related manner to alkylate DNA via its spiroaminal-derived iminium ion, which is reminiscent of the oxocarbenium ions proposed to account for the cephalostatins/OSW-1 relationship (Figure 6).

2.5. Simple Analogues

Although the biologically hyperactive cephalostatins and ritterazines are asymmetric and structurally complex, some simple symmetrical analogues (Figure 7) exhibited differential cytotoxicity (as well as in vivo anticancer activity in animal trials) for a *ras*-oncogene transfected cell line. These compounds were tested in mice and found to decrease tumor growth by 50–60%.¹² This observation is significant since testing the same compounds in the NCI 60 tumor panel

**Figure 6.** Solasodine and the antitumor agent solamargine.

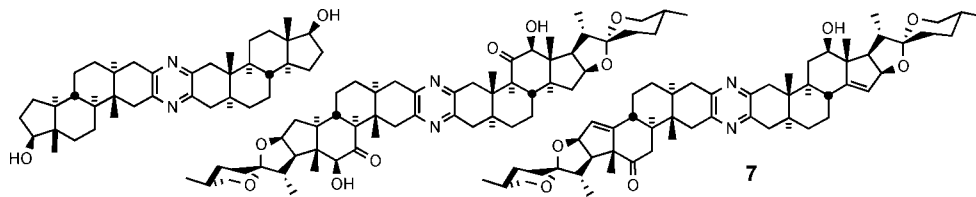


Figure 7. Simple bissteroidal pyrazine analogues.

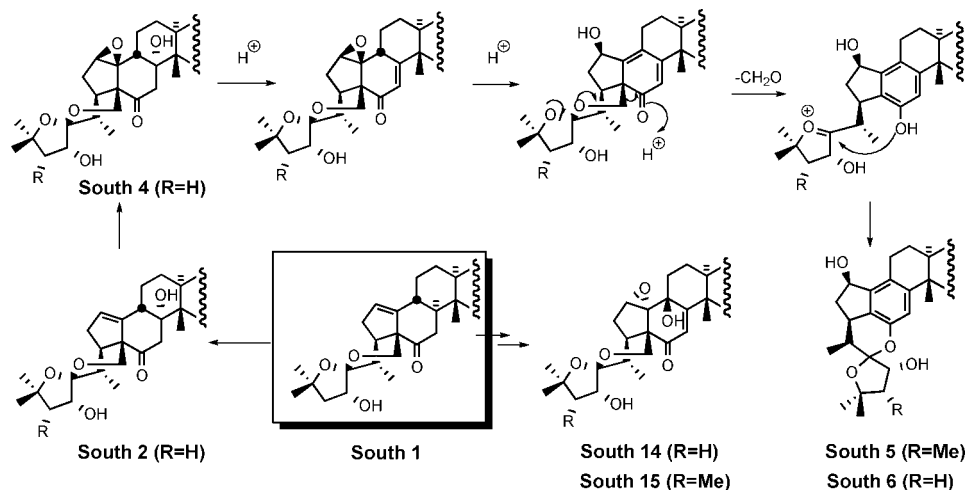


Figure 8. “South 1” similarities among certain cephalostatins.

failed to reveal any indication of anticancer activity. Unsymmetrical hydroxyketone **7** showed a low micromolar range of GI_{50} in the NCI 60-cell line panel. Surprisingly, this simple analogue displayed the same pattern of bioactivity as cephalostatin **1** (**1**), suggesting a common mode of action.

3. Pyrazine Synthesis

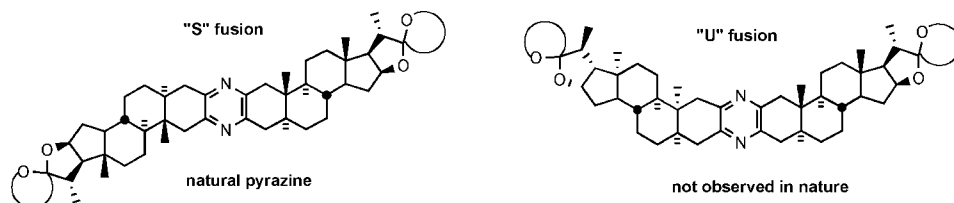
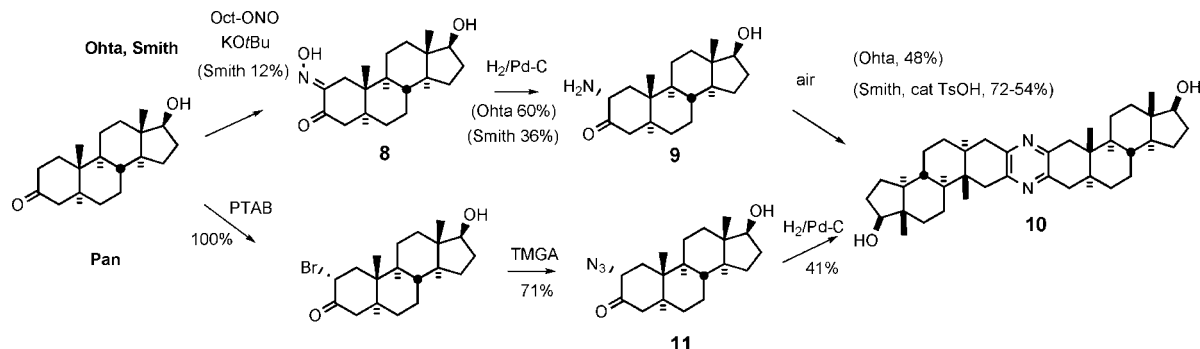
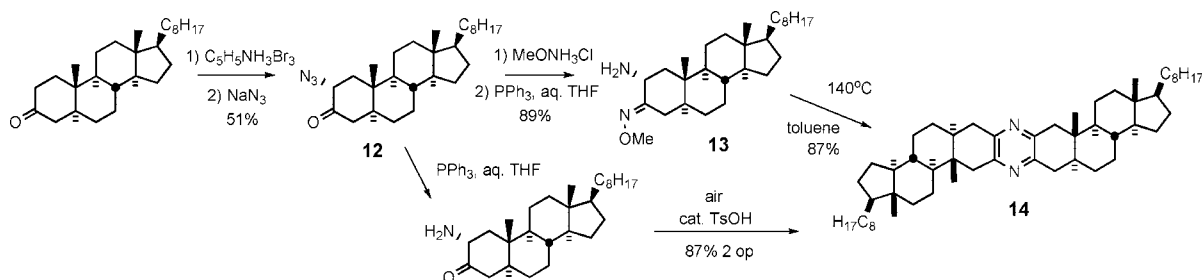
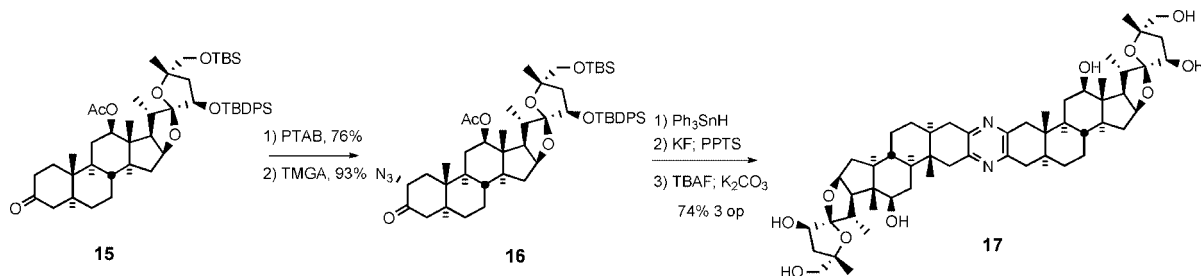
An approach to the cephalostatins must address the central heteroaromatic ring. The dominance of unsymmetrical pyrazines in the cephalostatin family presents a puzzle. Does nature modify symmetrical dimers, couple different subunits, or perform both pre- and postunion modifications? In his seminal contribution describing cephalostatin **1** (**1**), Pettit hypothesized that the pyrazine core structure was assembled via dimerization and oxidation of steroidal α -amino ketones, a spontaneous reaction in the laboratory.¹⁶

The Purdue group outlined two main scenarios distinguished by the timing of the dimerization.²⁸ The first hypothesis posits random coupling at equal rates of previously differentiated North 1 and South 7 α -aminoketones to form cephalostatin **7** along with C_2 symmetric dimers cephalostatin **12** and ritterazine **K**. Consonant with the preponderance of the North 1 unit in the cephalostatin branch (present in 18 of 19 cephalostatins) and the 10-fold lower yield of cephalostatin **7** relative to cephalostatin **12**, this view requires the presence of North 1 in much greater amounts than South 7. Evidence for trace amounts of ritterazine **K** (South 7 dimer) was detected among unassigned products from the *Cephalodiscus* worm, with matching chromatographic properties using synthetic ritterazine **K** as a guide. The analysis appears to break down with respect to the yield of the cephalostatin **1**, which is 100-fold greater than that of cephalostatin **12**, the North 1 dimer. Although unnoted in the literature, a similar dilemma attends the South 1 unit (present in 16 of 19 cephalostatins, substantially modified in cephalostatins **5**, **6**, and **8**), but no such South 1 dimer has been reported.

The second biogenetic scenario for cephalostatin **7** (**5**) projects differentiation of a homodimer, either by C23 monoreduction of cephalostatin **12** or C23 monooxidation of ritterazine **K**, with subsequent spiroketal isomerization. Ganesan outlined dimerization of a precursor α -amino ketone followed by unselective oxidations to achieve differential functionalization of the steroidal subunits, and cites the similarity between the two halves of cephalostatin **7** and the identification of dimeric cephalostatins **12**–**13**.^{9c,d} It is unclear why the high proportion of South 1/North 1 unions was ignored, although it was obvious then in 10 of the 17 known members, and despite recognition of the likely derivation of South 5 from South 1. The majority of “South” units in the cephalostatins could be easily derived from South 1 (Figure 8).

“Unselective” oxidations in the cephalostatins now appear unlikely. Indeed, modification of a homodimer in this branch would seem to be quite selective. On the other hand, the South 7 type was ubiquitous among ritterazines (13 of 26) but with no majority of any particular union apparent, and four of these (ritterazines **J**–**M**) were of high symmetry. Several of the subsequent 13 ritterazines also possess such symmetry, for a total of 9 near or exact homodimers out of 26 examples. Additionally, this branch displays consistently lower oxidation levels than the cephalostatins.

Another logical alternative seems worthy of consideration, wherein directed (not random) coupling of at least partially modified units prevails in the worm but not necessarily in the tunicate. Sole responsibility for production of these cytotoxins by putative common and very well-traveled symbiotic microflora²⁵ seems inconsistent with the observed divergence in character of the two pyrazine branches. Perhaps a common organism participates by fusing steroid stocks, which differ between the animals. Whatever the timing, only the “S” type pyrazine has been isolated (Figure 9), consistent with the sole mechanistically possible outcome of reaction between 2-amino-3-ketones. Unfortunately, although several “U” pyrazines have been synthesized, none have been tested

**Figure 9.** Possible bissteroidal pyrazine geometries.**Scheme 4.** Early Approaches for Preparation of Symmetrical Pyrazines**Scheme 5.** Smith/Heathcock Routes to Symmetrical Pyrazines**Scheme 6.** Jeong Synthesis of C_2 -Symmetric Cephalostatin North 1 Analogue

for biological activity.³⁰ No analogues featuring alternative fusions (e.g., benzene, pyridine, pyrrole, quinone, dioxane, etc.) have yet been prepared.

3.1. Symmetrical Pyrazine Synthesis

Symmetrical steroidal pyrazine synthesis via classical dimerization of an α -aminoketone was first reported in 1968 by Ohta and co-workers (Scheme 4).²⁹ Ohta reduced the 2-oximino-androstan-17 β -ol-3-one **8** in alcoholic HCl. Liberation of free amine **9** followed by brief warming in air provided symmetrical pyrazine **10** in fair yield. Smith and Hicks³⁰ partially characterized the intermediate dihydropyrazine and found that catalytic TsOH enhanced air oxidation at ambient temperature.

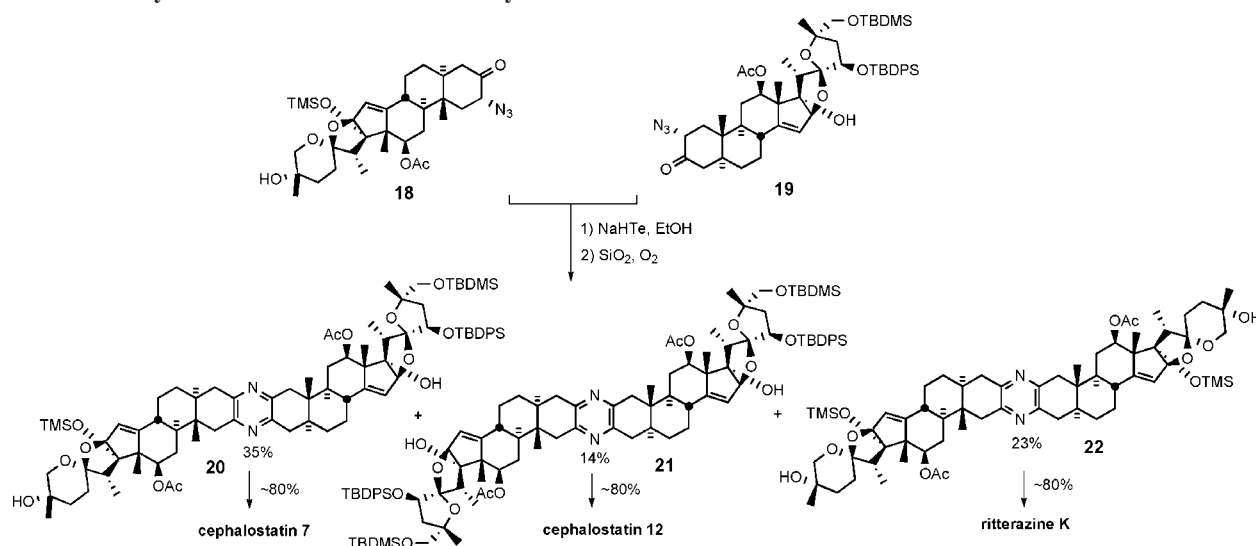
Disclosure of the cephalostatin structure renewed interest in such pyrazines as evidenced by a report by Pan et al., who developed¹² an improved pyrazine synthesis via reduc-

tive dimerization of α -azidoketone **11** upon catalytic hydrogenation (Scheme 4). Smith and Heathcock contemporaneously disclosed³¹ a similar route to α -azidoketone **12** and achieved improved access to pyrazine by a two-step method, Staudinger reaction followed by air oxidation (Scheme 5). Heathcock's second route employed conversion of α -azidoketone **12** to stable α -aminomethoxime **13**, which afforded pyrazine **14** in high yield. In 1994, Jeong reported³² synthesis of C_2 -symmetric cephalostatin analogue **17** via tin hydride reduction of α -azidoketone **16** (Scheme 6).

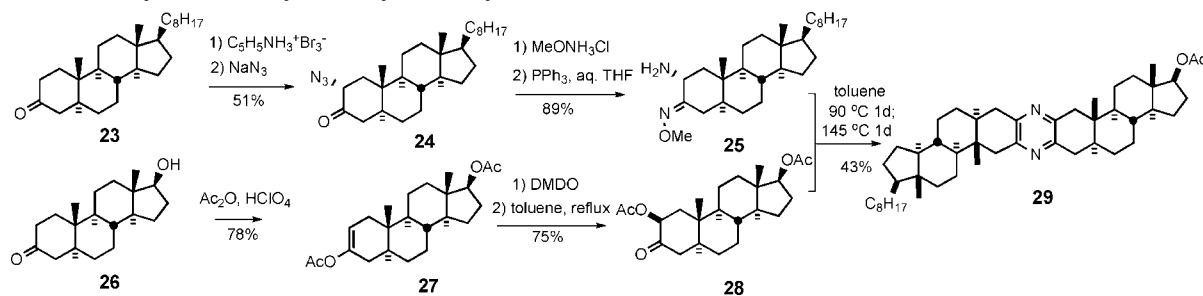
3.2. Biomimetic Random Coupling of α -Aminoketones

As discussed earlier, the composition of the cephalostatin and ritterazine families implies that nature may utilize random coupling of differentiated steroidal α -aminoketones to produce the bissteroidal pyrazines. Jeong's synthesis prepared unsymmetrical cephalostatin **7** and the

Scheme 7. First Synthesis of Natural Bissteroidal Pyrazines



Scheme 8. First Unymmetrical Pyrazine Synthesis by Smith/Heathcock



dimers of its subunits, cephalostatin 12 and ritterazine K, to explore this “pseudocombinatorial” hypothesis (Scheme 7).²⁰

The synthesis featured production of cephalostatins 7 and 12 and ritterazine K in one pot via in situ reduction of α -azidoketones (**18** and **19**) to α -aminoketones followed by statistical combination of the α -aminoketones. When a 1:1 mixture of the North 1 and South 7 unit was treated with ethanolic NaHTe in the presence of SiO₂ and O₂, α -aminoketones produced in situ afforded the expected pyrazines. The reaction provided the protected pyrazines cephalostatin 7 (**20**), cephalostatin 12 (**21**), and ritterazine K (**22**) in 35, 14, and 23% isolated yields, respectively. Individual deprotection of pyrazines (**20**, **21**, and **22**) with excess TBAF afforded the first synthetic samples of cephalostatin 7 (**5**), cephalostatin 12, and ritterazine K, respectively.

3.3. Unsymmetrical Pyrazine Synthesis

Earlier cephalostatin studies focused on preparing symmetric pyrazines. However, since most of cephalostatins and ritterazines are unsymmetrical dimers, and symmetrical dimers (e.g., cephalostatin 12, ritterazine K) universally exhibit substantially weaker cytotoxicity, efficient construction of unsymmetrical bissteroidal pyrazines was absolutely essential.

3.3.1. Heathcock Method

Smith and Heathcock provided the first synthetic route for unsymmetrical bissteroidal pyrazines in 1992 (Scheme 8).^{31a} α -Azidoketone **24** was obtained by α -bromination of 3-cholestanone **23**, followed by displacement of the secondary bromide with sodium azide. Treatment of **24** with *O*-methyl

hydroxylamine provided the *O*-methoxime, which was reduced with triphenylphosphine in aqueous THF to give 2-amino-3-methoxime **25**. To prepare a coupling partner, androstanone **26** was converted to enol acetate **27**, which was oxidized with dimethyldioxirane to 2 β -acetoxy 3-ketone **28**. Initial heating at 90 °C of aminomethoxime **25** with 3-ketoacetate **28**, followed by heating at 145 °C, provided the first unsymmetrical steroidal pyrazine **29**, probably via sequential imine formation followed by loss of AcOH and MeOH (Scheme 9).

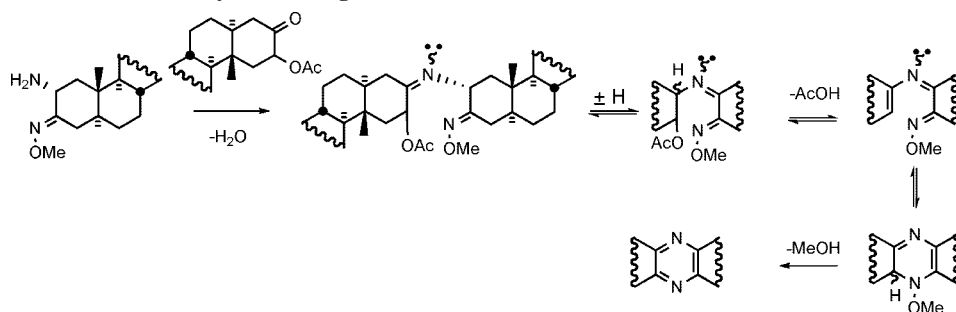
Since the cephalostatins contain spiroketals, the next logical step was to couple a steroid bearing this structural feature. Thus, α -acetoxyketone **30** was prepared by sequential enolate formation, MoOOPh-mediated α -hydroxylation, and acetylation (Scheme 10). Condensation of **30** with α -aminomethoxime **25** under the same conditions furnished spiroketal-containing unsymmetrical pyrazine **31**.

Although the yield of pyrazine is low, this protocol provided a breakthrough for the construction of unsymmetrical pyrazines, thereby enabling subsequent efforts to target the North and South segments of cephalostatin with expectation of unification late in the synthesis. Indeed, all synthetic trisdecacyclic analogues are prepared by late-stage pyrazine formation.

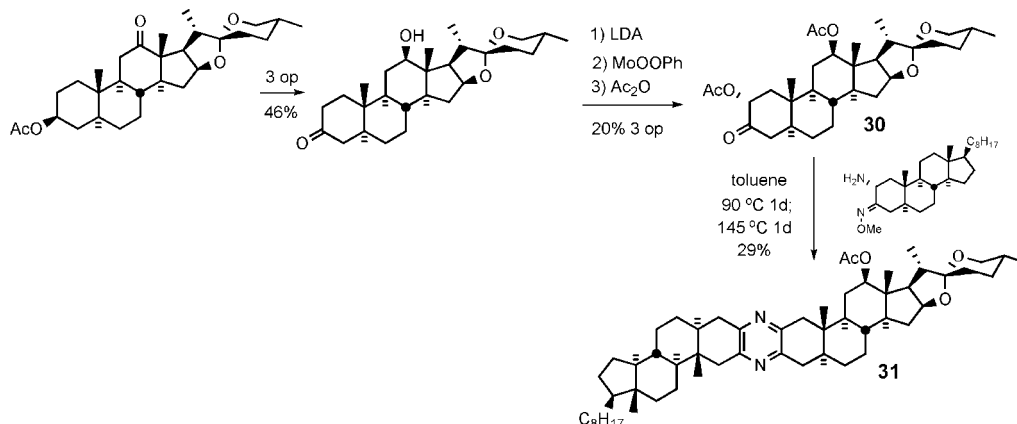
3.3.2. Winterfeldt Method

With respect to unsymmetrical pyrazine synthesis, the Winterfeldt group pursued both desymmetrization of homodimers and coupling of different steroids. In 1993, they reported³³ the first synthetic bissteroidal spiroketal pyrazines containing a Δ^{14} olefin moiety (Scheme 11). Desymmetri-

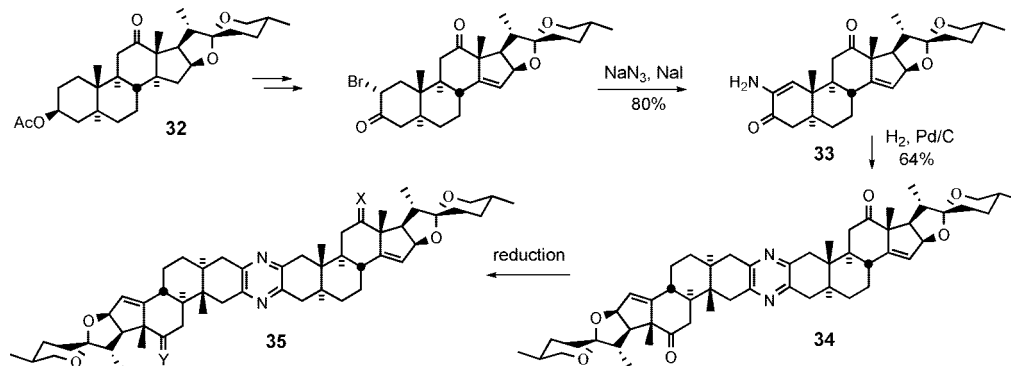
Scheme 9. Proposed Mechanism for Pyrazine Ring Formation



Scheme 10. Coupling of an Unsymmetrical Spiroketal-Bearing Steroid



Scheme 11. Winterfeldt Desymmetrization of Symmetrical Pyrazine 34



reduction condition	X	Y	yield (%)
0.7 equiv. L-selectride	α -OH, β -H	O	49
excess L-selectride	α -OH, β -H	α -OH, β -H	96
0.7 equiv. NaBH ₄	α -H, β -OH	O	47
excess NaBH ₄	α -H, β -OH	α -H, β -OH	98

zation began by installing the unsaturation into hecogenin acetate **32**, in the succinct words of the author, “by a photoprocess.”

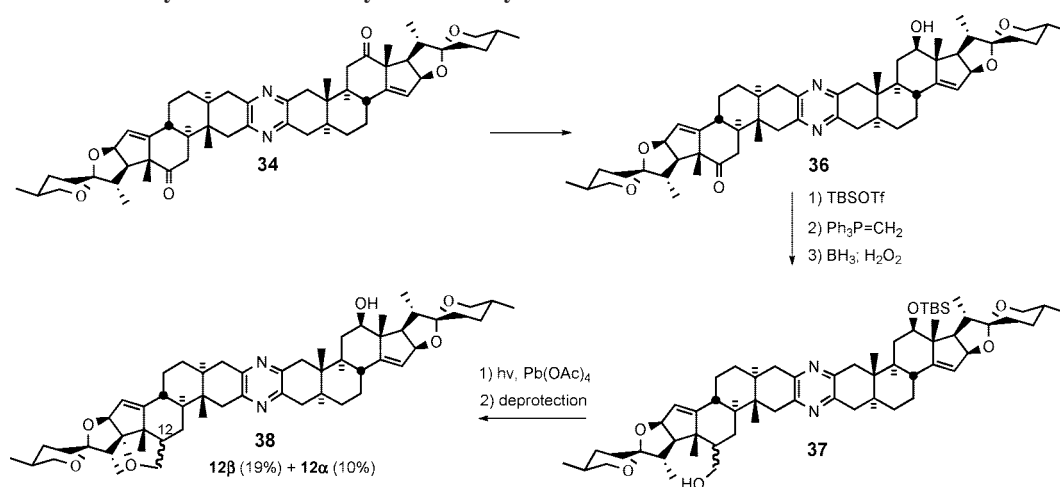
Aminoenone **33** was obtained in excellent yield and showed no tendency to thermally dimerize, but Pd-catalyzed hydrogenation afforded pyrazine **34**. Exhaustive NaBH₄ or L-selectride reductions of **34** furnished symmetrical derivative **35**.

Recently, the Winterfeldt group extended the desymmetrization strategy to proximally functionalize C17 via intramolecular alkoxy radical cyclization (Scheme 12).³⁴ After converting diketone **34** to keto-alcohol **36** by NaBH₄ reduction, silylation and Wittig olefination, followed by hydroboration/oxidation, provided alcohol **37**. Exposure of **37** to lead tetraacetate with irradiation furnished a mixture of isomeric tetrahydrofurans **38**.

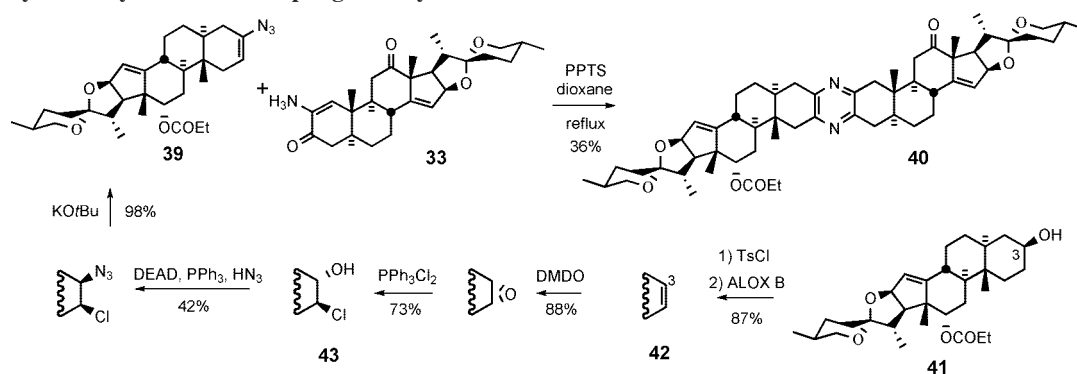
Winterfeldt's 1996 communication³⁵ disclosed an original protocol for unsymmetrical pyrazine coupling inspired by the thermal stability of α -aminoenones. He reasoned that azirines would be cyclic equivalents of reactive α -aminoenones yet resistant to dimerization and would, thus, perform well as coupling partners. Stilbene azirine (stilbene/IN₃, 0–60 °C, 94%) did indeed condense with an α -aminoenone under mild conditions. However, ring-fused azirines proved too strained to isolate, so their generation from steroidal vinyl azides **39** was conducted thermally in the presence of PPTS and aminoenone **33**. This strategy successfully furnished pyrazine **40** in 36% yield.

Synthesis of vinyl azide **39** from C3-OH **41** revealed substantial improvements to the Schweng-Zbiral protocols achieved by the German group (Scheme 13). Tosylation of

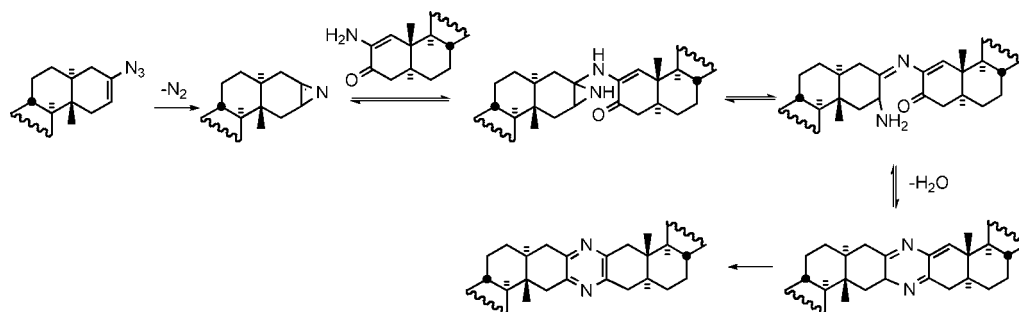
Scheme 12. Winterfeldt Desymmetrization of Symmetrical Pyrazine 34



Scheme 13. Pyrazine Synthesis via Coupling of Vinyl Azide 39 with α -Aminoenone 33



Scheme 14. Proposed Mechanism for the Pyrazine Ring Formation

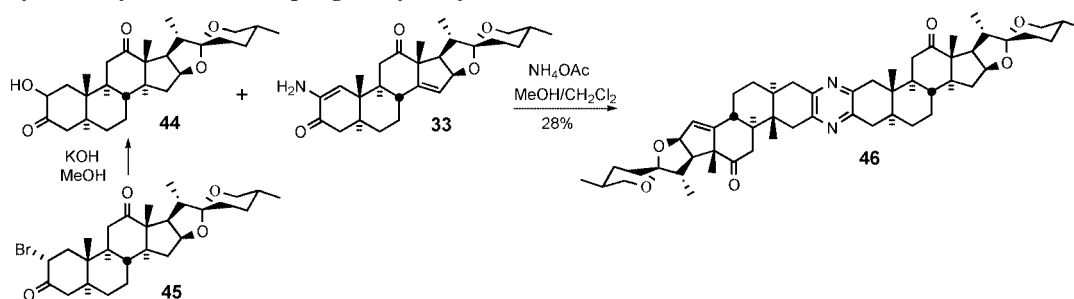


C3-alcohol **41** followed by ALOX B-assisted E₂-elimination provided Δ² olefin **42**, which was subjected to sequential treatment with DMDO and Ph₃PCl₂ to furnish 2β-chloro-3α-alcohol **43**. Exposure of **43** to Mitsunobu conditions gave vinyl azide **39** after treatment with KOtBu. The pyrazine synthesis mechanism involves in situ azirine generation via loss of molecular nitrogen, amination of the azirine, imine formation, loss of water, and aromatization (Scheme 14).

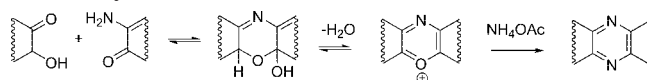
Although Winterfeldt's vinyl azide approach provided unsymmetrical pyrazines, the synthesis suffered from the length of preparing vinyl azide (six steps from **41**) and the low yield in the coupling reaction. The Hanover group later provided a partial remedy to their earlier approach (Scheme 15).³⁶ Hydroxyketone **44** was readily prepared in three steps from commercially available hecogenin and coupled with aminoenone **33**, pretreated with ammonium acetate to afford asymmetrical bissteroidal pyrazine **46**, probably via azapyrylium salt formation and nitrogen incorporation (Scheme 16).

3.3.3.3. Guo's Unsymmetrical Pyrazine Synthesis

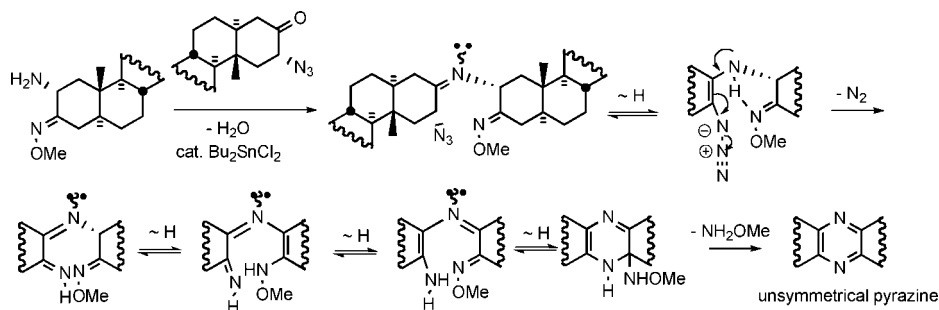
The Purdue group initially employed a biomimetic synthesis of cephalostatin 7, cephalostatin 12, and ritterazine K where the pyrazine ring was constructed by a statistical coupling of North and South α -amino ketosteroids. While the synthesis was informative in probing several biological questions, the strategy adopted was intrinsically incapable of efficiently providing an unsymmetrical coupling product such as cephalostatin 7 (**5**) since the substantially less active C_2 -symmetrical pyrazines (cephalostatin 12 and ritterazine K) were also formed. Inspired by Heathcock's concept of using α -amino methoxime as an imine progenitor, which fosters aromatization in the absence of additional oxidation, Guo devised an unsymmetrical pyrazine synthesis via coupling of an α -azidoketone and aminomethoxime in the presence of dibutyltin dichloride (Scheme 17).³⁷ This procedure is milder (80 °C, 3–6 h) and better yielding (60–90%, 28 examples) than the Heathcock–Smith protocol.

Scheme 15. Pyrazine Synthesis via Coupling of Hydroxyketone **44** with Aminoenone **33**

Scheme 16. Proposed Mechanism for the Pyrazine Formation



Scheme 17. Proposed Mechanism for the Guo Pyrazine Formation



which combined an α -aminomethoxime with an α -acetoxiketone at elevated temperatures (90–140 °C) for 2 days with yields of 29 and 43% for the two cases. The seemingly trivial substitution of an α -azidoketone for the α -acetoxiketone led to not only a more efficient preparation of the acceptor ($\sim 80\%$ in 2 steps versus $\sim 40\%$ in 3 steps) but also a probable change of mechanism. The evolution of gas and basic final pH of the reaction medium suggests that the azido moiety may not simply be serving as a leaving group as does the acetate in the Heathcock transformation (Scheme 17).

Guo evaluated the scope of the method using donor/acceptor pairs varying in distal functionality to synthesize several simple pyrazines (equimolar partners, ~ 0.02 M in

benzene, 0.1 equiv of Bu_2SnCl_2 , azeotropic removal of water for 7–12 h). Head-to-head comparisons between insoluble acidic and basic additives indicated superior catalysis by Nafion-H, but polyvinylpyridine (PVP) was more routinely utilized since many spiroketals are acid-sensitive.

The Guo protocol worked well even for the coupling of highly functionalized steroid spiroketals. For example, South 1 analogue **47** and North 1 partner **48** were smoothly united to provide protected dihydrocephalostatin **1** (**49**) (Scheme 18). The sequence was later used in the synthesis of various natural and unnatural bissteroidal pyrazines, such as cephalostatin **1**,³⁸ 23'-deoxycephalostatin **1**,³⁹ dihydro-ornithostatin

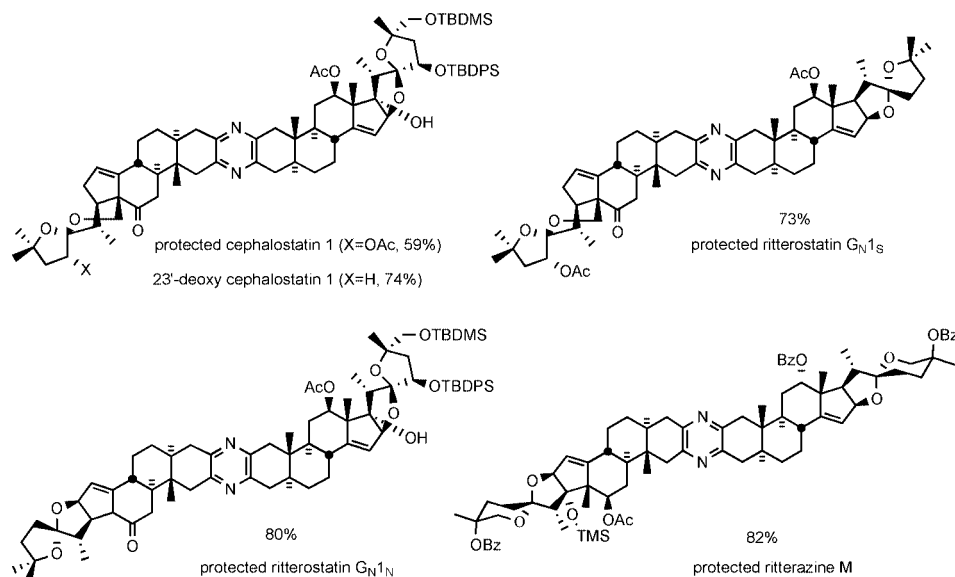
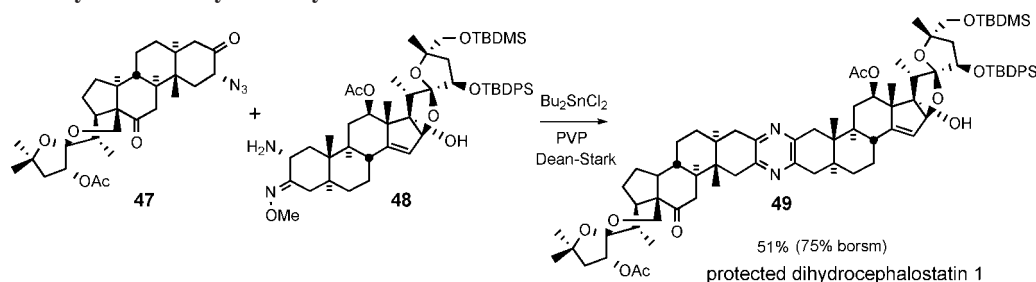
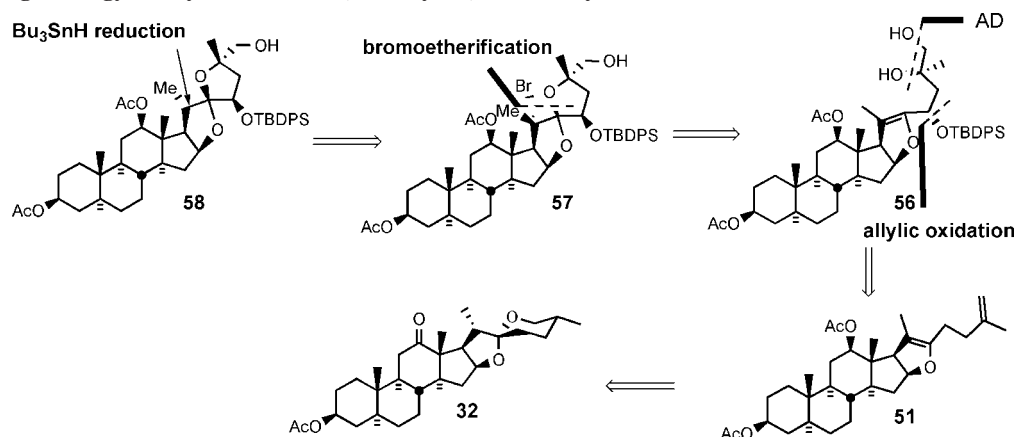


Figure 10. Some unsymmetrical bissteroidal pyrazines prepared by Guo coupling.

Scheme 18. Guo Unsymmetrical Pyrazine Synthesis**Scheme 19. Jeong Strategy for Synthesis of C14,15-Dihydro, C17-Deoxy North 1.**

O₁I_N, ritterostatins G_NI_S and G_NI_N,³⁷ and ritterazine M,⁴⁰ in good-to-excellent yields (Figure 10).

4. Classical First-Generation Syntheses

The two branches of the bissteroidal pyrazine family were isolated from *different phyla*: from the marine worm *Cephalodiscus gilchristi* (Hemichordata) in the Indian Ocean and from the tunicate *Ritterella tokioka* (Chordata) 7000 miles away off the coast of Japan. Surprisingly, they appear closely related, featuring the union of two C₂₇ steroids taken from an array of

six major subunits, variously substituted or isomerized. These subunits may themselves be seen as substituted isomers of the abundant plant-derived steroid hecogenin. Cephalostatins 1, 7 and ritterazine G are of particular interest since they feature the four “most active” of the six basic hemispheres common to the entire family (Figure 11).

Provocatively, the most potent pyrazines of the natural series were seen to utilize only the four basic units North 1, South 1, South 7, and North G. The mild unsymmetrical pyrazine fusions discussed above provided confidence for achieving late-stage

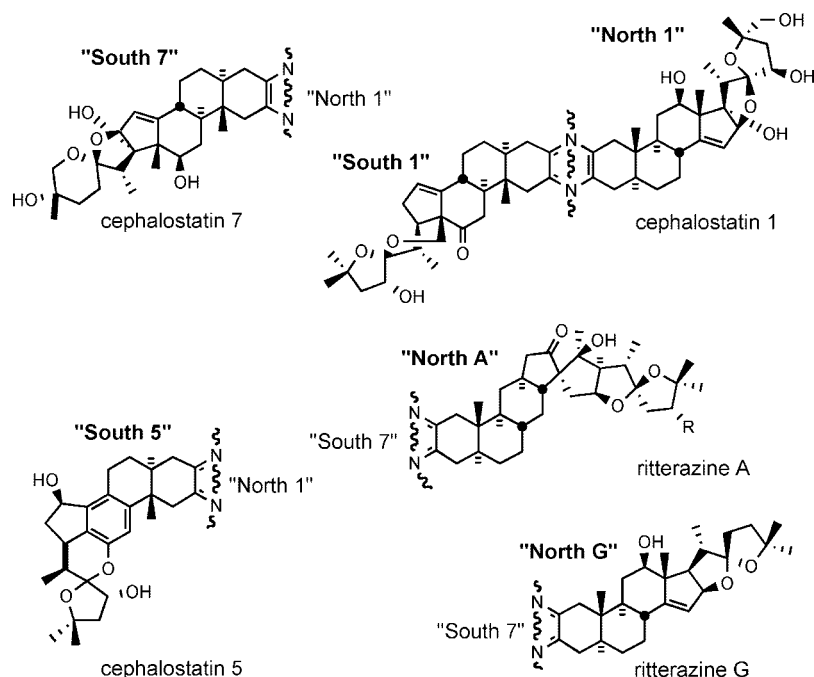
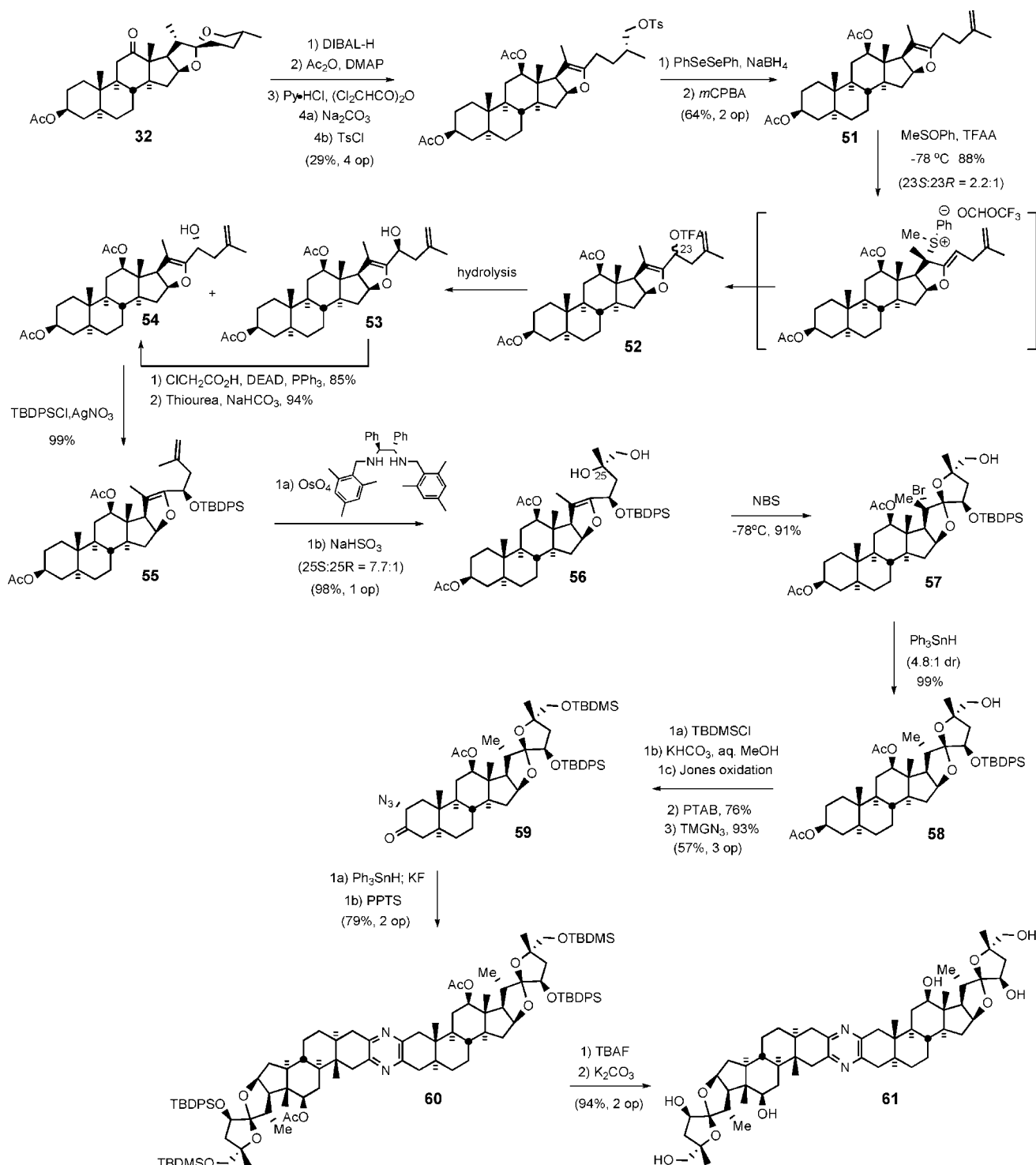


Figure 11. Six basic subunits of the cephalostatin family.

Scheme 20. Jeong Synthesis of C-17-Deoxy-C14,15-Dihydro North 1 and Its Dimer



coupling of North and South hemispheres derived from 3-ketosteroids. The many unknowns at the time of the first-generation cephalostatin syntheses necessitated employing strategies closely based upon steroid degradation of hecogenin acetate to pregnalone for constructing the two different hemispheres required for the late-stage pyrazine formation.

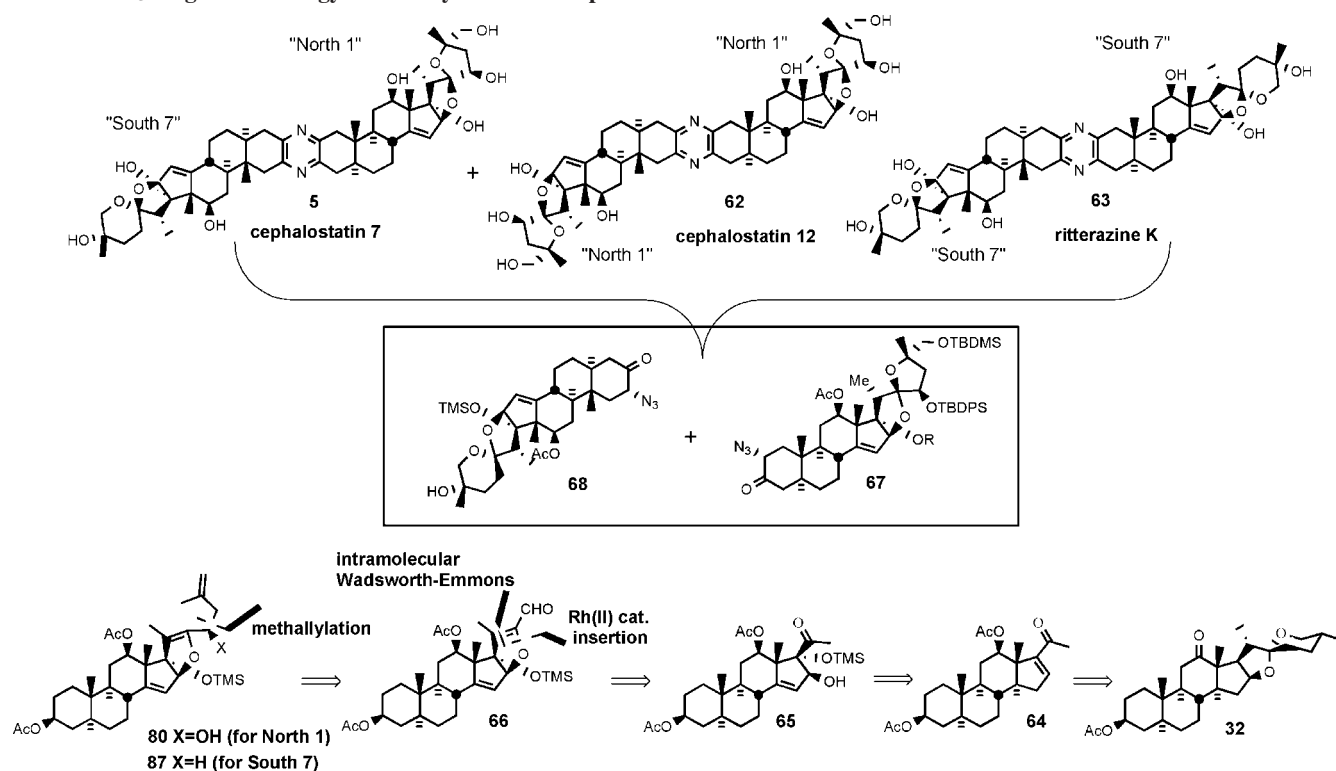
4.1. Synthesis of the C17-Deoxy-C14,15-Dihydro North Cephalostatin 1

Shortly after disclosing the syntheses of several simple, steroid-derived C_2 symmetric nonacyclic and trisdecacyclic cephalostatin analogues that possessed modest anticancer

activity in animal trials, the Purdue group reported synthesis of the model C17-deoxy-C14,15-dihydro derivative **58** of North unit of cephalostatin 1 (**1**) and its C_2 symmetric dimer by using hecogenin acetate **32** as starting material.³² The 1994 synthesis relied on (i) C23 alcohol introduction via TFAA/sulfoxide-mediated allylic oxidation, (ii) the establishment of a 5/5 spiroketal through bromoetherification, and (iii) stereoselective reduction of the tertiary bromide of **57** with Bu_3SnH (Scheme 19).

The Jeong synthesis started with the preparation of terminal olefin **51** from hecogenin acetate **32** using the protocol of Micovic and Piatak (Scheme 20).⁴¹ Reaction of

Scheme 21. Jeong/Guo Strategy for the Synthesis of Cephalostatin 7



enol ether **51** with TFAA-activated phenyl methyl sulfoxide afforded the C23 trifluoroacetates **52**, which were then hydrolyzed to give a mixture of C23 alcohols **53/54** (23S/23R = 2.2:1). Further supplies of C23R alcohol **54** were secured by Mitsunobu inversion of C23S alcohol **53** using $\text{ClCH}_2\text{CO}_2\text{H}$, providing chloroacetate, which was then chemospecifically deacylated⁴² with thiourea to alcohol **54**, which was protected as TBDPS silyl ether **55**. Acceptable dihydroxylation stereoselectivity with olefin **55** required doubly stereoselective stoichiometric osmylation in the presence of (*S,S*)-Corey ligand to give diastereomeric alcohols **56** in a C25S/C25R ratio of 7.7:1. While formation of a spiroketal from silyl ether diol **56** under acidic conditions was unsuccessful, N-Bromosuccinimide (NBS)-mediated cyclization at lower temperature exclusively afforded C20 brominated spiroketal **57**, which was then reduced with triphenyltin hydride to give a 4.8:1 mixture of C20 α /C20 β methyl **58** in essentially quantitative yield. Protection of alcohol **58**, hydrolysis of C3 acetate using KHCO_3 , Brown-Jones oxidation, PTAB-mediated α -bromination, and azide treatment gave α -azidoketone **59**. Reduction of **59** with triphenyltin hydride followed by cyclization of the resultant α -aminoketone using PPTS provided trisdecacyclic pyrazine **60**, which was then globally deprotected to afford North spiroketal dimer **61**. C₂ symmetric analogue **61** showed far less potency ($\text{GI}_{50} = 2.4 \mu\text{M}$) than the natural cephalostatins (Scheme 20).⁴³

4.2. Cephalostatin 7, Cephalostatin 12, and Ritterazine K

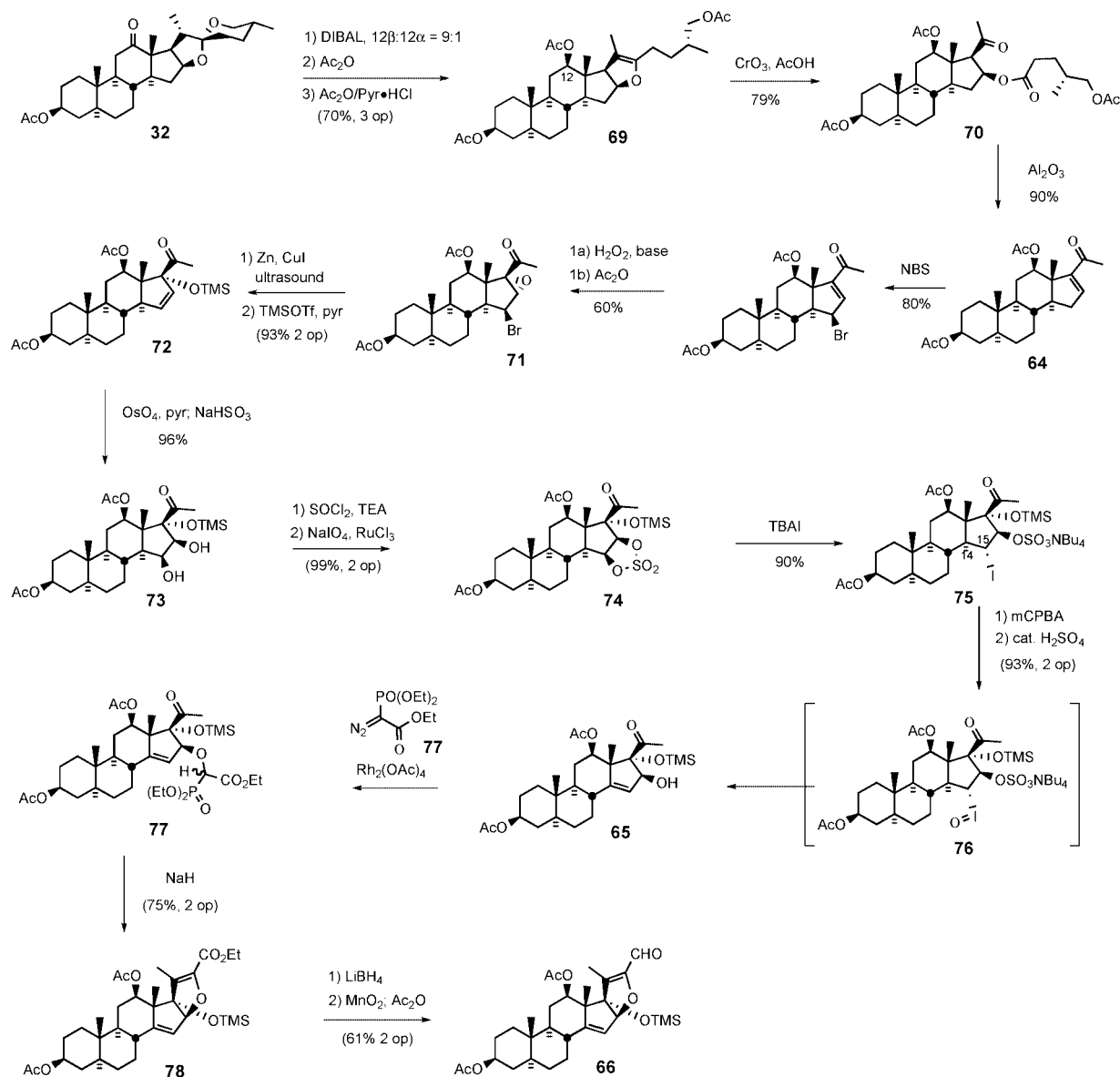
The Purdue group's biomimetic cephalostatin synthetic strategy²⁸ was based on Pettit's hypothesis^{1a} that the pyrazine core structure was assembled via dimerization and oxidation of steroidal α -aminoketones. The synthesis highlighted a statistical combination of α -aminoenones North 1 and South 7 to concomitantly produce cephalostatins 7 (**5**) and 12 (**62**)

and ritterazine K (**63**) in one pot. The key synthetic steps involved are as follows: (i) transformation of hecogenin acetate **32** to enone **64**, (ii) pentacyclic dihydrofuran-aldehyde **66** formation via rhodium[III]-catalyzed intermolecular oxygen alkylation of secondary neopentyl alcohol **65**, and (iii) subsequent intramolecular Wadsworth-Emmons reaction (Scheme 21). Aldehyde **66** served as a key common intermediate for preparing both hemispheres of the target pyrazines (North 1 (**67**) and South 7 (**68**)).

4.2.1. Construction of the North Hemisphere of Cephalostatin 1

The North 1 synthesis⁴⁴ began with the reduction of hecogenin acetate **32** with DIBAL-H followed by acylation to provide rockogenin diacetate (Scheme 22). Rockogenin diacetate was converted into pseudorockogenin triacetate **69** by pyridinium hydrochloride catalyzed reaction with acetic anhydride. Oxidation of triacetate **69** gave the known ketoester **70**, which was then treated with basic alumina to give enone **64** via β -elimination of the pentanoate side chain. Allylic bromination of **64** followed by epoxidation yielded epoxyketone **71**. After reacetylation to recover some C3 alcohol that arose in the epoxidation step, bromoepoxide was reductively cleaved with ultrasonicated zinc/copper couple to generate the tertiary allylic alcohol, which was protected as its TMS ether **72**. It is interesting to note that no larger silyl ether could be formed, and compound **72** was an easily handled material, presumably due to the crowded nature of its environment. After dihydroxylation of **72**, diol **73** was converted to cyclic sulfate **74** via the Sharpless protocol.⁴⁵ Reaction of sulfate **74** with excess tetrabutylammonium iodide afforded iodo ammonium sulfate **75**, which was oxidized with *m*-CPBA to C14,15 olefin **65** via Reich *syn*-elimination⁴⁶ of iodoso intermediate **76**. Acidic cleavage of ammonium sulfate **75** to alcohol **65** occurred *without any loss of the TMS ether moiety*.

Scheme 22. Preparation of Aldehyde 66

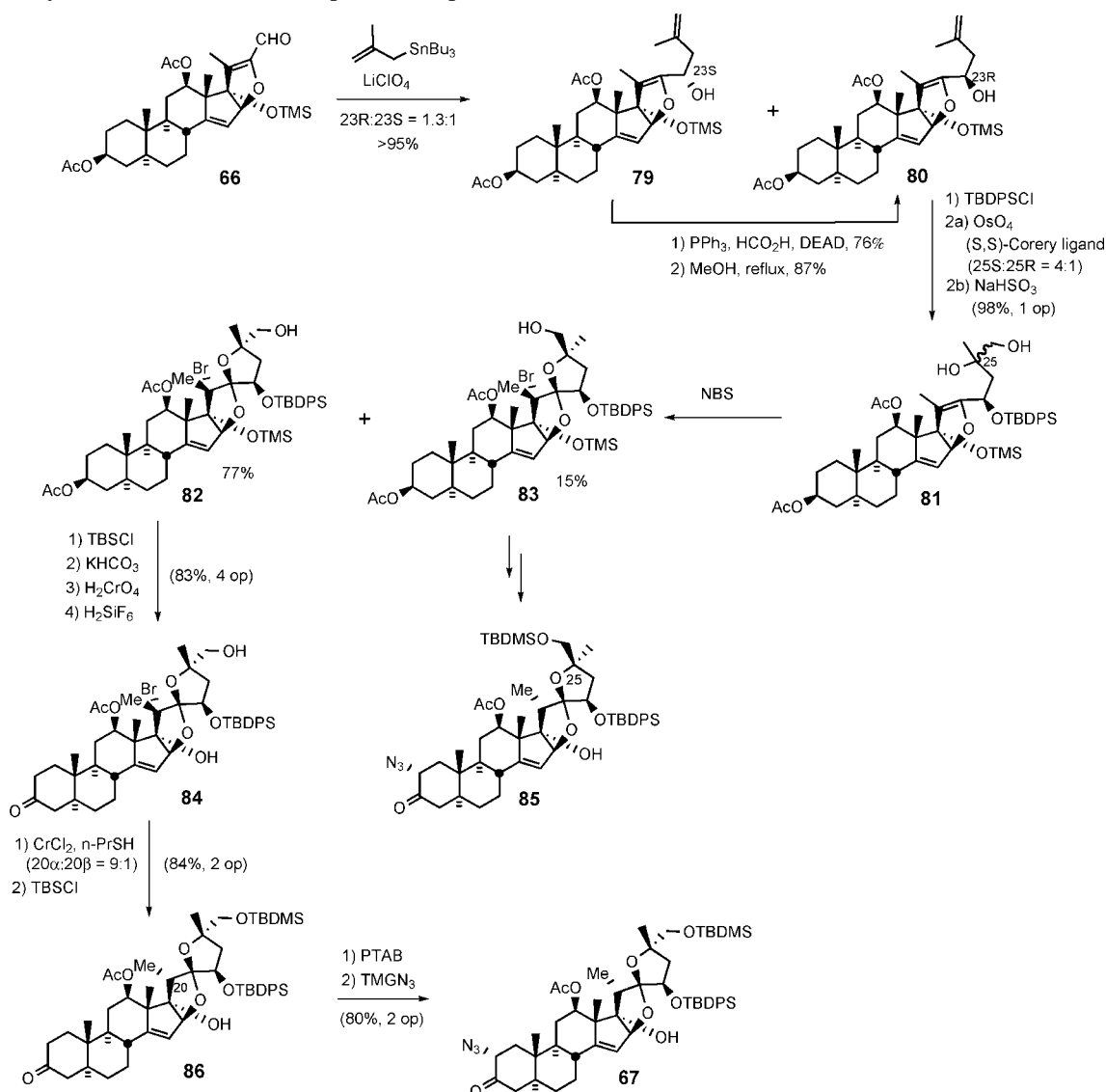


O–H insertion of allylic alcohol **65** with α -diazophosphonate ester using the Moody oxygen alkylation strategy⁴⁷ provided phosphonate ester **77** as a 1:1 mixture of diastereomers. Although hotly debated at the planning stage, the key intramolecular Wadsworth–Emmons reaction of **77** took place without difficulty to provide a high yield of complex dihydrofuran–ester **78**. Lithium borohydride reduction of **78** afforded a mixture of alcohols that were selectively oxidized to aldehyde **66** with MnO₂, although a finishing acetylation was needed to recover some C3 alcohol formed during ester reduction.

Lithium perchlorate mediated reaction of methallyl stannane with aldehyde **66** afforded a 1.3:1 mixture of allylic alcohols **79/80** (Scheme 23). In addition to providing additional supplies of alcohol **80** via Mitsunobu inversion, unnatural diastereomer **79** also served as progenitor of the South hemisphere of cephalostatin **7** via deoxygenation. Dihydroxylation of terminal olefin **80** gave a workable excess of C25S diastereomer, but again required the stoichiometric use of osmium tetroxide in conjunction with the (*S,S*) Corey ligand.

With the inseparable 4:1 mixture of diols **81** in hand, spiroketal ring formation was next surveyed. Once again,

direct reaction of the 4:1 diol mixture with a variety of acids was not successful. However, NBS-mediated spirocyclization afforded the C20 brominated 5/5 spiroketal **82** along with diastereomer **83** resulting from cyclization of the minor diol. After protecting the C26 hydroxyl moiety with a TBS group, the C3 acetate was cleaved and then subjected to chromic acid oxidation and bidesilylation with H₂SiF₆ to provide C17,26-diol **84**. The breakthrough to achieve the correct C20 stereochemistry involved conducting the reductive cleavage on the C17 alcohol **84**. Inspired by the classic chromium[II]-mediated halohydrin reductions described by Barton,⁴⁸ bromide **84** was treated with excess CrCl₂ in the presence of *n*-propylmercaptan to selectively deliver reductive cleavage product **86**. Completion of the synthesis of the targeted α -azidoketone **67** involved treatment of ketone **86** with phenyltrimethylammonium perbromide (PTAB) to give α -bromoketone, which reacted with tetramethylguanidinium azide (TMGA) to generate North 1 α -azidoketone **67** (Scheme 23). C25-*epi* North 1 α -azidoketone **85** was also prepared from **83** via a parallel reaction sequence.

Scheme 23. Synthesis of the North Hemisphere of Cephalostatin 1**4.2.2. South Unit of Cephalostatin 7**

Synthesis of the South hemisphere of cephalostatin 7 exploited the common intermediate **79**.⁴⁹ Deoxygenation was accomplished via the intermediacy of xanthate, via triphenyltin hydride to exclusively provide **87**. While osmylation of (*R*)-configured C23 TBDPS ether **80** resulted in good stereocontrol at C25, C23-unsubstituted substrate **87** suffered poor stereoselectivity (Scheme 24).

After a three-step MTM protection of the C25 tertiary alcohol to avoid 5/5 spiroketal formation, alcohol **88** was subjected to CSA catalyzed cyclization to give three 5/6 spiroketals as an inseparable mixture. Preparation of South 7 α -azidoketone **68** involved pyridine–CrO₃ oxidation of C3 alcohol **89**, followed by standard treatment of ketone **90** with PTAB and TMGN₃.⁴⁷

4.3. Cephalostatin 1 and C14',15'-Dihydrocephalostatin 1

After communicating the synthesis of C14',15'-dihydro derivative of the South hexacyclic steroid unit of cephalostatin 1 in 1995,¹⁴ the Purdue group fully described the synthesis of South 1 (**91**), as well as the first total syntheses of cephalostatin 1 and dihydrocephalostatin 1 (**92**).³⁸ Key

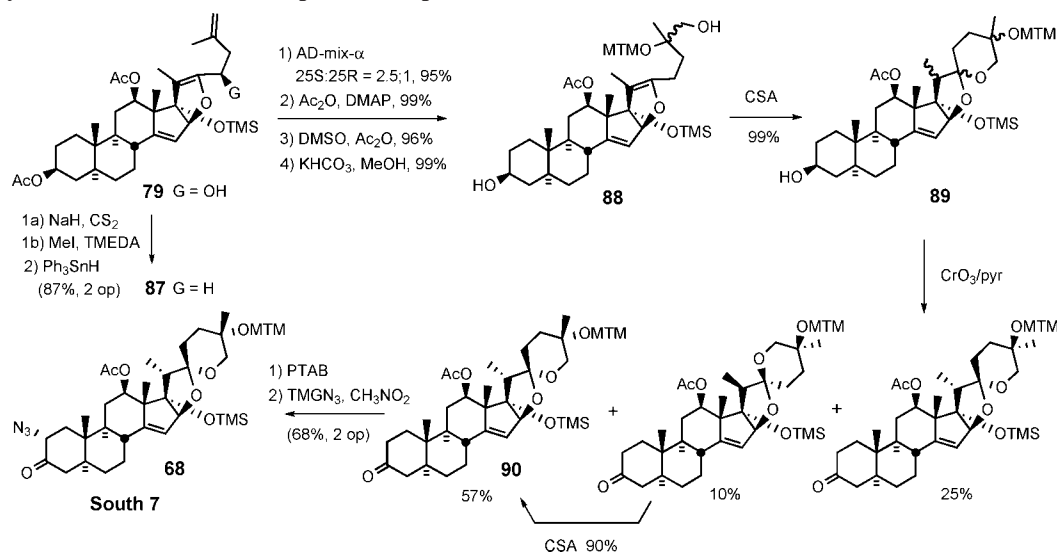
transformations included (i) introduction of Δ^{14} olefin via the Welzel/Prins procedure, (ii) methallylation, (iii) chemoselective Rh[II]-catalyzed intermolecular oxygen alkylation of a primary neopentyl alcohol, (iv) intramolecular Wadsworth–Emmons reaction, and (v) proximal functionalization of the C-18 methyl group via hypiodite-mediated alkoxy radical cyclization (Scheme 25).

4.3.1. South Unit of Cephalostatin 1

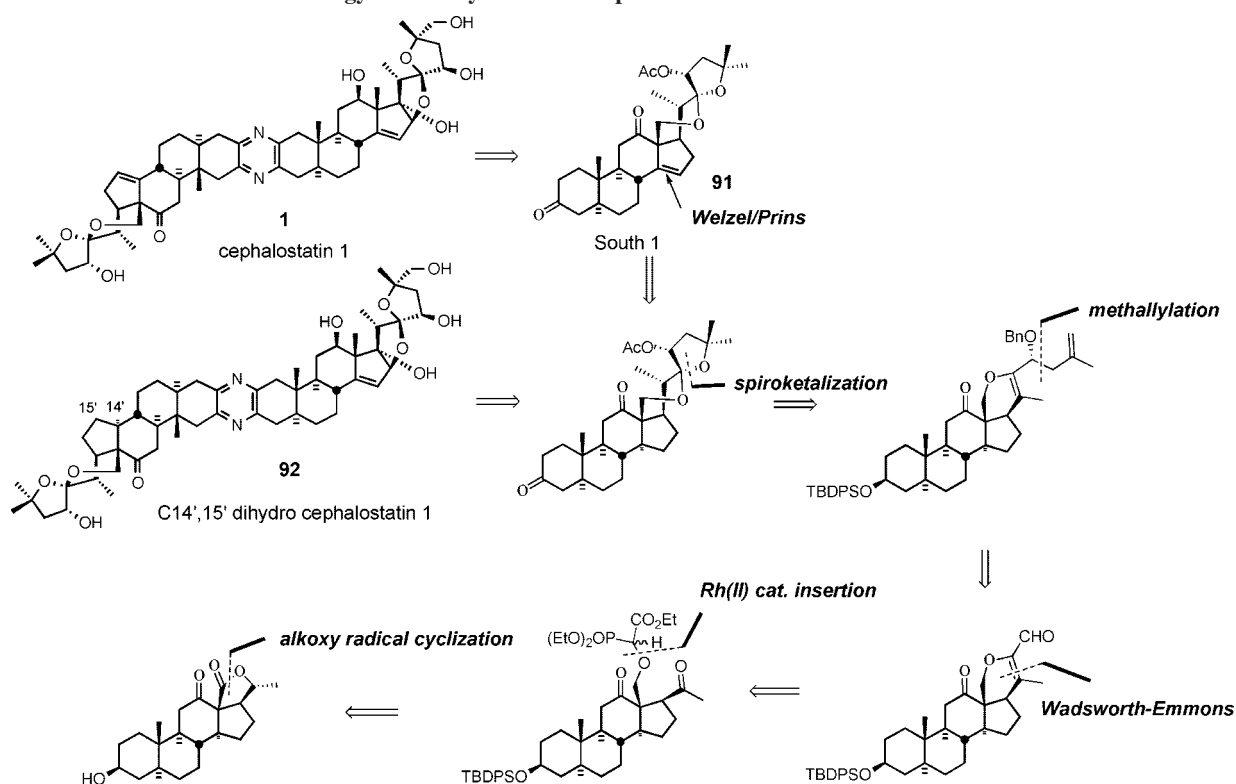
The South 1 synthesis started with conversion of hecogenin acetate **32** into enone **64** via a modified Dauben protocol (Scheme 26).⁵⁰ After ketalization of the C12 carbonyl, enone **64** was stereospecifically reduced to the allylic alcohol, which was then hydrogenated with platinum oxide to give, after ketal deprotection, the saturated alcohol **93**. Proximal functionalization of the C18 methyl group of **93** was accomplished via the hypiodite method of Meystre,⁵¹ which provided lactone **94** after chromic acid oxidation. Sequential hydrolysis of the C3 acetate group, silylation of the hydroxyl group, and LiAlH₄ reduction of the lactone moiety delivered triol **95**.

The key Bhandaru^{14a} transformation employed the unprecedented chemoselective insertion of a diazophosphonate

Scheme 24. Synthesis of the South Hemisphere of Cephalostatin 7



Scheme 25. LaCour/Bhandaru Strategy for the Synthesis of Cephalostatin 1

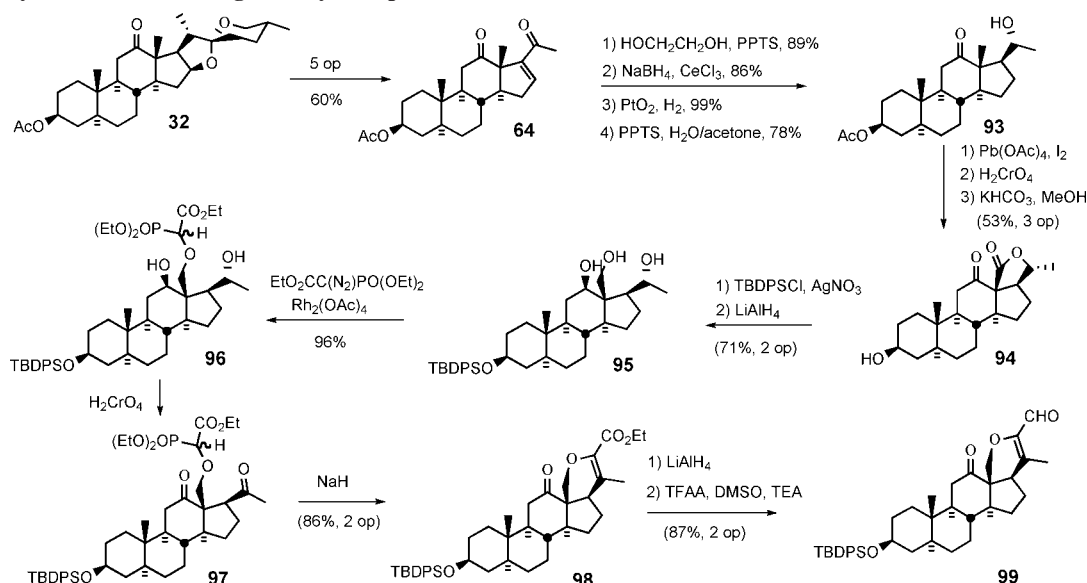


into the primary neopentyl hydroxyl group of triol **95**. Slow addition of ethyldiazophosphonate to triol **95** in the presence of catalytic $\text{Rh}_2(\text{OAc})_4$ regioselectively provided a 1:1 diastereomeric mixture of neopentyl α -alkoxyphosphonoacetates **96** in near-quantitative yield. Brown-Jones oxidation of diol **96** provided diketone **97** as another 1:1 mixture of phosphonate esters. Treatment of the diastereomeric mixture of **97** with sodium hydride effected the intramolecular Wadsworth–Emmons reaction, exclusively affording the dihydropyran ester **98**. Dihydropyran **98** was reduced by LiAlH_4 to a diol mixture, which was directly subjected to Swern oxidation, generating the key pentacyclic keto-aldehyde **99** (Scheme 26).

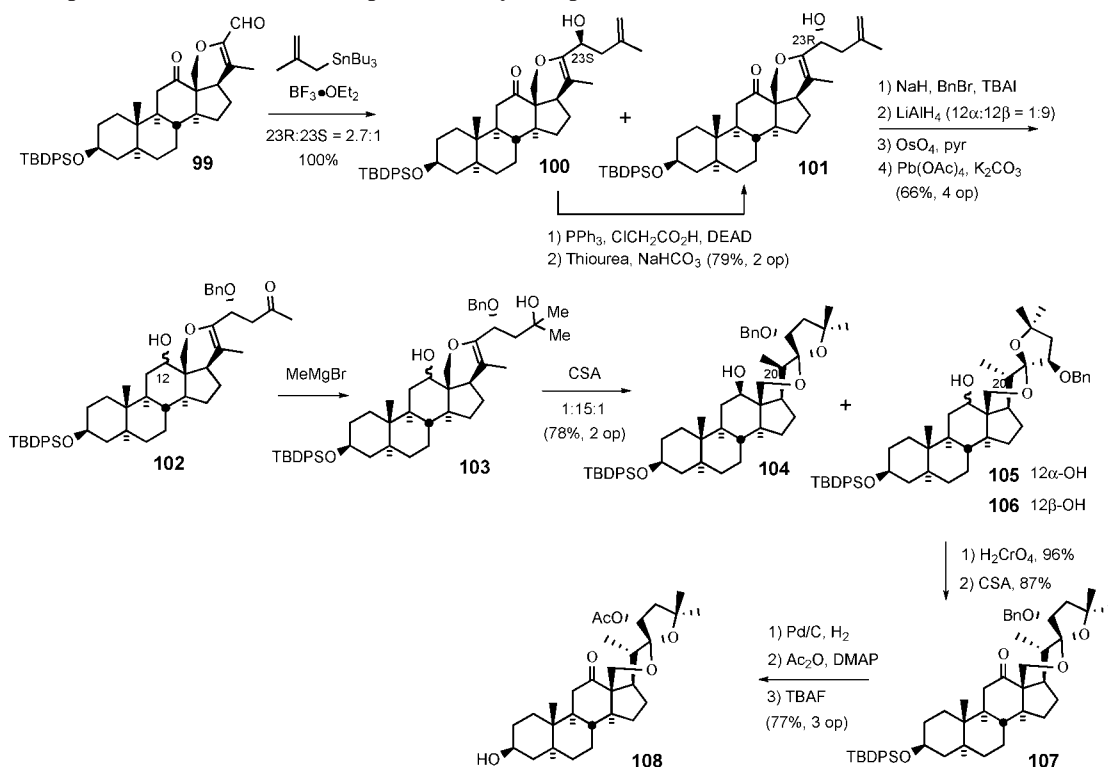
Reaction of aldehyde **99** with methallyl stannane in the presence of boron trifluoride etherate quantitatively produced a 1:2.7 mixture of homoallyl alcohols **100/101**. Mitsunobu

inversion of the undesired isomer **100** afforded additional alcohol **101**. After protecting C23 alcohol with a benzyl group, the ketone was reduced with LiAlH_4 to provide a diastereomeric mixture ($\alpha/\beta = 1:9$ at C12) of diols that were subjected to stoichiometric osmylation. Oxidative cleavage of diols with lead tetracetate gave a mixture ($\alpha/\beta = 1:9$ at C12) of keto-alcohols **102**. Addition of MeMgBr to C25 ketone **102** resulted in a mixture of diastereomeric diols **103**, which were smoothly converted to a mixture of three spiroketals **104/105/106** upon treatment with camphorsulfonic acid. Chromium oxidation followed by acid-catalyzed spiroketal isomerization established the natural C22 stereochemistry. Replacement of the C23 benzyl protecting group with acetate and subsequent removal of TBDPS group with TBAF provided the South hemisphere of dihydrocephalostatin 1 (**108**) (Scheme 27).

Scheme 26. Synthesis of the E-ring of Dihydrocephalostatin 1.



Scheme 27. Completion of the South 1 Hemisphere of Dihydrocephalostatin 1



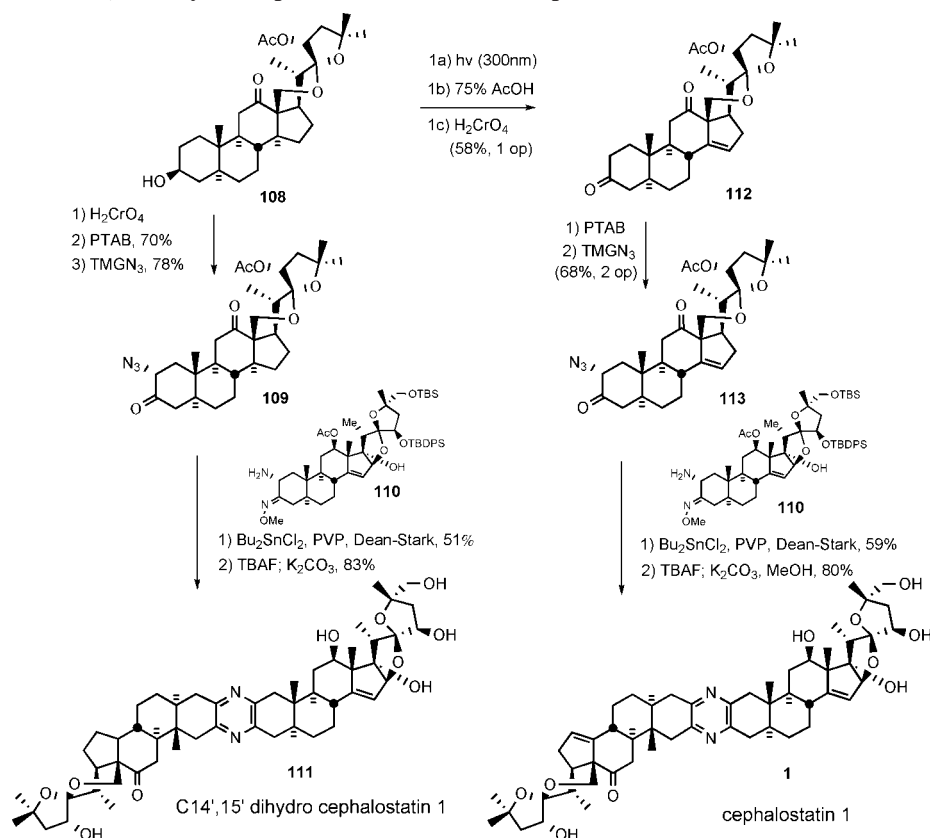
4.3.2. Cephalostatin 1 and C14',15'-Dihydrocephalostatin 1

In 1996, Guo and Bhandaru³⁷ reported the dihydrocephalostatin 1 (**1**) synthesis using the Guo unsymmetrical pyrazine coupling protocol (Scheme 28). Alcohol **108** was oxidized to the C3 ketone followed by α -bromination with PTAB and azide substitution to afford α -azido ketone **109**. Heating an equimolar mixture of azido ketone **109** and aminomethoxime **110** in the presence of PVP and dibutyltin dichloride with azeotropic distillation provided protected dihydrocephalostatin 1, which was then globally deprotected with TBAF and methanolic K_2CO_3 to unveil dihydrocephalostatin 1 (**111**).

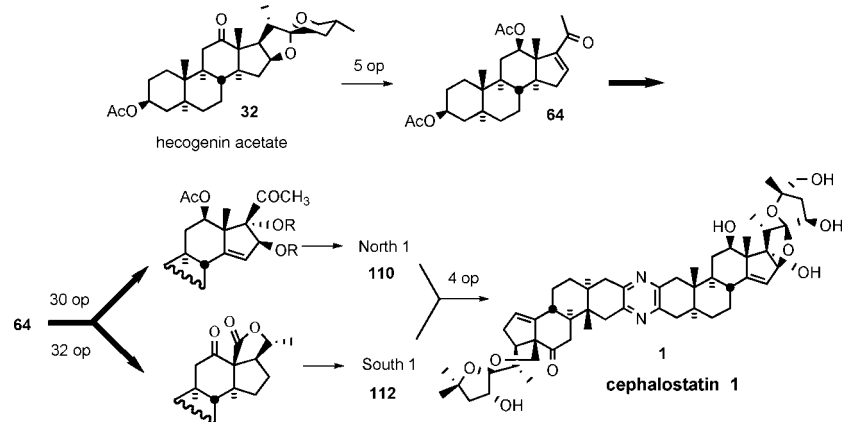
The final stage of 1999 cephalostatin 1 synthesis³⁸ involved a crucial three-step Welzel-Prins sequence to introduce the

Δ^{14} olefin moiety present in the South 1 (Scheme 28). Unlike photolysis of hecogenin acetate, the effects of the altered ring strain and steric repulsions on its reactivity during the photolytic opening and acid-catalyzed recyclization steps were nonobvious. Fortunately, photocleavage of ring-strained ketone **108** at 300 nm smoothly provided the desired aldehyde, which was then subjected to Prins reaction, cleanly affording the homoallylic alcohol. Subsequent chromic acid oxidation furnished C3,12-diketone **112**. Elaboration of ketone **112** to ketone **113** proceeded by the now standard bromination and azide substitution to give azido ketone **113**, which was coupled with North 1⁴³ (**110**) to give, after deprotection, the first sample of synthetic cephalostatin 1 (**1**) (Scheme 28).

Scheme 28. Synthesis of C14',15'-Dihydro Cephalostatin 1 (111) and Cephalostatin 1 (1)



Scheme 29. First-Generation “Cut and Paste” Synthesis of Cephalostatin 1 (1)



5. Second-Generation Synthesis

The initial synthetic strategy provided a cumulative total of ~50–300 mg of the key North 1, South 7, and South 1 steroid subunits, which permitted exploration of the anti-cancer structure–activity relationship and completion of a handful of total syntheses. Nevertheless, the first-generation approach suffered from the material-supply problems associated with any synthesis of ~35 linear steps per subunit (Scheme 29).

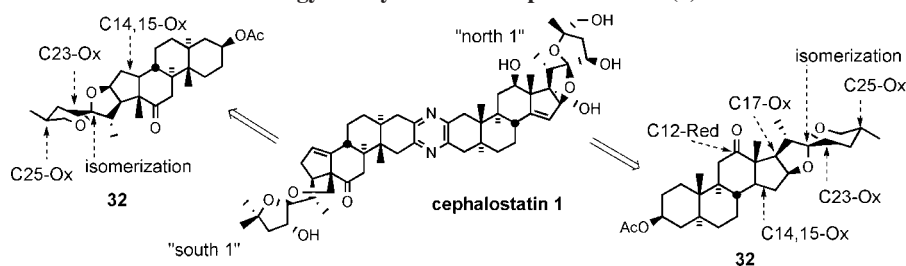
The classical synthesis was unattractive at the strategic level, requiring excision of the entire F-ring and subsequent reintroduction of the same atoms (“cut and paste approach”). Clearly, a new synthetic strategy was required to complete the definition of the minimum pharmacophore and provide compounds for clinical trials. The second-generation strategy envisaged a highly aggressive plan targeting preparation of both North and South hemispheres of cephalostatin 1 from

hecogenin acetate 32 without adding or deleting any carbon atoms. The new approach exploited oxidations, reductions, and spiroketal isomerizations (“Red-Ox” strategy) rather than the degradation/addition sequence used previously (Scheme 30).

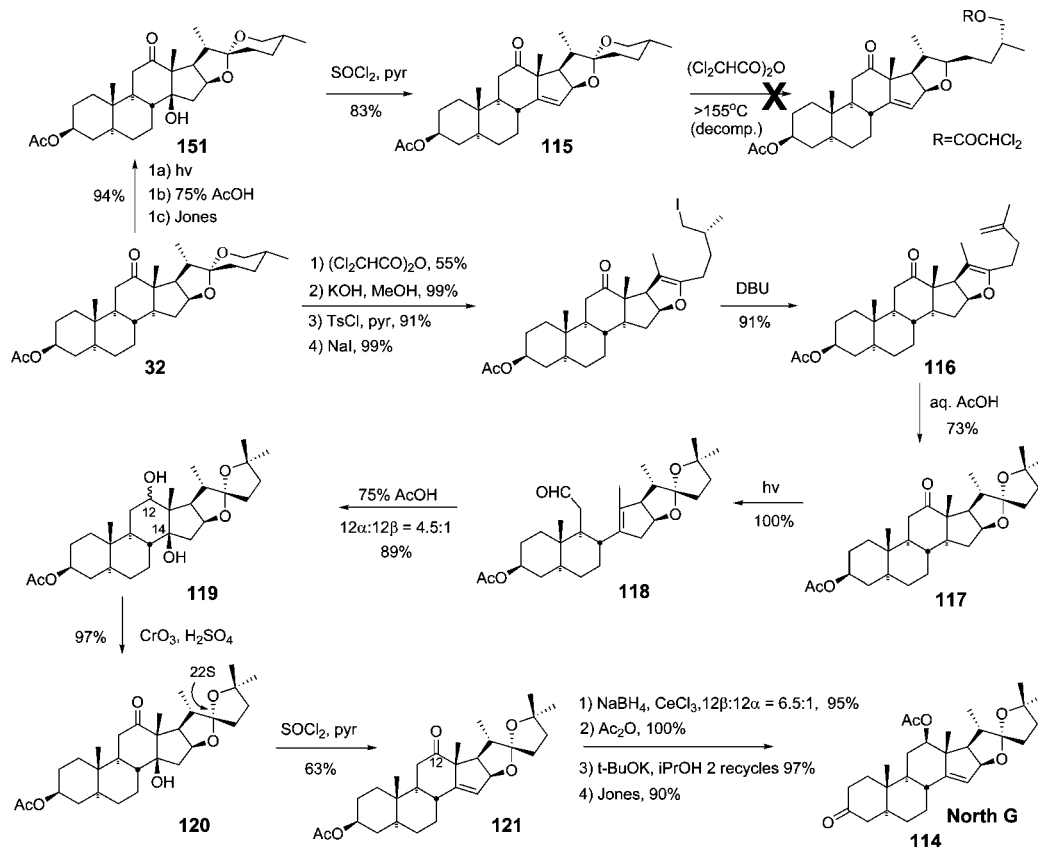
5.1. Ritterazine North Hemispheres B, F, G, and H

A 1998 full paper by LaCour et al. detailed the synthesis of the North G hemisphere 114 (Scheme 31).³⁸ Introducing the D-ring olefin at the first stage of this approach was successful, but the olefin moiety of 115 was unstable to spiroketal opening. Success was attained by constructing the 5/5 spiroketal ring prior to olefin introduction. Hecogenin acetate 32 was opened to the dichloroacetate, which was subjected to sequential deacylation, tosylation, iodination, and DBU-mediated elimination to provide enolether–olefin

Scheme 30. Second-Generation “Red-Ox” Strategy for Synthesis of Cephalostatin 1 (1).



Scheme 31. LaCour North G Synthesis



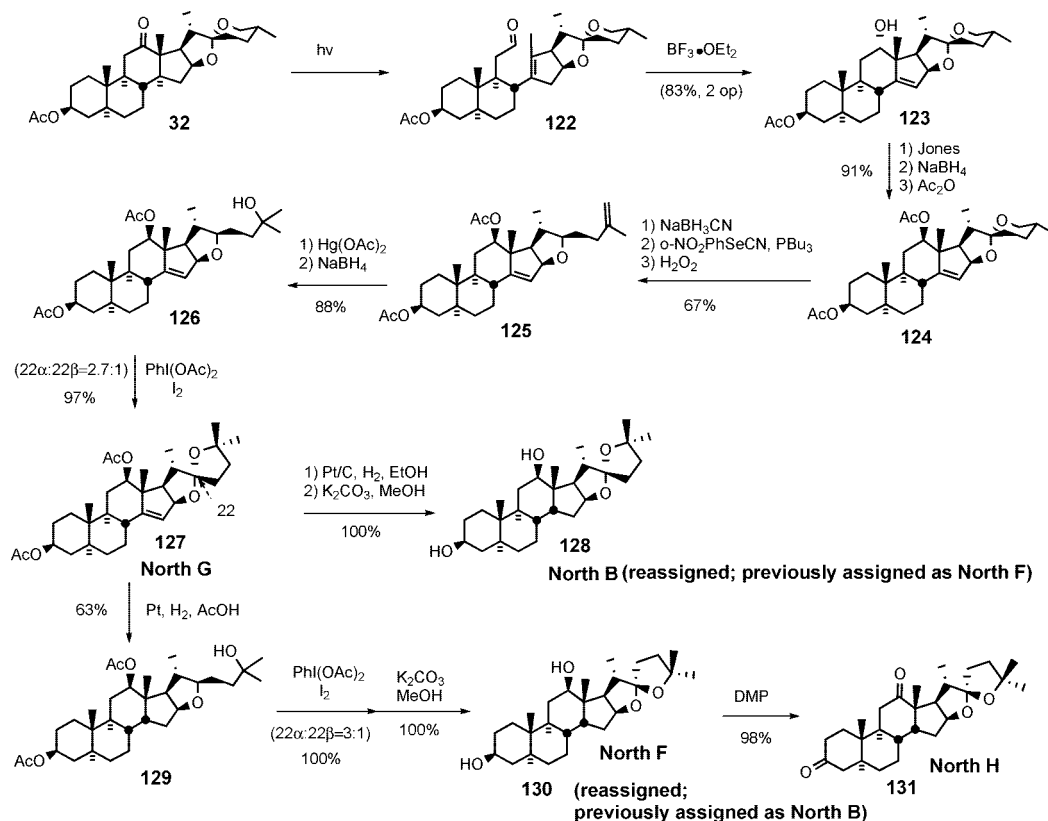
116. Treatment of **116** with hot aqueous acetic acid delivered 5/5 steroidal spiroketal **117** with desired C22S stereochemistry. Spiroketal **117** was photolyzed to secoaldehyde **118**, which afforded diol **119** by the Prins reaction. Jones oxidation followed by dehydration of **120** with thionyl chloride generated keto olefin **121**. Luche reduction of ketone **121** provided C12 alcohol ($12\beta:12\alpha = 6.5:1$), which was further transformed into North G (**114**) through straightforward functional group manipulations. The North G synthesis was accomplished in 15% yield over 13 operations, substantially better than the syntheses of the highly oxygenated South 7, North 1, and South 1 hemispheres (30–35 operations, ~1%).

In 2007, Phillips and Shair reported⁵² concise synthetic routes to the North hemisphere of ritterazines B, F, G, and H, and these syntheses lead to corrections of previously assigned structures of North B and F (Scheme 32). The Shair group's North G synthesis features an early-stage photolysis of the C12–C13 bond and a late-stage spiroketalization by Suárez oxidation. The synthesis began with Winterfeldt's Norrish type I photolysis of hecogenin acetate **32** to form aldehyde **122**, which was treated with $\text{BF}_3 \cdot \text{OEt}_2$ to stereoselectively give homoallylic alcohol **123**. After inversion of

the stereochemistry of the C12 alcohol, the 5/6 spiroketal ring was reductively opened and the resulting primary alcohol was converted to a terminal olefin **125** via Grieco's selenylation/oxidation protocol. Oxymercuration–demercuration of the olefin provided tertiary alcohol **126**, which was then subjected to Suárez alkoxy radical cyclization to give North G (**127**). The North G synthesis was, remarkably, accomplished in 31% overall yield over 10 steps from hecogenin acetate **32**.

Shair further manipulated North G (**127**) to synthesize North B (**128**), North F (**130**), and North H (**131**). North B (**128**) was prepared in one step from North G (**127**) by Pt/C-catalyzed hydrogenation (11 steps from hecogenin acetate **32** and 31% overall yield). Interestingly, the hydrogenation took place preferentially from the more-hindered β -face of the Δ^{14} olefin, probably via allylic ether-directed hydrogenation. North F (**130**) was prepared in two steps via Pt/C-catalyzed hydrogenation of North G (**127**) in acetic acid followed by Suárez oxidation of tertiary alcohol **129** (12 steps from hecogenin acetate **32** and 5% overall yield). North F (**130**) was further converted into North H (**131**) via Dess–Martin periodinane oxidation. The Shair group reassigned the spiroketal stereochemistry for North B and North F by

Scheme 32. Phillips/Shair Ritterazine North B, F, G, and H Syntheses



comparing ^1H NMR chemical shifts for ritterazine B, F, G, and H with those of their synthetic counterparts.

5.2. North M and Ritterazine M

The 2002 Lee ritterazine M synthesis⁵³ depended on Suárez alkoxy radical cyclization to establish the 5/6 spiroketal moiety (Scheme 33). This synthesis enabled correction of the originally assigned stereochemistry at C12, 22, and 25 of the North hemisphere of ritterazine M via comparison of NMR chemical shift differences^{3c}

The North M synthesis began with sequential photocleavage of hecogenin acetate **32**, was followed by Lewis acid-catalyzed ene reaction of aldehyde **122**, and was concluded by benzoylation of the homoallylic alcohol. Treatment of 5/6 spiroketal **132** with triethylsilane– $\text{BF}_3 \cdot \text{OEt}_2$ stereospecifically provided primary alcohol **133**. Conversion of alcohol **133** to the primary iodide, followed by elimination with DBU, afforded terminal olefin **134**. Catalytic double stereoselective dihydroxylation of the olefin provided a 5.9:1 mixture of inseparable diols **135**. Sequential monosilylation of the primary alcohol, benzoylation of the tertiary alcohol with benzoic anhydride and magnesium bromide/triethylamine, followed by removal of TBS protecting group with $\text{BF}_3 \cdot \text{OEt}_2$ provided tertiary monoprotected diol **136**. Suárez $\text{PhI}(\text{OAc})_2/\text{I}_2$ -mediated alkoxy radical cyclization of alcohol **136** provided spiroketals **137**, which were hydrolyzed and then oxidized to the C-3 ketone **138**. Lee et al. prepared four other North M spiroketal isomers via similar synthetic routes (not shown) and, based upon NMR difference correlation with the values published by Fusetani, demonstrated that North M possesses C12 α –OH, C22 α –spiroketal, and C25–axial OH instead of C12 β –OH, C22 β –spiroketal, and C25–equatorial OH (**141** vs **142**). Thus, from hecogenin acetate **32**, aminomethoxime North M (**139**) was prepared

in 15% overall yield over 16 steps. The structural assignment was confirmed by providing the first total synthesis of ritterazine M (**141**) using the standard sequence (Scheme 33).

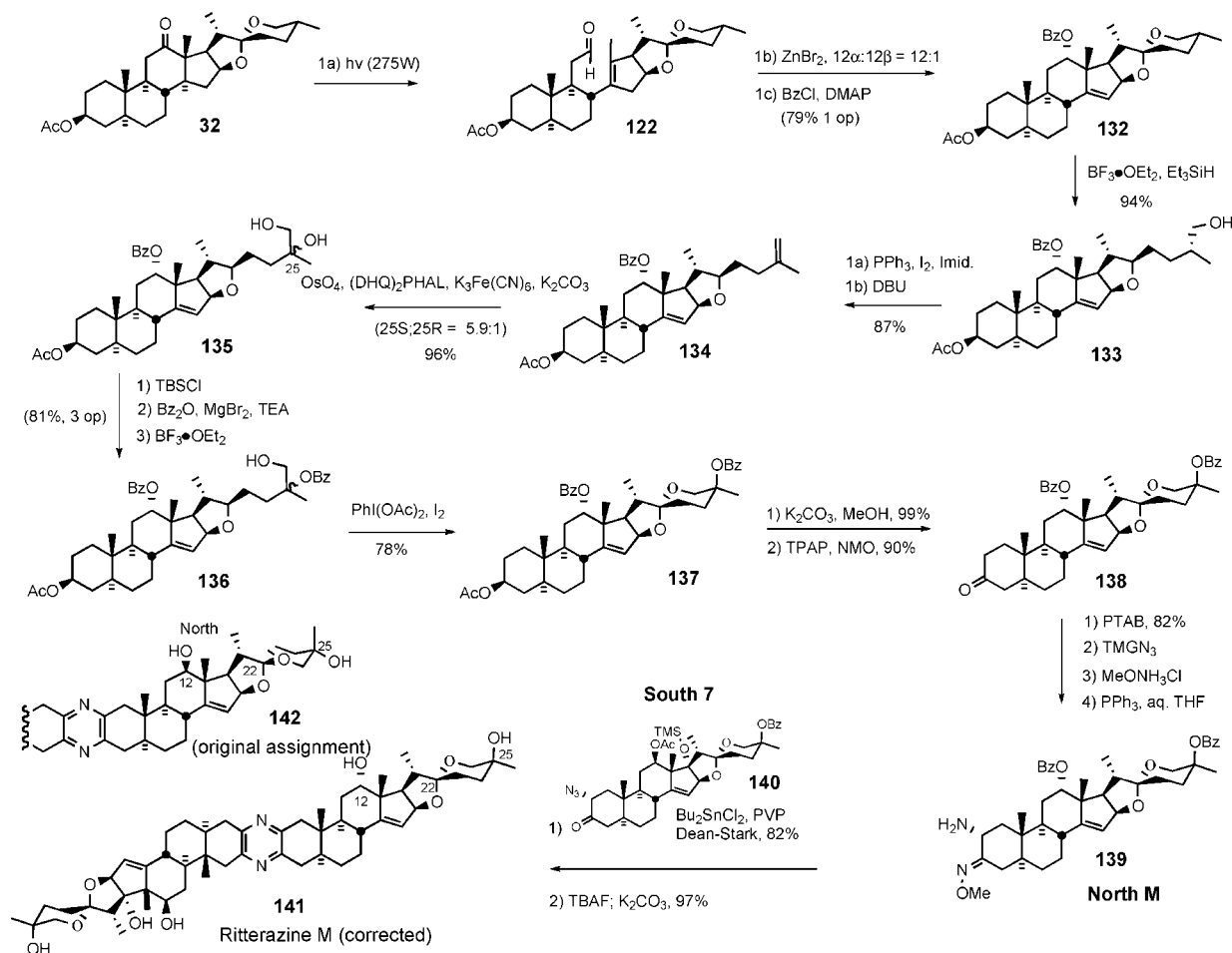
5.3. North 1 Analogues

Contemporaneously with the Lee ritterazine M synthesis, the Suárez group reported a North 1 analogue synthesis featuring their hypiodite-mediated alkoxy radical cyclization (Scheme 34).⁵⁴ The synthesis commenced with regioselective C23 oxidation of 3-methoxytigogenin **143** with $\text{NaNO}_2/\text{BF}_3 \cdot \text{OEt}_2$ to give C23–oxotigogenin **144**, which was reduced to a mixture of C23 alcohols **145** with L-selectride. Regio- and stereoselective spiroketal ring-opening with $\text{Ph}_2\text{SiH}_2/\text{TiCl}_4$, protection of the resultant primary alcohol with pivaloyl group and of the secondary alcohol with TBS group, and subsequent removal of pivalate with KOH afforded alcohol **146**. Terminal olefin **147** was obtained via nitrophenylselenenylation of primary alcohol **146** followed by H_2O_2 -mediated *syn*-elimination. Sequential osmylation and acetylation provided tertiary alcohol **148**, which was then transformed into a mixture of 5/5 spiroketal **149/150** via the Suárez alkoxy radical cyclization. These analogues are devoid of both the C-12 oxygen functionality and the D-ring olefin present in the natural products.

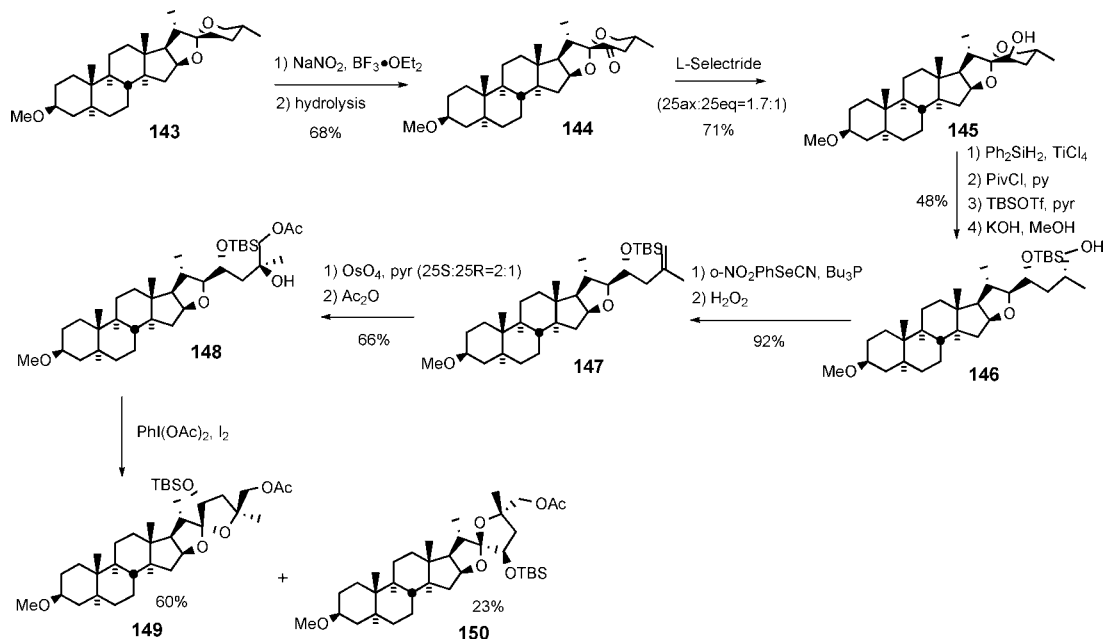
Shortly after the Suárez report, Lee disclosed⁵⁵ a more highly functionalized North 1 analogue synthesis exploiting the hypiodite alkoxy radical cyclization to establish the 5/5 spiroketal (Scheme 35). The key transformations featured (i) DMDO-mediated C–H oxidation at C16, (ii) dehydrative hemiacetal opening with SOCl_2/pyr , and (iii) C23R alcohol introduction via sequential stereoselective DMDO-mediated epoxidation and regioselective opening of the oxirane.

The analogue synthesis began with an improved transformation of hecogenin acetate **32** to β -hydroxyketone **151** in

Scheme 33. Lee Ritterazine M Synthesis



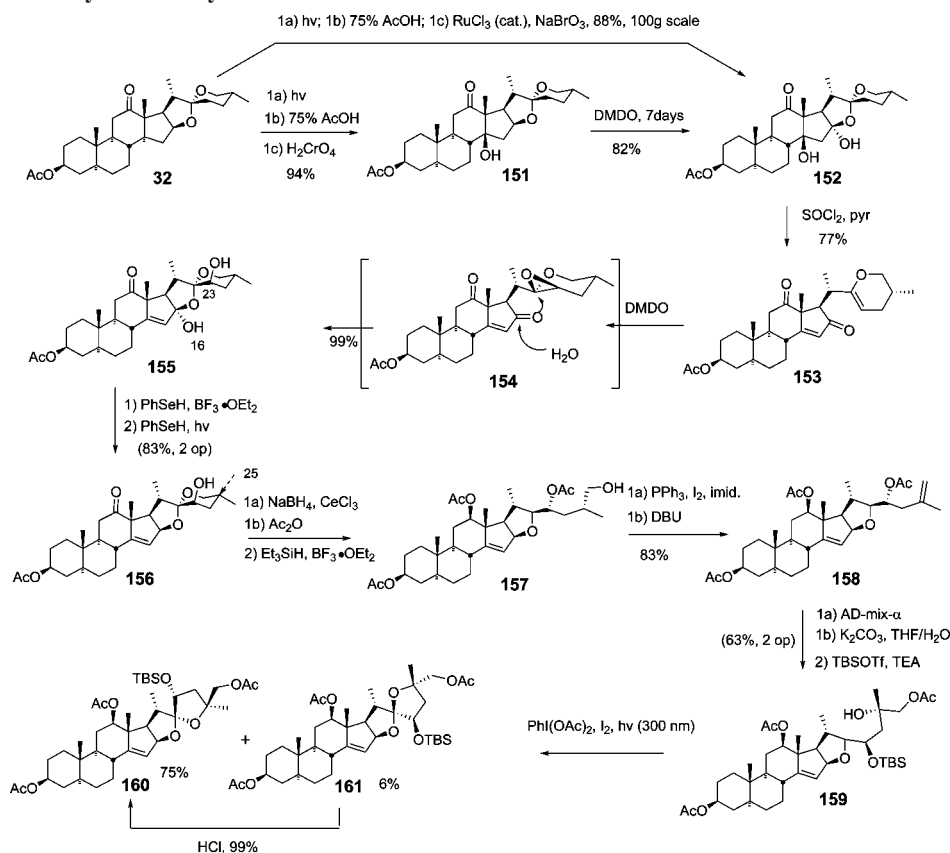
Scheme 34. Suárez North 1 Analogue Synthesis



a one-pot 94% yield (cf. 27%).³⁸ Treatment of the 5/6 spiroketal **151** with dimethyldioxirane provided diol **152** in 82% yield. More recently, the inconvenient large-scale DMDO oxidation was avoided by combining the photo/Prins sequence with a ruthenium-catalyzed oxidation that smoothly provided **152** in 88% overall yield on the 100 g scale.⁵⁶ Dehydration of tertiary alcohol **152** with thionyl chloride and

pyridine afforded vinyl ether **153**, which was then immediately subjected to DMDO oxidation to stereospecifically establish C-23 axial alcohol **155**, presumably via the intermediacy of epoxide **154**. Treatment of lactol **155** with PhSeH in the presence of boron trifluoride–etherate gave C16-phenylselenide (not shown), which was further reduced with PhSeH with irradiation to give 5/6 spiroketal **156**. After

Scheme 35. Lee C17-Deoxy North 1 Synthesis



unrewarding attempts at C23 alcohol-directed oxygenation at the C-25 position of **155** or **156**, Lee returned to the alkoxy radical cyclization strategy used earlier in the ritterazine M synthesis.⁴⁰

After C-12 reduction and acetylation, the 5/6 spiroketal of **156** was converted into terminal olefin **158** via sequential reductive spiroketal ring-opening, iodination, and DBU-mediated elimination. Sharpless asymmetric dihydroxylation of olefin **158** gave C26 acetate **159**, presumably via sequential *double intramolecular transacylation*. Treatment of alcohol **159** with PhI(OAc)₂ and I₂ induced Suárez alkoxy radical cyclization to preferentially give unnatural 5/5 spiroketal isomer (**160/161**, unnatural/natural = 12:1). Control experiments revealed that *unnatural isomer 160* was the exclusive thermodynamic product (Scheme 35).

5.4. Interphylal Hybrid Ritterostatins G_N1_N and G_N1_S

In 1998, LaCour et al. detailed synthesis of the interphylal hybrids, ritterostatins G_N1_N and G_N1_S, where the North G was used as an easily prepared surrogate for the “Southern hemisphere”, to test the hypothesis that mechanism-based biological activity resulted exclusively from the Northern spiroketal, and the primary role of the nonpolar South spiroketal was for delivery (Scheme 36).³⁸

After converting ketone **114** (Scheme 31) to azidoketone **162** by the standard procedure, coupling with the North hemisphere of cephalostatin **1** (**48**) via the Guo protocol gave the first hybrid ritterostatin G_N1_N (**163**) after global deprotection. In a parallel fashion, azidoketone **162** was transformed into aminomethoxime **164** and united with the South 1 azidoketone **165** to provide ritterostatin G_N1_S (**166**) (Scheme 36).

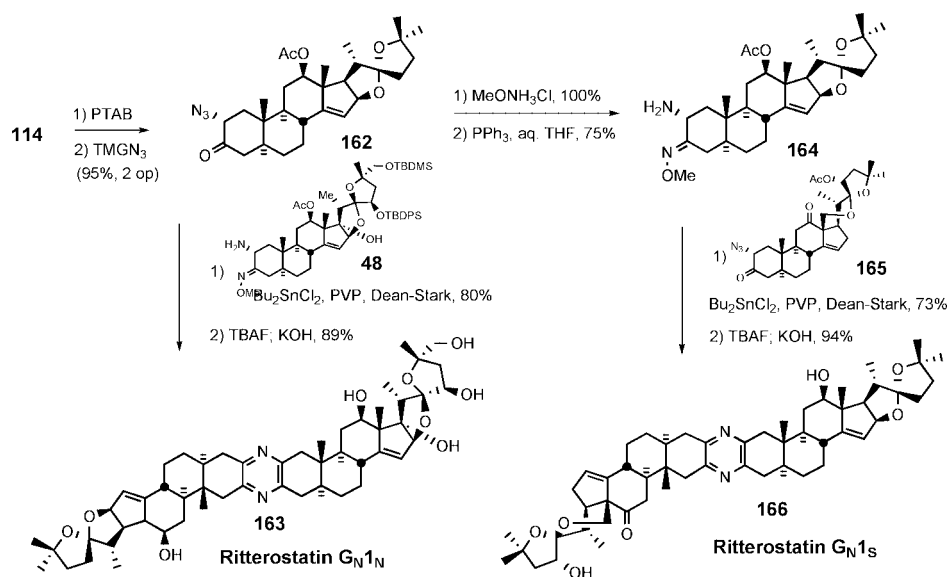
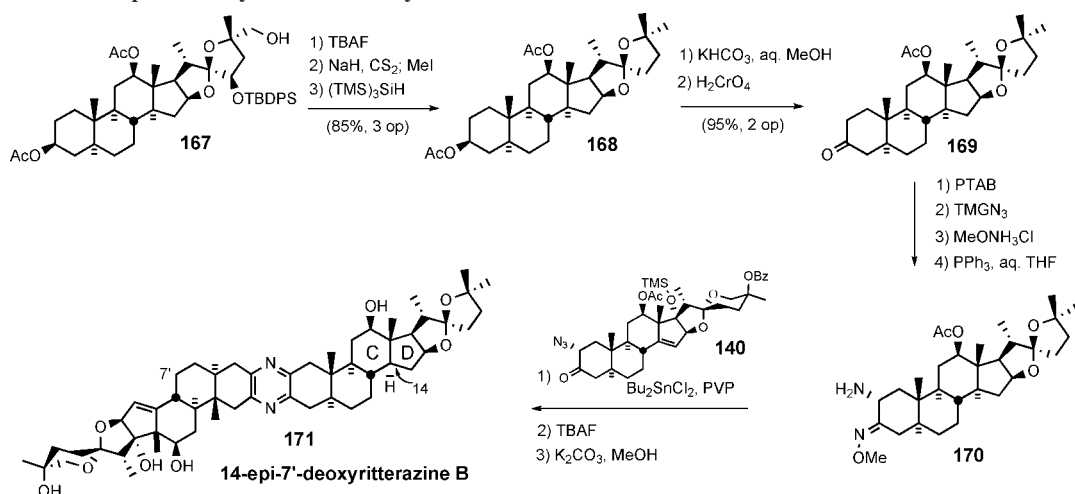
Testing of the two analogues against natural cephalostatin **1** (**1**) in the NCI in vitro human cancer cell panel revealed that ritterostatin G_N1_N displays exceptionally high potency (avg. GI₅₀ = 12.6 nM). Finding that ritterostatin G_N1_N retains most of the activity of cephalostatin **1** represents a significant advance, since preparation of **162** requires only one-third of the number of steps compared to synthesis of the “real” South 1 hemisphere **113** (Scheme 28), a net 1500% increase in yield. Ritterostatin G_N1_S, by contrast, was significantly weaker than ritterostatin G_N1_N (avg. GI₅₀ = 900 nM), presumably due to lack of a 17-OH group, a feature present in at least one hemisphere of the most active ritterazines and cephalostatins.

In 1999, LaCour et al. reported the preparation of B'/D ring-modified analogues starting from 14αH-17-deoxy-North 1 (**167**) (Scheme 37).⁴³ Desilylation and double Barton deoxygenation gave diacetate **168**. Selective hydrolysis of the 3β-acetate followed by Jones oxidation furnished 14-*epi*-North B as the 3-ketone **169**, which was converted to aminomethoxime **170** via standard procedures and then coupled with azidoketone **140** to give 14-*epi*-7'-deoxyritterazine B (**171**), after deprotection.

Ritterostatin G_N7_S, 12'β-hydroxycephalostatin **1**,^{14b} and 20- and 25'-epimers⁵⁷ of cephalostatin **7** were also synthesized via the Guo protocol from the appropriate azidoketones and aminomethoximes followed by standard deprotection (Figure 12).

6. Third-Generation Biomimetic Synthesis

The first-generation synthesis of the South 1 subunit employed the traditional Marker spiroketal degradation and a standard Pb-mediated hypoiodite proximal functionalization of the C18 angular methyl group.⁴⁹ Although this “classical”

Scheme 36. Synthesis of Ritterostats G_{N1N} and G_{N1S} Scheme 37. LaCour 14-*epi*-7'-Deoxyritterazine B Synthesis

synthesis provided ~300 mg of South 1, the strategy adopted was far from optimal. Thus, the third generation plan sought to biomimetically synthesize cephalostats while retaining all 27 carbon atoms present in the hecogenin starting material.

Fusetani proposed⁵⁸ that biosynthesis of the spiro-C/D junction, which was manifested in 13 of the 26 ritterazines, involved Wagner–Meerwein rearrangement during hydration and oxidation of a hypothetical 22-*epi*-North G (172). Li

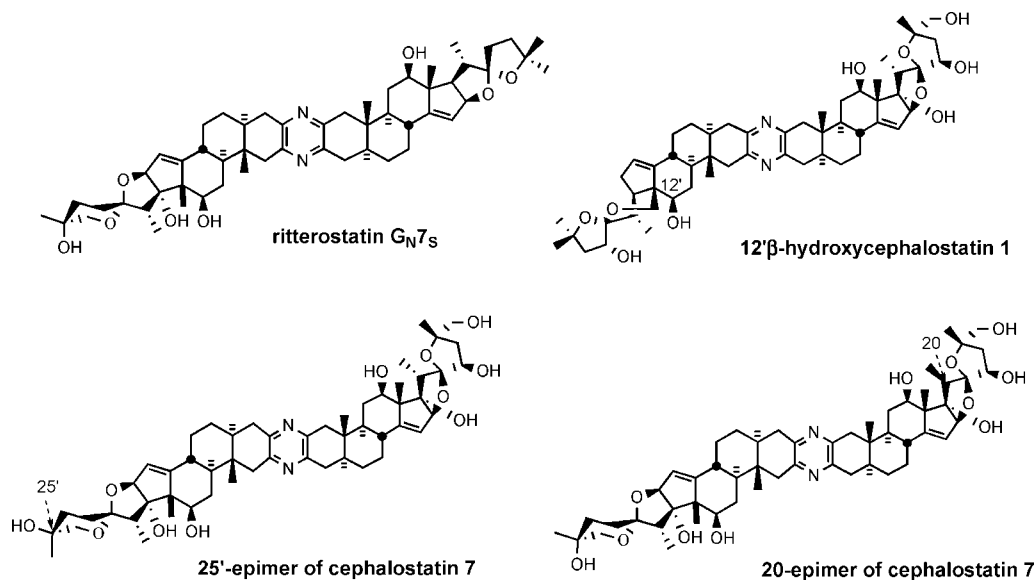
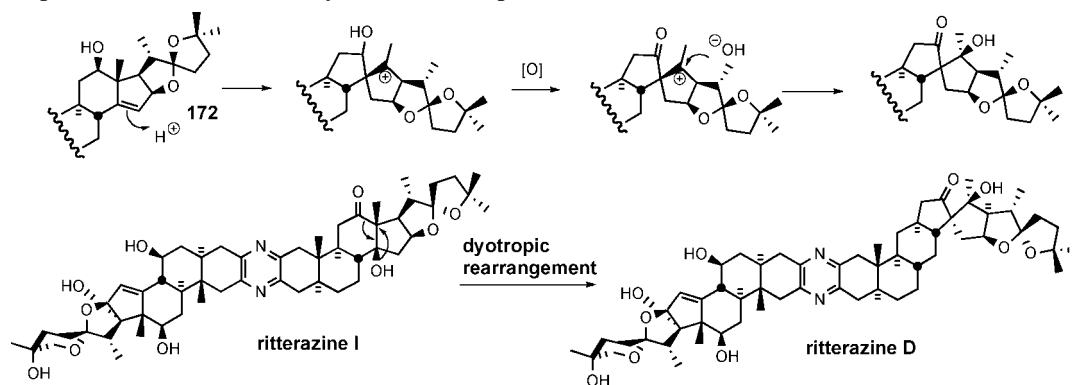
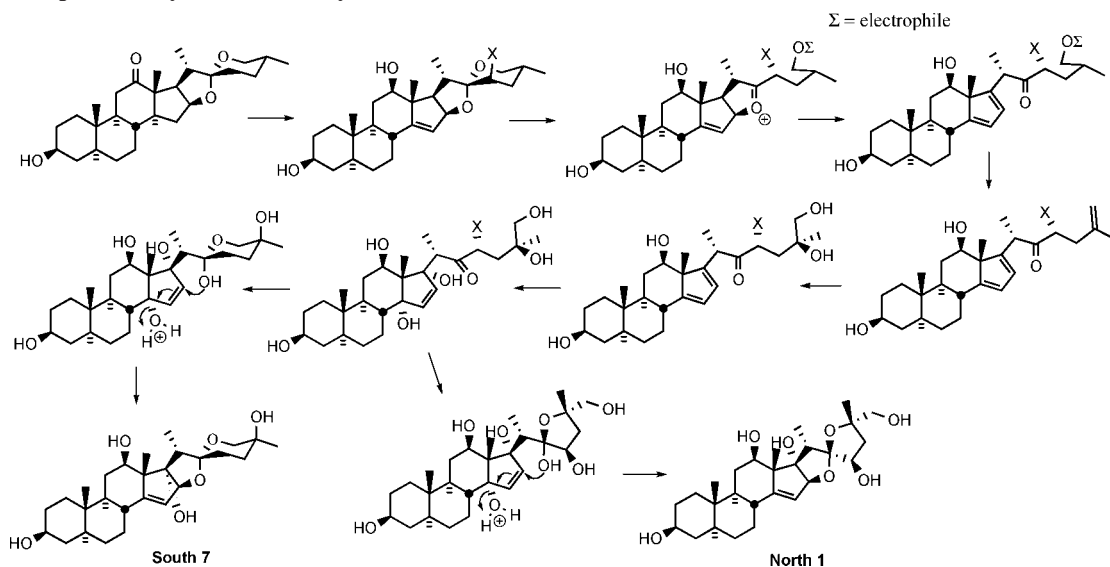


Figure 12. Ritterostatin G_{N7S} and B–D ring-altered cephalostatin analogues.

Scheme 38. Proposed Mechanisms for Biosynthesis of the Spiro-C/D Junction



Scheme 39. Proposed Biosynthetic Pathways for South 7 and North 1



later proposed that a dyotropic processes, as originally defined by Reetz⁵⁹ as the “simultaneous” intramolecular migration of two sigma-bound groups, afforded a rationale for biosynthesis of the cephalostatin family (e.g., North I to North D) (Scheme 38).

In 2005, Lee proposed⁶⁰ biosynthetic pathways for the North 1 and South 7 hemispheres of cephalostatins, which involve (i) electrophilic spiroketal ring-opening to form the diene; (ii) a [4 + 2]-cycloaddition of singlet oxygen; and (iii) an acid-catalyzed cyclization cascade (Scheme 39).

6.1. C23'-Deoxy South Unit of Cephalostatin 1

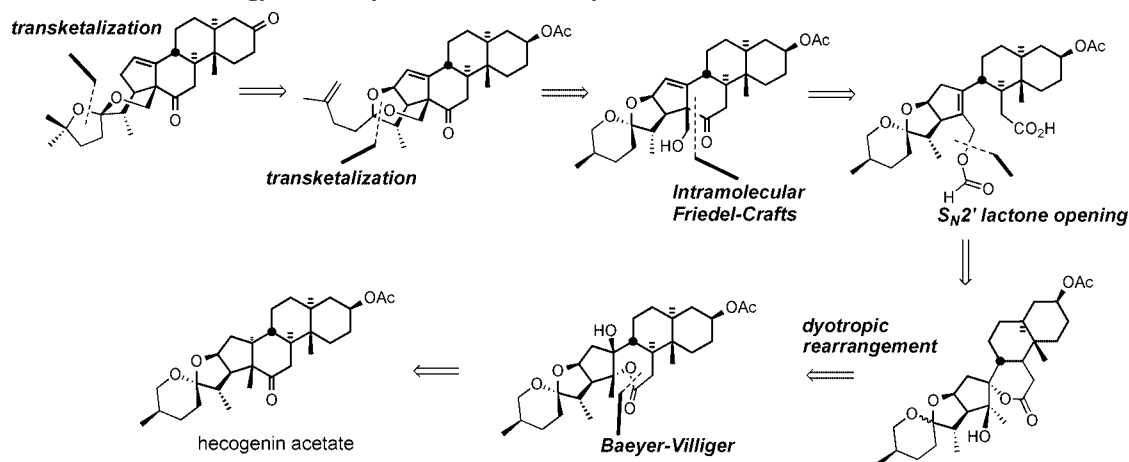
In 2002, Li et al. disclosed³⁹ a biomimetic route to the South 1 hemisphere of cephalostatin 1. The synthesis featured (i) biomimetic proximal functionalization via dyotropic rearrangement, (ii) lactone ring-opening by S_N2' , (iii) intramolecular Friedel–Crafts reaction, and (iv) transketalizations (Scheme 40).

The synthesis started with transformation of hecogenin acetate **32** to β -hydroxyketone **151** (Scheme 41).³⁹ Bayer–Villiger oxidation of ketone **151** afforded lactone **174**, which was subjected to sequential treatment with catalytic TBSOTf followed by pyridine/ SOCl_2 to deliver exomethylene spiro-lactone **177**. Interruption of the sequence after rearrangement provided an equilibrium mixture (1:2) of the hydroxyspiro-lactones **175** and **176**. Elimination of a mixture of these alcohols gave exomethylene spiro-lactone **177** as a single

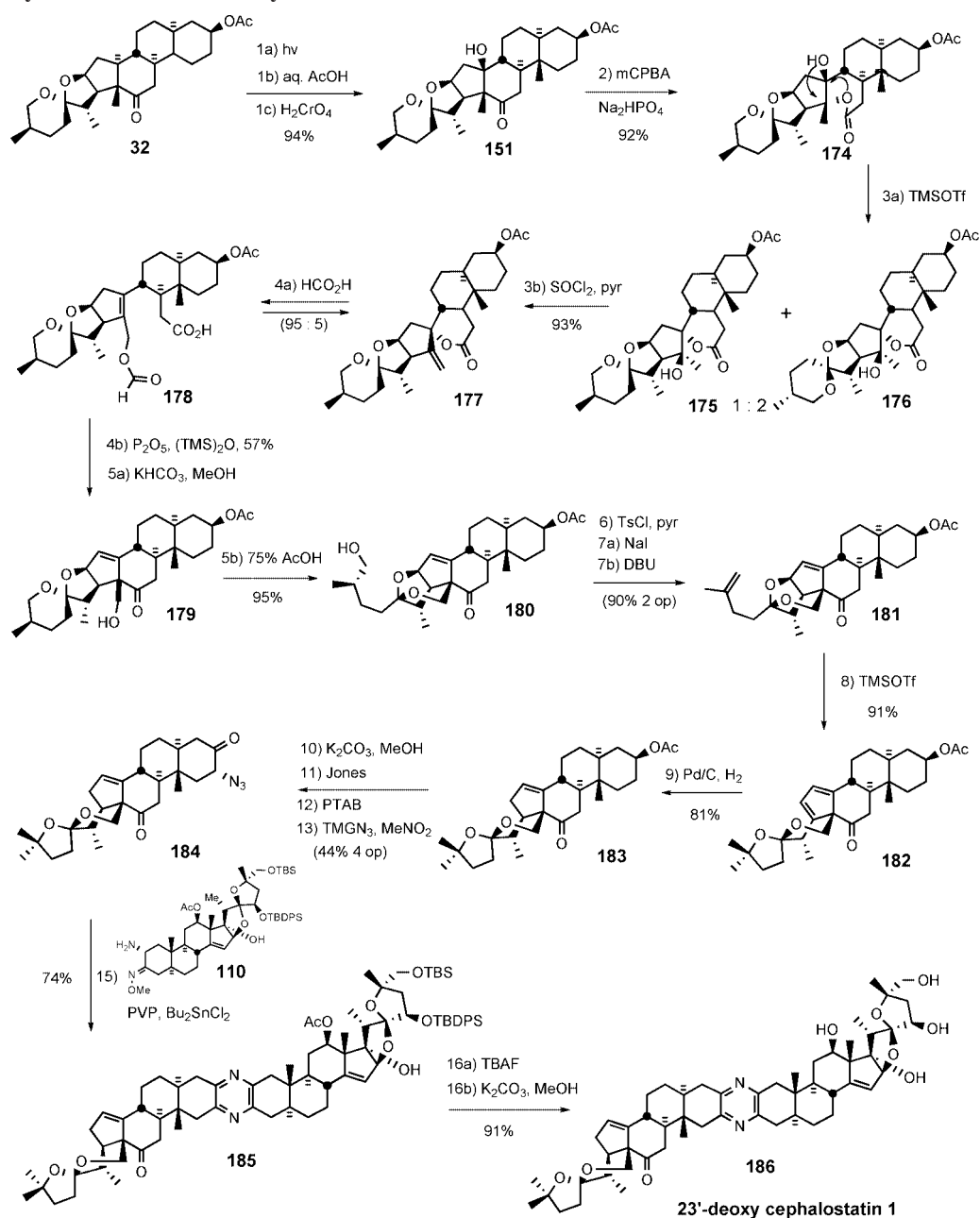
isomer. Spirolactones **175/176** arose via unprecedented stereospecific dyotropic ring contraction of the seven-membered lactones to their more stable six-ring counterparts. Smooth S_N2' opening of the spiro-lactone moiety **177** with formic acid provided an equilibrium mixture (95:5) of allylic formate **178** and starting **177**. Polyphosphoric acid trimethylsilyl ester (PPSE)-promoted intramolecular Friedel–Crafts acylation of olefin **178** was employed⁶¹ to give an intermediate hexacyclic formate, which was deprotected with catalytic bicarbonate to afford alcohol **179**. It is noted that the South unit of cephalostatin 8 has the same C18 alcohol, which could undergo transketalization to form E-ring of South 1. The action of warm 75% aqueous AcOH established an equilibrium mixture (1:2.2) of transketalization product **180** and starting material **179**.

Conversion of C26-alcohol **180** to tosylate, iodide substitution, followed by DBU-assisted elimination provided terminal olefin **181**, setting the stage for a TMSOTf-mediated rearrangement to transketalized diene **182**. Hydrogenation of diene **182** proceeded with reasonable regio- and stereo-selectivity to afford $17\alpha\text{H}$ olefin **183** with modest over-reduction. Methanolysis of C3 acetate **183** followed by Jones oxidation gave the C3-ketone. Application of the previously described two-operation method gave azidoketone **184**. Guo coupling of azidoketone **184** with the North 1 partner **110** provided masked pyrazine **185**, which was globally deprotected to give 23'-deoxy cephalostatin 1 **186**.

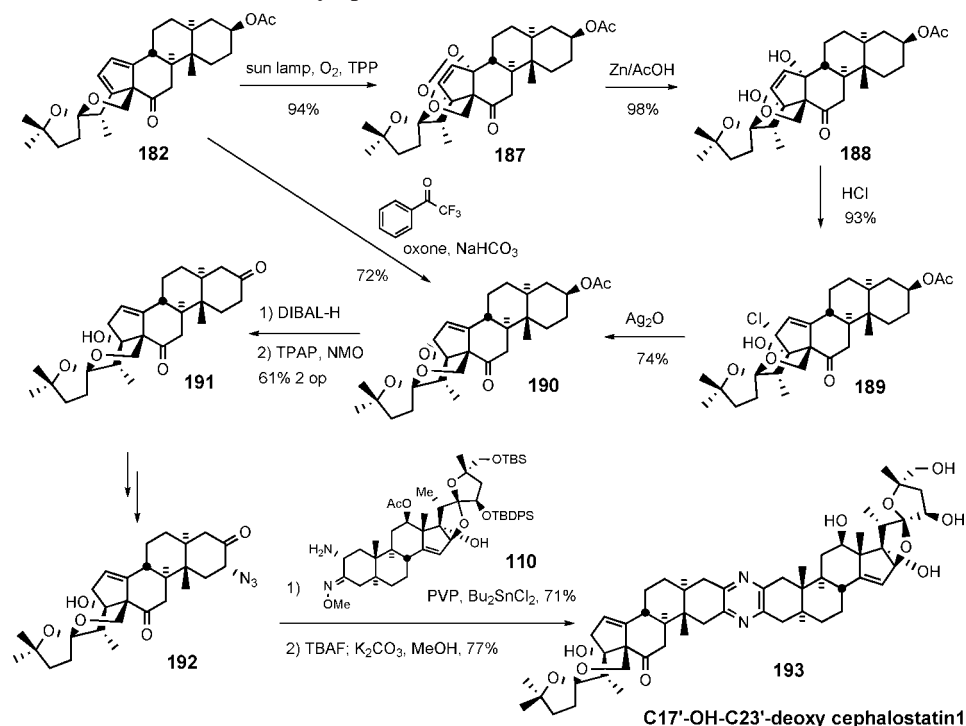
Scheme 40. Li Biomimetic Strategy for the Synthesis of C23-Deoxy South 1



Scheme 41. Li Synthesis of the C23-Deoxy South 1



Scheme 42. Li Synthesis of C17'-OH-C23'-Deoxycephalostatin 1



The new South 1 hemisphere synthesis relied on oxidative functionalization of the C18 methyl group via dyotropic rearrangement combined with spiroketal equilibration studies. The synthesis of 23'-deoxy South 1 (**183**) was accomplished in only 12 operations (23% overall yield) from hecogenin acetate and also afforded diene **182** in 11 steps (28% overall). The total synthesis of 23'-deoxy cephalostatin 1 (**186**) was completed in 16 operations from starting material **32** (9% overall; average 86% yield per operation).

Li et al. later reported⁶² the preparation of C17'-OH-C23'-deoxy cephalostatin 1 starting from diene **182** used in the above synthesis (Scheme 42). Steroidal diene **182** reacted with singlet oxygen to stereospecifically provide [4 + 2]-cycloaddition adduct **187**. Reductive cleavage of **187** by treatment with Zn/AcOH gave diol **188** in near-quantitative yield. Subjection of alcohol **188** to hydrochloric acid led to *syn*-halohydrin **189**, which was exposed to silver oxide to furnish allylic epoxide **190**. Oxirane **190** was also obtained directly by regioselective epoxidation of diene **182** with dioxiranes derived from sterically demanding trifluoroacetophenone analogues.⁶³ Regioselective reductive opening of epoxide **190** with DIBAL-H followed by TPAP oxidation afforded diketoalcohol **191**.

Compound **191** was converted to azidoketone **192** using standard procedures and then condensed with North 1 coupling partner **110** by the Guo pyrazine protocol to give the protected cephalostatin 1 analogue, which was globally deprotected to afford C17'-OH-C23'-deoxy cephalostatin 1 (**193**).

6.2. South Hemisphere of Cephalostatin 7

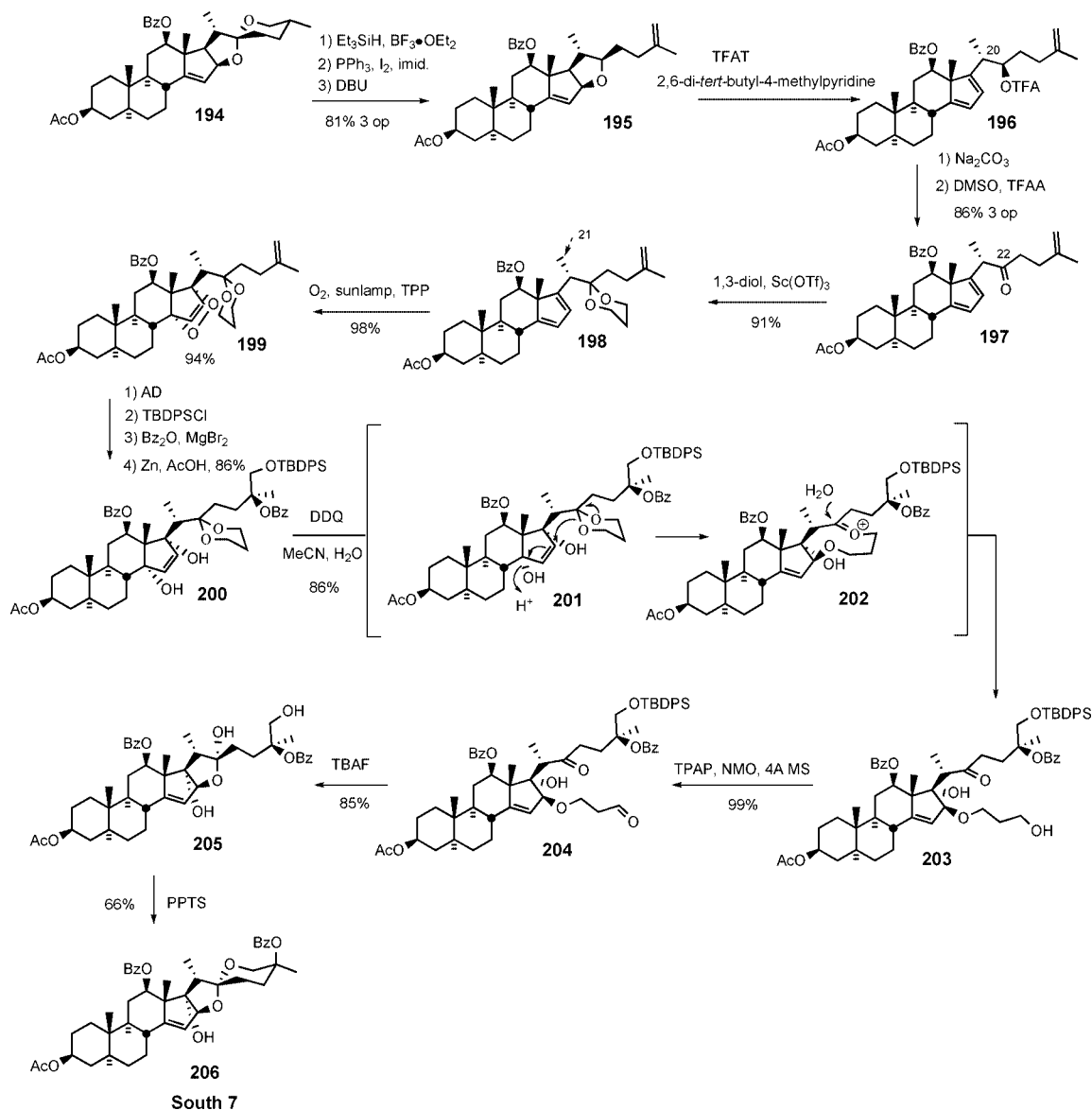
The 2005 Lee biomimetic South 7 synthesis⁶⁰ began with preparation of terminal olefin **195** from 5/6 spiroketal **194**,⁴⁰ via sequential reductive spiroketal ring-opening, iodination, and DBU-mediated elimination (Scheme 43). Treatment of tetrasubstituted tetrahydrofuran **195** with trifluoroacetyl triflate (TFAT)⁶⁴ in the presence of a hindered pyridine base

smoothly afforded dienyl trifluoroacetate **196** at $-78\text{ }^{\circ}\text{C}$, without affecting the stereochemistry at C20. Removal of the trifluoroacetyl group by mild basic hydrolysis followed by Swern oxidation produced key dienyl ketone **197** in 86% yield over three operations.

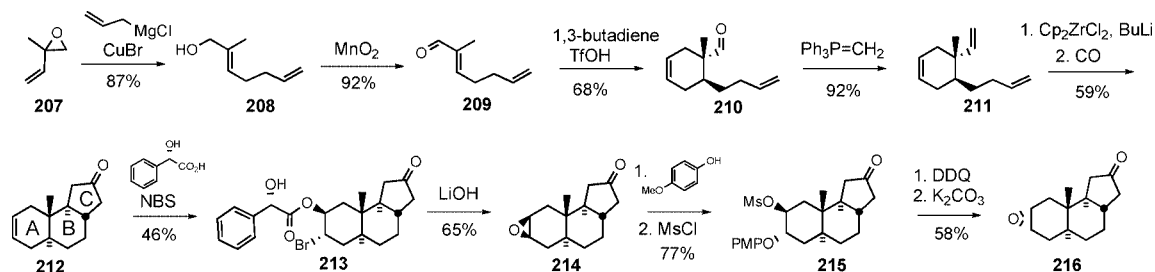
Oxyfunctionalization of D-ring diene **197** again utilized singlet oxygen to give the cycloaddition product in high yield but with no facial selectivity. This selectivity issue was resolved by employing a substrate **198** bearing a C22 propylene glycol ketal. [4 + 2]-Cycloaddition between D-ring diene **198** and singlet oxygen stereospecifically occurred at $-78\text{ }^{\circ}\text{C}$ to furnish only α -face adducts. In stark contrast, the unnatural C-21 β -methyl ketal (not shown) exclusively gave the β -face adduct. This striking reversal of singlet oxygen preference suggests that the stereochemistry of the C-21 methyl moiety determines the facial selectivity of the cycloaddition via conformational control of the side chain.^{60,65} Adduct **199** was transformed into differentially protected C-25,26-diol in three operations with a 4.3:1 ratio of C25S/C25R, in favor of the desired stereochemistry. Under the influence of Zn/AcOH, the O—O bond of **199** was reductively cleaved to ketal—diol **200**. Treatment of **200** with aqueous DDQ, via slow hydrolytic release of HCN, led to the unexpected formation of hydroxypropyl ether **203**, presumably via ketal participation of **201** followed by hydrolysis of intermediate oxonium ion **202**. TPAP oxidation of primary alcohol **203** afforded aldehyde **204**, which was treated with TBAF to give hemiacetal **205**. Acid-catalyzed spiroketalization of hemiacetal **205** provided the South 7 hemisphere **206**.

The Lee South 7 synthesis paved the way for the multigram synthesis of cephalostatin analogues. The synthesis was completed in 20% overall yield over 16 operations from commercially available hecogenin acetate **32**. Compared with the first-generation South 7 synthesis (2% overall yield,

Scheme 43. Lee Synthesis of the South 7 Hemisphere



Scheme 44. Preparation of A–B–C Carbocyclic Core of Ritterazine N (216)



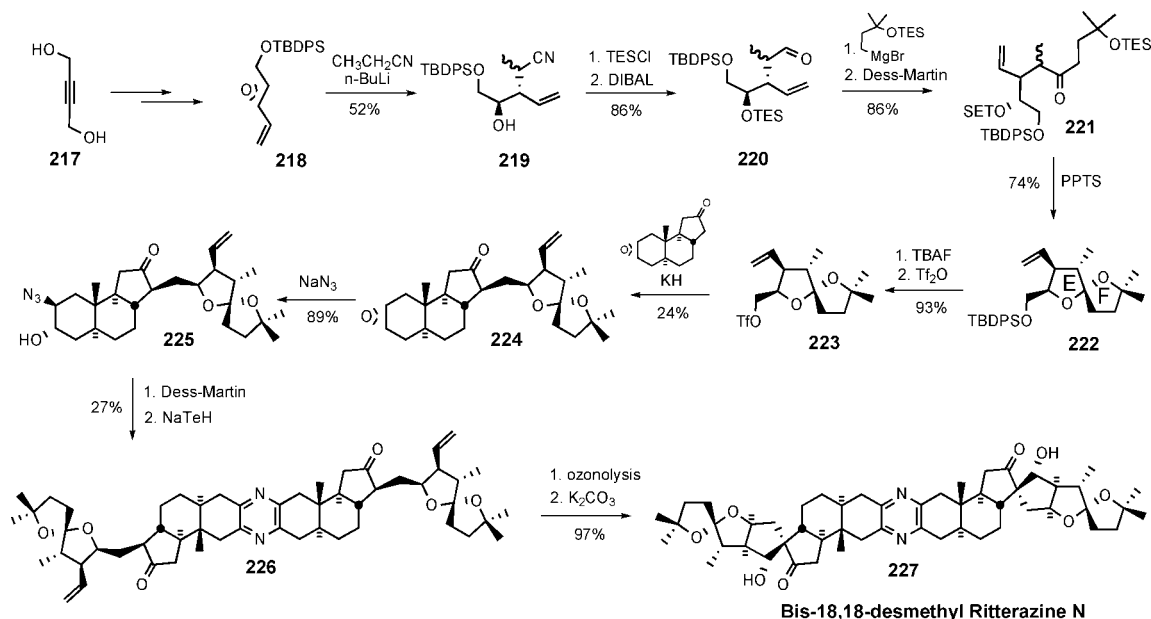
25 operations), this synthesis is vastly improved and provides a more practical route for South 7-bearing cephalostatin analogues.

7. Related Syntheses

In 2008, the Taber group reported synthesis of bis-18,18'-desmethyl ritterazine N (**227**).⁶⁶ The synthesis involved a key coupling of ABC carbocycle **216** and E–F spiroketal **223**, which were prepared from nonsteroid starting materials (see Scheme 44). The ritterazine synthesis began with opening of oxirane **207** with vinylmagnesium chloride to give

allylic alcohol **208**, which was subjected to sequential allylic oxidation and Diels–Alder cyclization to provide cyclohexene **210**. After converting aldehyde **210** to terminal olefin **211** via Wittig olefination, the triene **211** reacted with zirconocene dichloride in the presence of butyl lithium to give a zirconacycle (not shown), which was then treated with carbon monoxide to afford ABC core **212** of ritterazine N. Exposing ketone **212** to mandelic acid and *N*-bromosuccinimide led to the formation of enantiopure ketone **213** after column chromatography. Saponification of bromomandolate **213** yielded β -epoxide **214**, which was inverted by sequential

Scheme 45. Taber Synthesis of Bis-18,18'-Desmethyl Ritterazine N (227)



opening of oxirane ring **214** with *p*-methoxyphenol, mesylation, DDQ oxidation, and base-mediated intramolecular cyclization to give α -epoxide **216**.

The construction of spiroketal **222** for ritterazine N started with regioselective opening of oxirane **218** to provide the secondary alcohol **219**. After TES ether formation, the nitrile was reduced with DIBAL to furnish aldehyde **220**, which was converted to ketone **221** via Grignard addition followed by Dess-Martin oxidation. Treatment of ketone **221** with PPTS removed both TES protecting groups, and the resulting diol (not shown) underwent spiroketal formation to yield the desired E/F-spiroketal **222** as the major product. The *t*-butyldiphenylsilyloxy (TBDPSO) group in **222** was converted to triflate **223**, which was coupled with ketone **216** to furnish **224** in low yield. Diaxial opening of oxirane **224** with azide delivered C3-alcohol **225**, which was transformed into dimer **226** via sequential Dess-Martin oxidation and NaTeH-mediated pyrazine formation. Ozonolysis of alkene **226** followed by base-catalyzed aldol condensation delivered bis-18,18'-desmethyl ritterazine N (**227**). Although it suffered from low overall reaction yield (0.04%), the Taber synthesis of ritterazine N analogue represents the first successful construction of the 6/6/5/5 ring framework present in several ritterazines (see Scheme 45).

8. Structure–Activity Relationships

The 45 members of the cephalostatin/ritterazine family isolated to date, together with the growing number of analogues (>40) and related monosteroidal antineoplastics (>30), provide the basis for elucidating some structure–activity relationships (SAR) of these potent cytotoxins.

The cephalostatins and ritterazines are bissteroidal pyrazines with pseudo C_2 -symmetry (see Figure 9). The symmetry arises from the “S” fusion of two C_{27} steroids, with the 19-Me of each subunit (C19, C19') on the same face of the molecule and each C2–C3 set *para* to its mate in the pyrazine core. Because no variants on this fusion have been tested, the type of attachment required (e.g., rigid, “S”, aromatic or not) is currently unknown. The most active of these pyrazines (≤ 10 nM) are unsymmetrical, featuring a pair of significantly different steroids taken from the six

natural basic subunits (North 1, North A, North G, South 1, South 5, and South 7; see Figure 11).

Consideration of these disparate structures suggests that four features conspire to provide active in vitro materials: (i) a molecular dipole consisting of covalently linked lipophilic “nonpolar” and hydroxylated “polar” domains, with a molecular length of $\sim 30\text{\AA}$; (ii) a spiroketal or other latent precursor of an oxacarbenium ion; (iii) one or more homoallylic oxygen arrays; and (iv) a 17-OH function. The pyrazine ring, though present in most examples, is absent in several subnanomolar active monosteroids. Questions regarding the necessity, location, and molecular function for the latter two features remain, but both are present in the most potent natural and analogue examples, whereas one or more of these distinctive units are missing in structures with notably inferior in vitro activity including all “simple” cephalostatin analogues and most saponins.

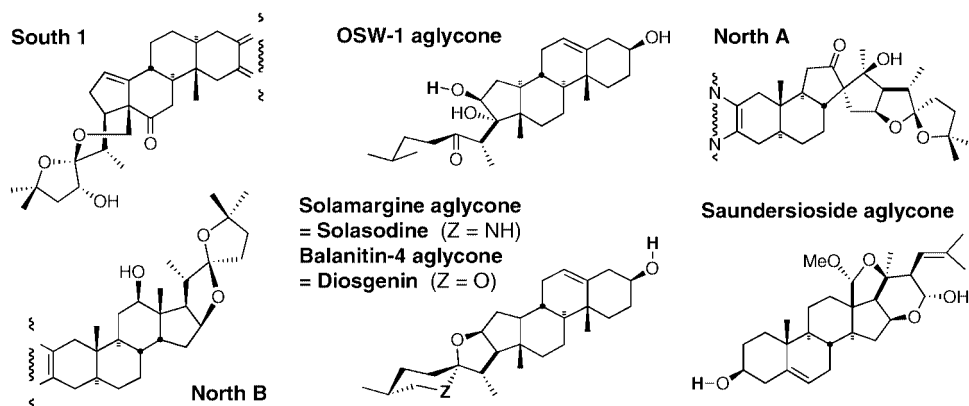
8.1. Appropriate Pairing of Polar/Nonpolar Subunits

A covalent union of a polar (hydrophilic) domain with a nonpolar or lipophilic domain appears required, although total polarity may vary widely within certain limits (Figure 13). Tests on free steroids and sugars, alone or together (North 1 and South 7 pentols, the North G diol, solasodine and/or added rhamnose or other sugars, diosgenin, dihydro-OSW-1 aglycone, etc.) show little or no cytotoxicity. Even the best monosteroids (North G aminomethoxime, OSW-1 aglycone-ethylene ketal) are several orders of magnitude less active than cephalostatin **1** (**1**).

Solasodine displays a provocative apparent exception to this trend. Although essentially inactive against human cells, it appears quite potent against DNA-repair-deficient yeast strains. The activity of this monosteroid is proposed to be related to its spiroaminal function, which can also afford a heterocarbenium ion moiety. These results add weight to the apparent importance of such pro-oxacarbenium sites in steroidal antineoplastics.

All symmetric bissteroidal pyrazines display inferior cytotoxicity (10^2 – 10^6 nM). The activity of symmetrical

Nonpolar Domains



Polar Domains

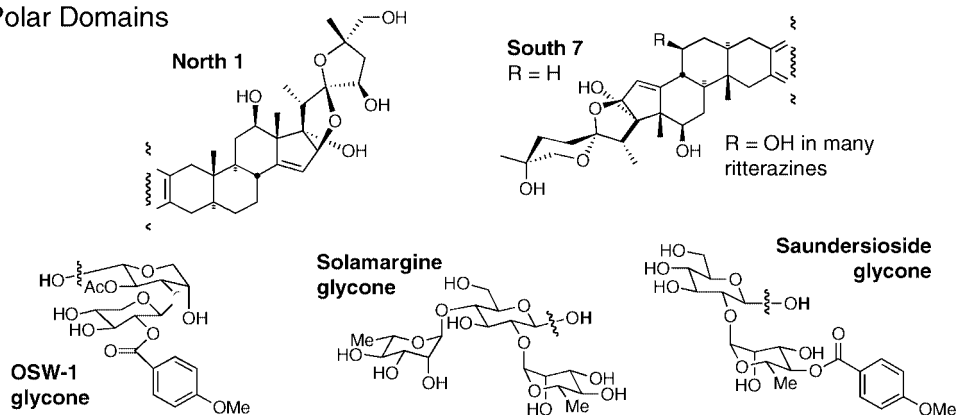


Figure 13. Polarity groupings of steroidal and glycone subunits.

(polar/polar) natural ritterazine K approaches that of unsymmetrical (polar/polar) cephalostatin 7, underscoring the need for pairing of subunits with quite disparate polarities.

Decreased activity associated with a diminished “molecular dipole” is evident with increased polarity in the lipophilic domain (ritterazines D/A and I to ritterazines F/B), or by decreased polarity in the hydrophilic domain (cf., e.g., ritterazines Y to B or T to A).

Such decreased polarity in the hydrophilic domain may account for the fact that natural South 7 makes a somewhat inferior substitute for North 1 or the 7'-OH-South 7 present in the strongest ritterazines (G_{N1N} is more active and affects many more lines (14 nM, 59/60 lines) than does G_{N7S} (>34 nM, 44/60 lines). The latter situation also applies to comparison of cephalostatins 17 versus 2. Here, removal of the 26-OH from the polar domain in cephalostatin 2 results in a dramatic $\geq 10^4$ loss of potency against P388 but a modest 4-fold drop against the NCI panel for cephalostatin 17, which highlights the sometimes disparate SAR indicated for cephalostatins by P388 and the 60-cell NCI panel. Unfortunately, for cephalostatins 10–19, comparison of the SAR indicated by human leukemia lines to that by P388 is not possible, as detailed NCI results have not been made available.

Excessive disparity also results in inferior in vitro potency. Such may be the case if the hydrophilic domain becomes too polar for its formerly appropriate nonpolar partner. This situation is seen with OSW-1a,b versus OSW-1 (removal of acyl groups reveals additional free hydroxyl functions). Likewise, when the lipophilic domain becomes too nonpolar relative to its polar partner, decreased potency results (e.g., 12-acetyl-ritterazine B and ritterazine H vs ritterazine B: loss

of the 12-OH function by acetylation or oxidation; ritterostatin G_{N1N} vs cephalostatin 1, loss of the South ketone and 23'-OH functions, retaining only a secondary 12-OH polarizing function). Comparison of the latter pair might be questioned on the grounds that the spiroketal (pro-oxacarbenium ion) moieties of their nonpolar units have different spatial relationships to the common polar unit. However, it will be seen that the comparison is not unreasonable because, like the total polarity of a given union of subunits, the relative locations of the spiroketals have an acceptable range of values (vide infra) and that of ritterostatin G_{N1N} falls within that range.

The high cytotoxicity associated with unsymmetrical pairing of appropriate polar with nonpolar domains occurs for molecules with a range of overall polarity. A “lower” limit is seen for mainly nonpolar unions, whether unsymmetrical or not. The “upper” limit on total polarity is not apparent, which bodes well for possible alterations to give increased water solubility, a desirable feature in drugs administered orally. The most dramatic range of overall polarity is demonstrated by the total hydrophilicity of three highly potent (all ~ 1 nM) steroidal antineoplastics: ritterazine B, cephalostatin 2, and OSW-1.

8.2. Homoallylic Oxygen

No reported bis-*trans*-saturated C/D bissteroidal pyrazines are highly active (all are poorly differentiated/polarized), but several monounsaturated C/D compounds are extremely cytotoxic, most notably ritterazine B (*cis*) and dihydrocephalostatin 1 (*trans*). No bis-*cis*-saturated C/D compound has

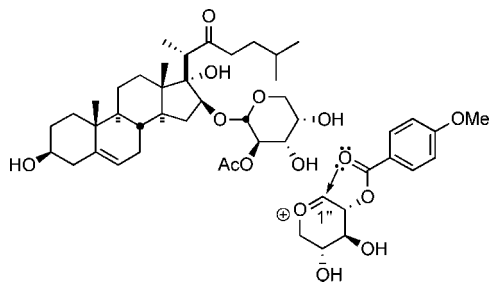


Figure 14. 1''-Oxacarbenium ion of OSW-1.

been prepared. The possibilities of alkylation via oxacarbenium ion, nucleophilically susceptible carbonyl, or Wagner-Meerwein or dyotropic rearrangements have been proposed (See Schemes 38 and 39).

8.3. 17-OH Function Is Beneficial

A 17-OH function in one hemisphere is beneficial to high in vitro activity. For bissteroidal pyrazines, it is always in the polar domain. Removal of 17-OH results in ~10–100-fold loss of activity (Ritterazine Y = 0.0045 nM; Ritterazine B = 0.000025 nM, part due to loss of 7'OH; Ritt *T* > 1500 nM; Ritt A = 0.007 nM, part due to 7'OH loss). No glaring exceptions to this rule have been noted, but there may be a flaw in the in vitro approach to SAR. Neither saundersioside B nor solamargine are powerful in vitro, but solamargine (4680 nM NCI) is extremely (100%) efficacious in vivo and is nontoxic to healthy tissue. Future work is needed to define the role of the 17-OH heteroatom.

8.4. An Aromatic Moiety Is Not Necessary

An aromatic group appears beneficial to high in vitro activity but is likewise not a requisite for in vivo efficacy. Although one is present in all cephalostatins and some OSW types, solamargine is wholly aliphatic. The aromatic group's main contribution may be hydrophobic attractive interactions, but the ease with which nitrogenous aromatic heterocycles undergo nucleophilic aliphatic substitution should not be ignored. The fully substituted pyrazine has, as its protonated (pyrazinium) salt, $pK_a \approx 5$, and it is known to hydrogen bond over the ring, like benzene, rather than edge-on like pyridines.⁶⁷ The carbonyl of the pMeOBz group of OSW-1 is calculated to greatly stabilize formation of a 1''-oxacarbenium ion, the lowest energy ion available to OSW 1 (Figure 14).⁶⁸

8.5. Hydrogen-Bonding: Sugars and Spiroketal

If, as seems likely, the polar domains in cephalostatin and OSW compounds function as a network of H-bond donors/acceptors and mimic the recognition role demonstrated for solamargine, future computer modeling may reveal critical overlap. A postentry role for these spatially defined hydroxyl groups may also be important. Attached sugars are often cleaved on admittance within the cell, but the hydroxylated spiroketals of cephalostatins cannot be easily removed. These functions may facilitate transport to the target, binding, or orientation once delivered. The possibility that OSW-1 retains its glycal linkage for such purposes is necessarily considered.

Although NCI COMPARE studies reveal a strong correlation (0.83) with cephalostatins and OSW-1, different biological effects⁶⁹ of 23'-deoxy-cephalostatin 1 and OSW-1 on mitochondria and cytotoxicity data of C22 deoxy OSW-1

analogues,⁷⁰ which cannot form E-ring oxacarbenium ion (Scheme 3), suggest that the mechanism of action of OSW-1 may be somewhat different from that of cephalostatins. Both OSW-1 and cephalostatin 1 (**1**) induce apoptosis at similar concentration and exposure,⁷¹ but reactive functionality usually associated with anticancer agents is absent in these classes, so particular attention should be paid to the fate of the spiroketals and sugars.

8.6. Two or More Pro-(stabilized)carbenium Ion Moieties

At least two pro-carbenium ion sites with some spatial separation appear requisite for high in vitro activity. It is possible that the interannular homoallylic oxygen (in many cases, the 17OH and the 12OH are both homoallylic) and spiroketal (or equivalent spiroaminal, ketone, imine, hemiacetal, glycosidic acetal, etc.) moieties serve as masked stabilized carbenium ion sites, probably unveiled as alkylation centers via biological acid or metal ion-catalyzed processes (Figure 15). Among such bissteroidal pyrazines, one spiroketal is often in a high-energy isomeric form (e.g., 22 β) and the other is in its thermodynamic form (22 α). The requisite spatial relationship of the pro-oxacarbenium ion sites is poorly defined and, in compounds with high activity, varies significantly between the glycoconjugate and pyrazine families, and to a lesser degree within the cephalostatin (pyrazine) family itself. In saponin OSW-1, no fixed angle relates the steroid side-chain C22 ketone and the two glycal centers (C1' and C1''), although models indicate that rotation about the pertinent connecting bonds does appear somewhat restricted. Its homoallylic oxygen array, like that of solamargine, bears different spatial relationships compared to the bissteroids. In cephalostatins/ritterazines, the spiroketals are rigidly fixed by the steroid ring system, but small, apparently remote, changes in the hexacyclic system can result in large attenuation of biological activity.¹⁴

8.7. Discussion

Limited information regarding effects on activity by stereochemical variation in the spiroketal rings is available from natural epimers, such as ritterazine F versus ritterazine B, and from analogues of cephalostatin 7, 20-*epi*-cephalostatin 7, and 25'-*epi*-cephalostatin 7, and by 5/6 versus 5/5 isomerization in ritterazine B, ritterazine C (Figure 16). Additional indications of the importance of this functionality are evident by considering cephalostatin 1 (**1**) versus its nearly equipotent hemiketal cephalostatin 9 and ritterazine B versus its dramatically less cytotoxic 22-H reduction product 22'-H ritterazine B.

Surprisingly, inversion at either C20 (as in 20-*epi*-cephalostatin 7) or at C25' (as in 25'-*epi*-cephalostatin 7) similarly diminished the activity. In addition to a substantial increase in many GI₅₀s relative to cephalostatin 7, the number and kinds of tumor lines affected by 20-*epi*-cephalostatin 7 and 25'-*epi*-cephalostatin 7 was considerably reduced, and in strikingly similar fashion. Functionality alteration or polarity match rationales do not apply to 20-*epi*-cephalostatin 7 and 25'-*epi*-cephalostatin 7, and topographical responsibility for their similar losses of activity was deemed unlikely. A simple explanation based on relative hydrophilicity or general hydrogen bonding seemed inadequate. Analysis of altered directional H-bonding capacities likewise did not account for the parallel losses of cytotoxicity. A kinetic

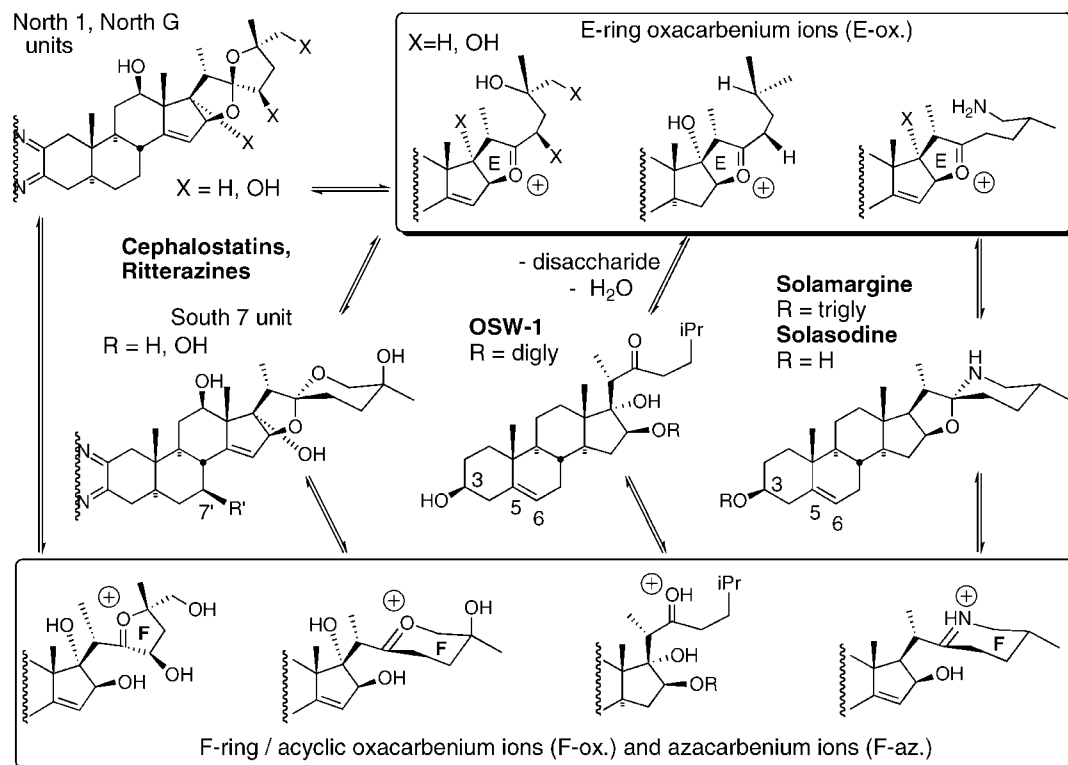


Figure 15. Heterocarbenium ions proposed as potential biological electrophiles.

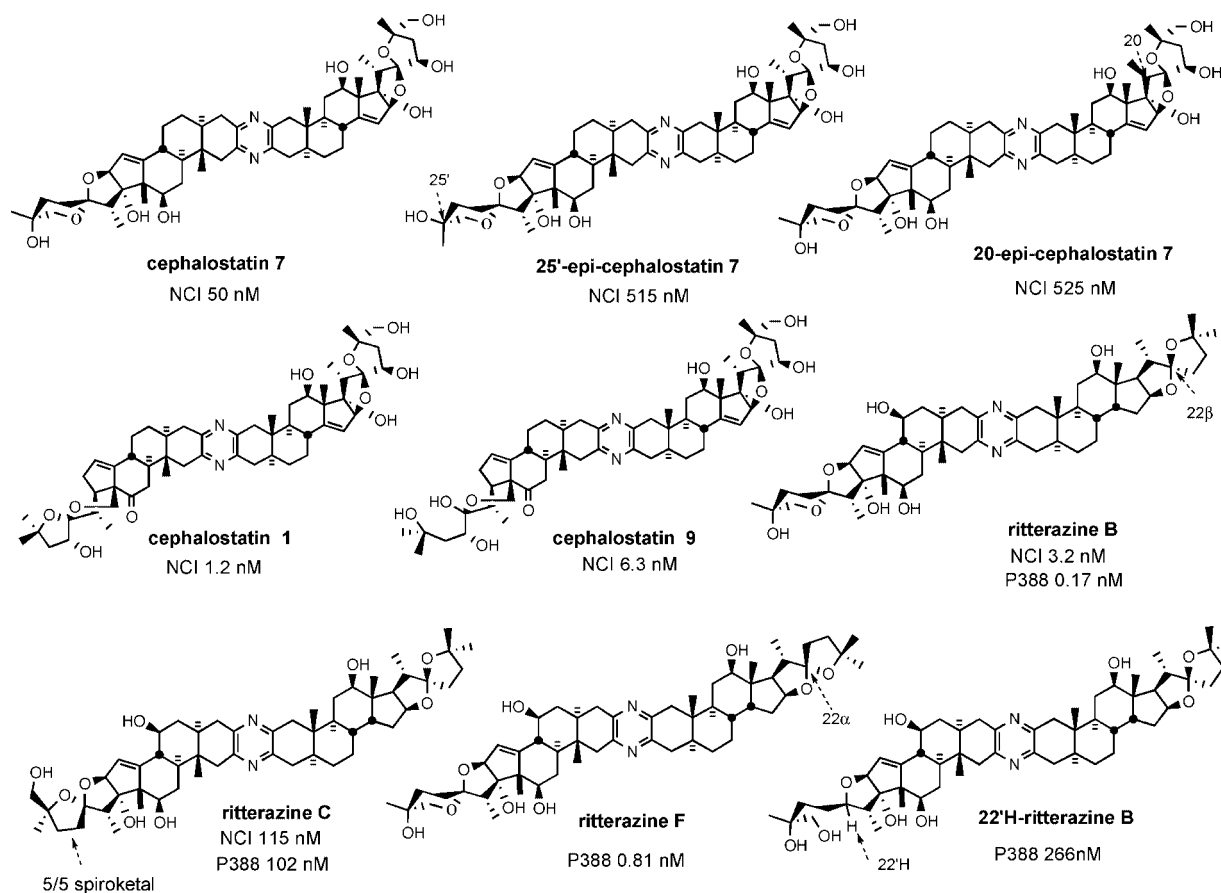


Figure 16. Bissteroid bioactivity as a function of spiroketal alteration.

protonation argument was considered untenable, especially since the 25'-*epi*-South 7 series was far more acid labile, and stereoelectronics suggest that the axial lone pair of O26' in South 7 units, the one "more hindered" in 25'-*epi*-

cephalostatin 7, is kinetically less basic than either the equatorial or O16' (E'-ring) lone pairs.⁷²

Spiroketal (or equivalent functionality) appear to be masked oxocarbenium sites, and biological activity bears an

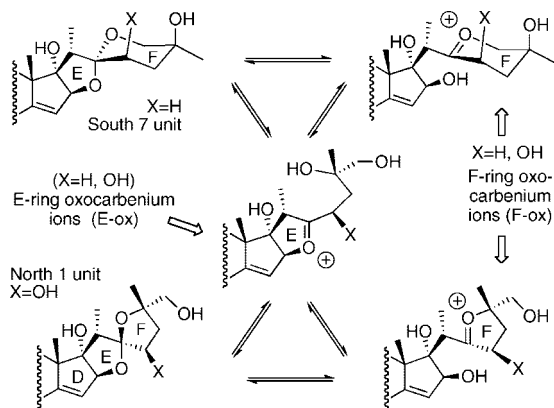


Figure 17. E- and F-ring oxocarbenium ions.

inverse relationship to the calculated energy cost to form such ions for topographically similar series.⁵⁷ Calculated geometries⁵⁷ showed only modest conformational alteration by epimerization at C20 in the North 1 subunit of cephalostatin 7 as in 20-*epi*-cephalostatin 7 and virtually no topographical alteration due to epimerization at C25' as in 25'-*epi*-cephalostatin 7. Rather, it seems 20-*epi*-cephalostatin 7 and 25'-*epi*-cephalostatin 7 suffer unfavorable oxocarbenium ion formation pathways compared to the parent cephalostatin 1 (**1**), and this rationale may explain their diminished cytotoxicity.

The South units were calculated⁵⁷ to favor the E'-ring oxonium ion (E'-ox.) via equatorial F'-ring protonation, with E'-ox. formation (relative to pyrazine protonation) 3.1 kcal/mol more endothermic in 10-fold less cytotoxic 25'-*epi*-cephalostatin 7 than in cephalostatin 7 (Figure 17). The computational study showed that the North 1 units also favor F-ring protonation, and E-ox. formation, while more endothermic, lies accessibly within ~1 kcal/mol of the protonated spiroketal. However, the E-ox. of 20-*epi*-cephalostatin 7 experiences greater steric repulsion than cephalostatin 7 as the ring flattens, with the 21 β -Me forced into unfavorable interactions with the concave side of the [3.3.0] D/E moiety. Oxocarbenium ion formation in 20-*epi*-cephalostatin 7 appeared 3.0 kcal/mol less favorable than that in cephalostatin 7, with about the same increased cost as for 25'-*epi*-cephalostatin 7. The similar potencies of 20-*epi*-cephalostatin 7 and 25'-*epi*-cephalostatin 7 implies oxocarbenium ion activity in both North and South subunits.

"Pro-oxocarbenium ion moieties" now seem to be critical components in SAR. Can evidence be found that suggests the spiroketals in these small antineoplastics assault the

comparably huge tumor target with oxocarbenium ions? If so, does such a moiety constitute a previously unrecognized but widely disseminated medicinally significant function?

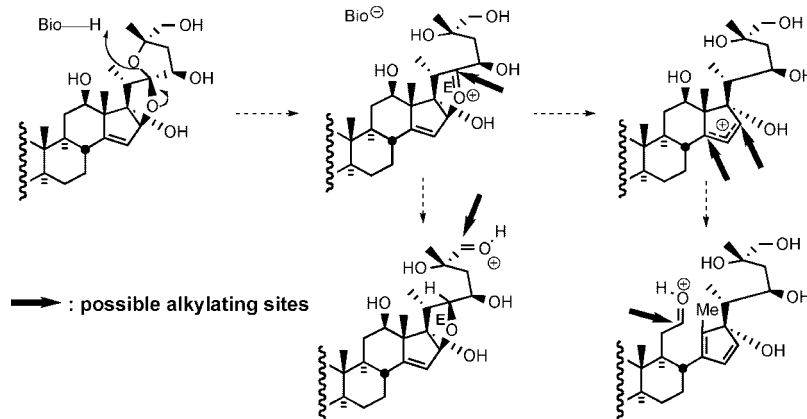
Such oxocarbenium ions may serve as direct electron-accepting agents or may sire rearranged intermediates capable of biological alkylation or oxidation (Scheme 46). At this juncture, the electrophiles will be considered as cations generated upon interaction with a cellular Bronsted or Lewis acid by analogy to known laboratory reactions and biological glycosidations. However, no evidence precludes neutral (zwitterionic) forms stabilized by hydrogen bonding or metal ligation.

Mathematical models relating the energies of chemical interactions to bioactivity are valuable for QSAR and drug design. Active functionality typically associated with anti-tumor agents includes radical-generating, intercalating, redox-active, and electronic centers, particularly as unveiled in vivo by processes such as bioreductive alkylation.⁷³ By contrast, spiroketals or equivalents (e.g., sugars, spiroaminals, etc.), present in diverse apoptoxins such as cephalostatins, spongistatins,⁷⁴ and clinically significant solamargine, have not been generally considered of similar consequence. Binding modes with "passive" spiroketal contributing structural rigidity and sometimes ion attraction or hydrogen bonding have been advanced for many classes, e.g., dunainycins (immunosuppression)⁷⁵ and novobiocin (antibiotic).⁷⁶ Dependence on spiroketal variations in halichondrins⁷⁷ and pectenotoxins⁷⁸ was similarly attributed to conformational effects (Figure 18). However, bioactivation of these widely disseminated latent electrophiles by metals, H-bonding, or acids could unmask a cascade of oxocarbenium ions competent to effect toxic modification(s) of susceptible sites in biopolymers.

Hecht has detailed oxidative alkylation of DNA following metabolic activation (α -oxygenation) of cyclic nitrosamines (Figure 18).⁷⁹ Iminium ions (cf. solasodine) were implicated in saframycins's reversible covalent binding to double-stranded DNA.⁸⁰ In the series of events leading to observed cytotoxicity, formation of participating ions might be energetically determinant and, therefore, predictive of activity and detectable by calculation in silico.

LaCour has proposed a semiempirical calculation⁶⁸ to rationalize the SAR of the entire 80-compound class of bissteroidal pyrazine antineoplastics. Application of this calculation method indicated an inverse exponential correlation ($r^2 \approx 0.970$), suggestive in form of the Arrhenius equation, between relative cytotoxicity and endothermicity of oxocarbenium ion formation (Figure 19). The correlation

Scheme 46. Oxocarbenium Ions As Putative Alkylating Intermediates



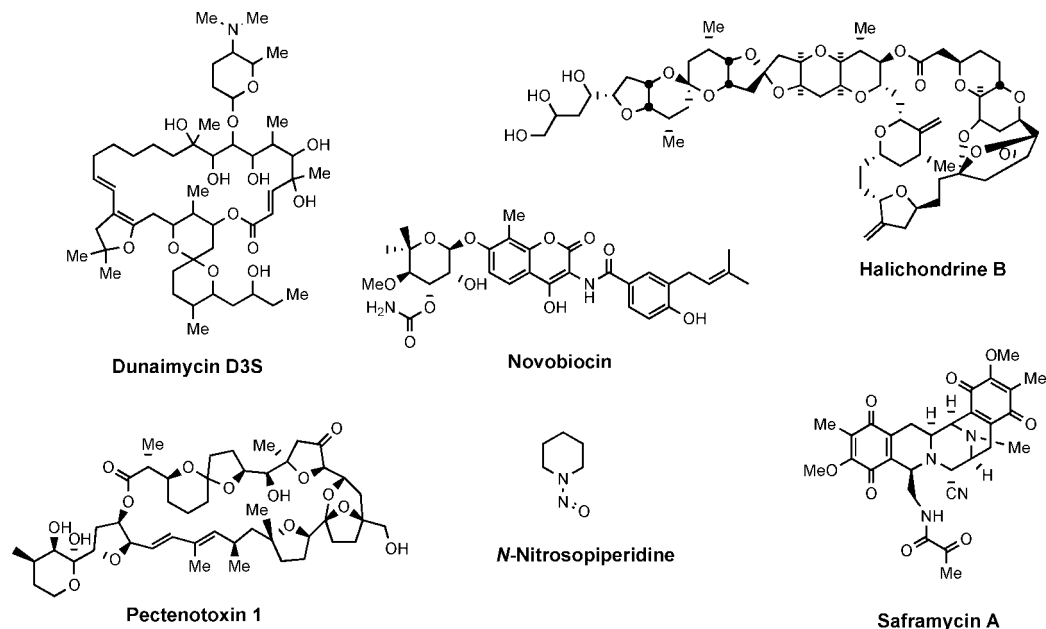


Figure 18. Potential heteroatom-stabilized carbenium ion precursors.

is periodic and appears regulated by accompanying polar functionality. The correlation originally showed that the biological activities of cephalostatin 8 and 16 and ritterazine M appeared substantially out of place.⁶⁸ In all three instances, *the structures had been assigned incorrectly*.⁸¹ The calculation method also correctly predicted that compounds 23'-deoxy cephalostatin 1³⁹ and 17'-OH-23'-deoxy cephalostatin 1³⁸ would exhibit activity within a factor of 10 of cephalostatin 1 (1) (Figure 20).

9. Conclusions and Medicinal Prospects

Cephalostatin is among the most powerful anticancer agents tested by the National Cancer Institute. These challenging bissteroidal pyrazine targets have provided a platform

for developing new synthetic strategies and methodologies over the last 15 years. The successful syntheses of these challenging molecular architectures, such as cephalostatin 1, 7, and 12, ritterazine K and M, highlighted the state of the art of contemporary organic synthesis. Significant progress toward developing efficient and scalable synthetic pathways to natural cephalostatin and analogues has been made (e.g., South 7: 25 operations, 2% overall yield (1995); 16 operations, 24% overall yield (2005)).

The growing number of natural cephalostatin and their analogues provides valuable structure–activity relationships, which aids the design of future analogues. The ongoing biological study of cephalostatin is gradually unveiling the antineoplastic mechanism of the cephalostatin. The bioac-

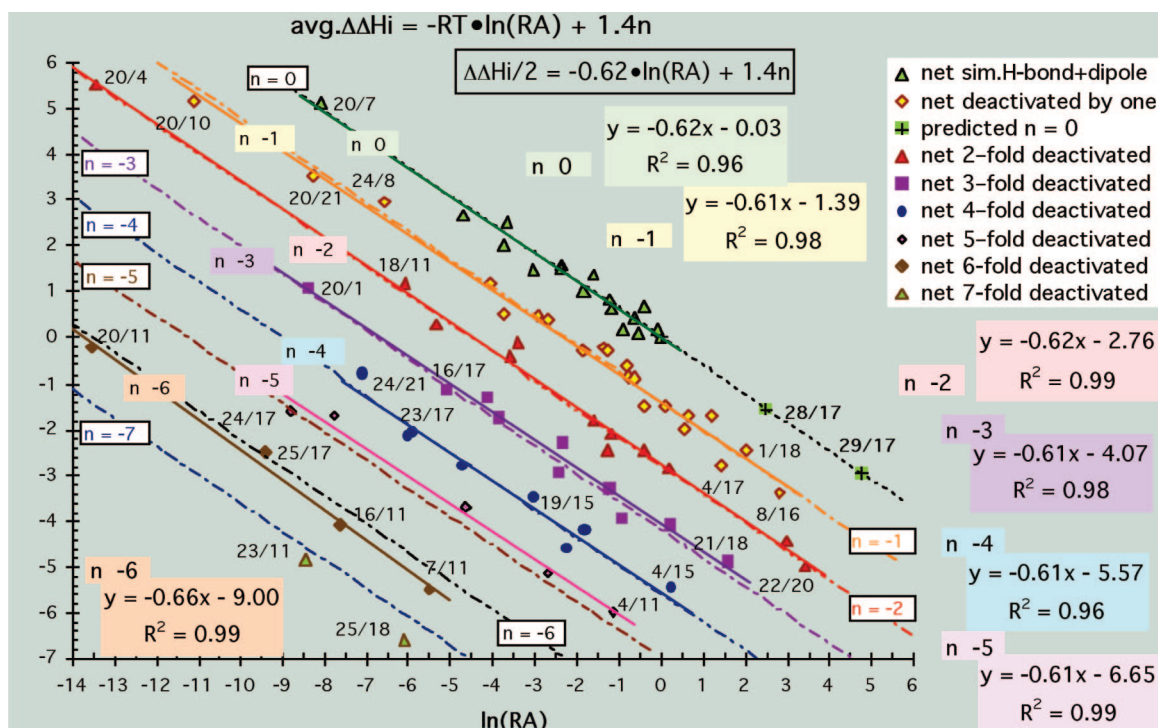


Figure 19. Plot of energy (ΔH_{pr}) vs $\ln(GI_{50})$ with 14 kcal/mol ring corrections.

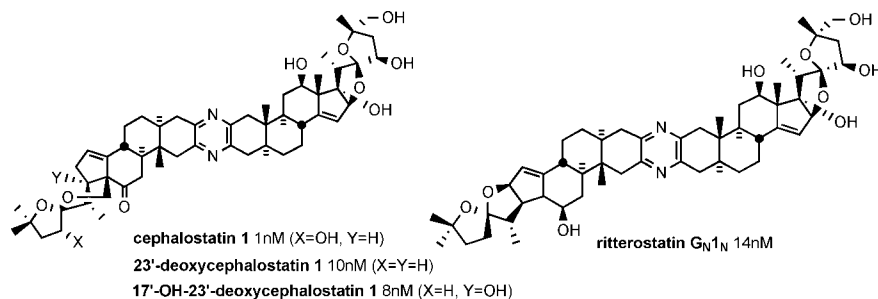
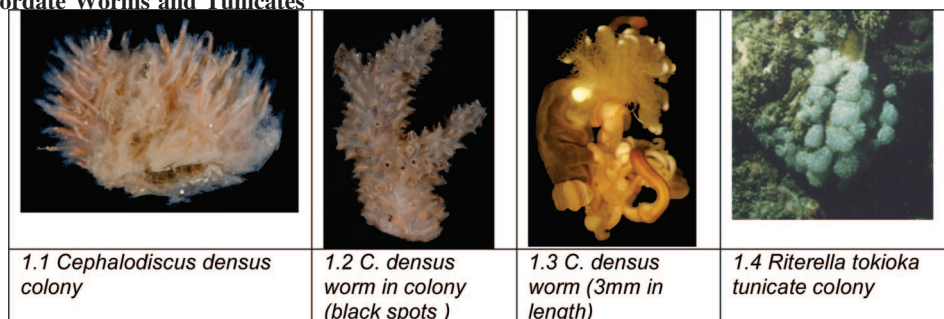


Figure 20. Cephalostatin analogues and their biological activities.

Chart 1. Hemichordate Worms and Tunicates



tivity pattern of cephalostatins has been found to be quite different from known anticancer agents, indicating a new mechanism of action, possibly offering the potential for treatment of drug-resistant cancers.

Clinical trials of cephalostatin **1** (**1**) have been delayed largely due to the supply problem. Progress in the practical and scalable cephalostatin synthesis should make the bissteroidal pyrazines more accessible, thereby enabling the clinical trials as well as providing tools for probing the biological and biochemical evaluation of the cephalostatins. Identification and structural elucidation of the biological target of cephalostatins coupled with QSAR studies are essential to facilitate the rational design of hyperactive analogues.

10. Acknowledgments

This review covers more than 75 person-years of cephalostatin research in the Fuchs group and is dedicated to the outstanding individuals whose names are given in the accompanying citations. We gratefully thank the National Institutes of Health (CA 60548) for financial support of this project. Additional thanks are due to Biogen Idec for recent financial contributions. Dr. Douglas Lantrip has provided extensive technical help on the project and in manuscript preparation. The cover art Earth map is used under terms described in "NASA's Earth Observatory" website. Pettit, Fusetani, and most recently Schiaparelli have provided invaluable assistance during the course of the entire research program.

11. Abbreviations

AIBN	azobisisobutyronitrile
CSA	camphorsulfonic acid
DABCO	1,4-diazabicyclo[2.2.2]octane
DBU	1,8-diazabicyclo[5.4.0]undec-7-ene
DDQ	2,3-dichloro-5,6-dicyano-1,4-benzoquinone
DEAD	diethyl azodicarboxylate
DIBAL	diisobutylaluminum hydride
DMAP	4- <i>N,N</i> -(dimethylamino)pyridine

DMDO	dimethyldioxirane
HMDS	hexamethyldisilazane
KHMDS	potassium hexamethyldisilylamide
LDA	lithium diisopropylamide
MCPBA	<i>meta</i> -chloroperbenzoic acid
MOM	methoxymethyl
MTM	methylthiomethyl
Ms	methanesulfonyl
NBS	<i>N</i> -Bromosuccinimide
NMO	<i>N</i> -methylmorpholine- <i>N</i> -oxide
PCC	pyridinium chlorochromate
PDC	pyridinium dichromate
PMB	<i>p</i> -methoxybenzyl
PPTS	pyridinium <i>para</i> -toluenesulfonate
PTAB	phenyltrimethylammonium tribromide
PVP	polyvinyl pyridine
Py	pyridine
TBAF	tetrabutylammonium fluoride
TBAI	tetrabutylammonium iodide
TBDPS	<i>tert</i> -butyldiphenylsilyl
TBDPSO	<i>t</i> -butyldiphenylsilyloxy
TBS	<i>tert</i> -butyldimethylsilyl
TBSOTf	<i>tert</i> -butyldimethylsilyl trifluoromethanesulfonate
TEA	triethylamine
TFA	trifluoroacetic acid
TFAA	trifluoroacetic anhydride
TFAT	trifluoroacetyl triflate
TIPS	triisopropylsilyl
TMS	trimethylsilyl
TPAP	tetraisopropylammonium perruthenate
TPP	5,10,15,20-tetraphenyl-21H,23H-porphine

12. References

- (1) (a) Pettit, G. R.; Inoue, M.; Herald, D. L.; Krupa, T. S. *J. Am. Chem. Soc.* **1988**, *110*, 2006. (b) Pettit, G. R.; Inoue, M.; Kamano, Y.; Herald, D. L. *J. Chem. Soc., Chem. Commun.* **1988**, 1440. (c) Pettit, G. R.; Xu, J. P.; Schmidt, J. M. *Bioorg. Med. Chem. Lett.* **1995**, *5*, 2027.
- (2) The unavailability of color photographs of *C. gilchristi* from the Pettit collection inspired a thorough web search for closely related *Cephalodiscus* species. A key paper (Schiaparelli, S.; Cattaneo-Vietti, R.; Mierzejewski, P. *Polar. Bio.* 2004, *27*, 813.) led us to contact professor Schiaparelli, who graciously provided the first three pictures shown in Chart 1. Comparison of a drawing of *C. gilchristi* provided by Professor Pettit with *C. densus* photo 1.3 revealed the minute (3 mm) worms to be nearly identical. Schiaparelli collected *C. densus* from

- Terra Nova Bay, Ross Sea, Antarctica, begging the question of whether it also hosts an assortment of trisdecacyclic pyrazines.
- (3) (a) Fukuzawa, S.; Matsunaga, S.; Fusetani, N. *J. Org. Chem.* **1994**, *59*, 6164. (b) Fukuzawa, S.; Matsunaga, S.; Fusetani, N. *J. Org. Chem.* **1995**, *60*, 608. (c) Fukuzawa, S.; Matsunaga, S.; Fusetani, N. *Tetrahedron* **1995**, *51*, 6707. (d) Fukuzawa, S.; Matsunaga, S.; Fusetani, N. *J. Org. Chem.* **1997**, *62*, 4484. (e) Fukuzawa, S.; Matsunaga, S.; Fusetani, N. *Tetrahedron Lett.* **1996**, *37*, 1447.
- (4) Full NCI-60 results for cephalostatins 1–9 (NSC# 363979–81, 378727–36) are on the Web at <http://dtp.nci.nih.gov>.
- (5) LaCour, T. G.; Guo, C.; Ma, S.; Jeong, J. U.; Boyd, M. R.; Matsunaga, S.; Fusetani, N.; Fuchs, P. L. *Bioorg. Med. Chem. Lett.* **1999**, *9*, 2587.
- (6) (a) Kubo, S.; Mimaki, Y.; Terao, M.; Sashida, Y.; Nikaida, T.; Ohmoto, T. *Phytochemistry* **1992**, *31*, 3969. (b) Mimaki, Y.; Kuroda, M.; Kameyama, A.; Sugita, K.; Beutler, J. A. *Bioorg. Med. Chem. Lett.* **1997**, *7*, 633.
- (7) Kim, Y. C.; Che, Q. M.; Gunatilaka, A. A. L.; Kingston, D. G. I. *J. Nat. Prod.* **1996**, *59*, 283.
- (8) Daunter, B.; Cham, B. E. *Cancer Lett.* **1990**, *55*, 209.
- (9) Reviews: (a) Atta-ur-Rahmann; Choudary, M. I. *Nat. Prod. Rep.* **1997**, *14*, 191. (b) Atta-ur-Rahmann; Choudary, M. I. *Alkaloids* **1999**, *52*, 233. (c) Ganensan, A.; Heathcock, C. H. *Angew. Chem., Int. Ed. Engl.* **1996**, *35*, 611. (d) Ganensan, A.; Heathcock, C. H. *Stud. Nat. Prod. Chem.* **1996**, *18*, 875. (e) Jacobs, M. F.; Kitching, W. *Curr. Org. Chem.* **1998**, *2*, 395. (f) Urban, S.; Hickford, S. J. H.; Blunt, J. W.; Munro, M. H. G. *Curr. Org. Chem.* **2000**, *4*, 765. (g) Gryszkiewicz-Wojtkielewicz, A.; Jastrzebska, I.; Morzycki, J. W.; Romanowska, D. B. *Curr. Org. Chem.* **2003**, *7*, 1257. (h) Flessner, T.; Jautelat, R.; Scholz, U.; Winterfeldt, E. *Fortschr. Chem. Org. Naturst.* **2004**, *1*. (i) Moser, B. R. *J. Nat. Prod.* **2008**, *71*, 487.
- (10) The “North unit”, the upper steroidal nucleus of the cephalostatins, has also been designated “right side” by Pettit and “east unit” by Fusetani. On the other hand, the “South unit” refers to the lower half of the cephalostatins.
- (11) (a) Ganesan, A.; Heathcock, C. H. *Chemtracts* **1988**, *1*, 311. (b) Ganesan, A. *Stud. Nat. Prod. Chem.* **1996**, *18*, 875.
- (12) Pan, Y.; Merriman, R. L.; Tanzer, L. R.; Fuchs, P. L. *Bioorg. Med. Chem., Chem. Lett.* **1992**, *2*, 967.
- (13) (a) Kramer, A.; Ullmann, U.; Winterfeldt, E. *J. Chem. Soc., Perkin Trans. 1* **1993**, 2865. (b) Jautelat, R.; Müller-Fahrnow, A.; Winterfeldt, E. *Chem.—Eur. J.* **1999**, *5*, 1226.
- (14) (a) Bhandaru, S.; Fuchs, P. L. *Tetrahedron Lett.* **1995**, *36*, 8347. (b) Bhandaru, S.; Fuchs, P. L. *Tetrahedron Lett.* **1995**, *36*, 8351.
- (15) (a) Tamura, K.; Honda, H.; Mimaki, Y.; Mimaki, Y.; Sashida, Y.; Kogo, H. *Br. J. Pharmacol.* **1997**, *121*, 1796. (b) Kuroda, M.; Mimaki, Y.; Sashida, Y.; Hirano, T.; Oka, K.; Dobashi, A. *Tetrahedron* **1997**, *53*, 11549.
- (16) (a) Pettit, G. R.; Kamano, Y.; Inoue, M.; Dufresne, C.; Boyd, M. R.; Herald, C. L.; Schmidt, J. M.; Doubek, D. L.; Christe, N. D. *J. Org. Chem.* **1992**, *57*, 429. (b) Pettit, G. R.; Tan, R.; Xu, J.-p.; Ichihara, Y.; Williams, M. D.; Boyd, M. R. *J. Nat. Prod.* **1998**, *61*, 955.
- (17) Müller, I. M.; Dirsch, V. M.; Rudy, A.; Lopez-Anton, N.; Pettit, G. R.; Vollmar, A. M. *Mol. Pharmacol.* **2005**, *67*, 1684.
- (18) Dirsch, V. M.; Müller, I. M.; Eichhorts, S. T.; Pettit, G. R.; Kamano, Y.; Inoue, M.; Xu, J. P.; Ichihara, Y.; Wagner, G.; Vollmar, A. M. *Cancer Res.* **2003**, *63*, 8869.
- (19) (a) López-Antón, N.; Rudy, A.; Barth, N.; Schmitz, L. M.; Pettit, G. R.; Schulze-Osthoff, K.; Dirsch, V. M.; Vollmar, A. M. *J. Biol. Chem.* **2006**, *181*, 33078. (b) Rudy, A.; López-Antón, N.; Dirsch, V. M.; Vollmar, A. M. *J. Nat. Prod.* **2008**, *71*, 482.
- (20) Jeong, J. U.; Guo, C.; Fuchs, P. L. *J. Am. Chem. Soc.* **1999**, *121*, 2071.
- (21) Komiya, T.; Fusetani, N.; Matsunaga, S.; Kubo, A.; Kaye, F. J.; Kelley, M. J.; Tamura, K.; Yoshida, M.; Fukuoka, M.; Nakagawa, K. *Cancer Chemother. Pharmacol.* **2003**, *51*, 202.
- (22) (a) Kubo, S.; Mimaki, Y.; Terao, M.; Sashida, Y.; Nikaida, T.; Ohmoto, T. *Phytochemistry* **1992**, *31*, 3969. (b) Mimaki, Y.; Kuroda, M.; Kameyama, A.; Sashida, Y.; Hirano, T.; Oka, K.; Maekawa, R.; Wada, T.; Sugita, K.; Beutler, J. A. *Bioorg. Med. Chem. Lett.* **1997**, *7*, 633.
- (23) Guo, C.; LaCour, T. G.; Fuchs, P. L. *Bioorg. Med. Chem. Lett.* **1999**, *9*, 419.
- (24) (a) Cham, B. E.; Daunter, B. *Cancer Lett.* **1990**, *55*, 221. (b) Cham, B. E.; Meares, H. M. *Cancer Lett.* **1987**, *36*, 111. (c) Cham, B. E.; Daunter, B.; Evans, R. A. *Cancer Lett.* **1991**, *59*, 183. (d) Beardmore, G. L.; Hart, V.; Wilson, P.; Francis, D. *Med. J. Aust.* **1989**, *150*, 351. (e) Evans, R. A.; Cham, B.; Daunter, B. *Med. J. Aust.* **1989**, *150*, 350.
- (25) (a) Evans, R. A.; Cham, B.; Daunter, B. *Med. J. Aust.* **1990**, *152*, 329. (b) Millward, M.; Powell, A.; Daly, P.; Tyson, S.; Ferguson, R.; Carter, S. *J. Clin. Oncol.* **2006**, *24*, 2070.
- (26) (a) Hu, K.; Kobayashi, H.; Dong, A.; Jing, Y.; Iwasaki, S.; Yao, X. *Planta Med.* **1999**, *65*, 35. (b) Roddick, J. G.; Weissenberg, M.; Leonard, A. L. *Phytochemistry* **2001**, *56*, 603. (c) Eschevarria, A. J. *Braz. Chem. Soc.* **2002**, *13*, 838.
- (27) (a) Hsu, S.-H.; Tsai, T.-R.; Lin, C.-N.; Yen, M.-H.; Kuo, K.-W. *Biochem. Biophys. Res. Commun.* **1996**, *229*, 1. (b) Kuo, K.-W.; Hsu, S.-H.; Li, Y.-P.; Lin, W.-L.; Liu, L.-F.; Chang, L.-C.; Lin, C.-C.; Lin, C.-N.; Sheu, H.-M. *Biochem. Pharmacol.* **2000**, *60*, 1865. (c) Liu, L. F.; Liang, C. H.; Shiu, L. Y.; Lin, W. L.; Lin, C. C.; Kuo, K. W. *FEBS Lett.* **2004**, *577*, 67.
- (28) Jeong, J. U.; Sutton, S. C.; Kim, S.; Fuchs, P. L. *J. Am. Chem. Soc.* **1995**, *117*, 10157.
- (29) Ohta, G.; Koshi, K.; Obata, K. *Chem. Pharm. Bull.* **1968**, *16*, 1487.
- (30) Smith, H. E.; Hicks, A. A. *J. Org. Chem.* **1971**, *36*, 3659.
- (31) (a) Smith, S. C.; Heathcock, C. H. *J. Org. Chem.* **1992**, *57*, 6379. (b) Heathcock, C. H.; Smith, S. C. *J. Org. Chem.* **1994**, *59*, 6828. (c) Heathcock, C. H.; Smith, S. C. *J. Org. Chem.* **1995**, *60*, 6641.
- (32) Jeong, J. U.; Fuchs, P. L. *J. Am. Chem. Soc.* **1994**, *116*, 773.
- (33) Kramer, A.; Ullmann, U.; Winterfeldt, E. *J. Chem. Soc., Perkin Trans. 1* **1993**, 2865.
- (34) Baesler, S.; Brunck, A.; Jautelat, R.; Winterfeldt, E. *Helv. Chim. Acta* **2000**, *83*, 1854.
- (35) Drogemüller, M.; Jautelat, R.; Winterfeldt, E. *Angew. Chem., Int. Ed. Engl.* **1996**, *35*, 1572.
- (36) Haak, E.; Winterfeldt, E. *Synlett.* **2004**, 1414.
- (37) Guo, C.; Bhandaru, S.; Fuchs, P. L.; Boyd, M. R. *J. Am. Chem. Soc.* **1996**, *118*, 10672.
- (38) LaCour, T. G.; Guo, C.; Bhandaru, S.; Boyd, M. R.; Fuchs, P. L. *J. Am. Chem. Soc.* **1998**, *120*, 692.
- (39) Li, Wei.; LaCour, T. G.; Fuchs, P. L. *J. Am. Chem. Soc.* **2002**, *124*, 4548.
- (40) Lee, S. M.; Fuchs, P. L. *Org. Lett.* **2002**, *4*, 317.
- (41) Micovic, I. V.; Ivanovic, M. D.; Piatak, D. M. *Synthesis* **1990**, 90, 591.
- (42) (a) Cook, A. F.; Maichuk, D. T. *J. Org. Chem.* **1970**, *35*, 1940. (b) Naruto, M.; Ohno, K.; Naruse, N.; Takeuchi, H. *Tetrahedron Lett.* **1979**, 251.
- (43) LaCour, T. G.; Guo, C.; Ma, S.; Jeong, J. U.; Boyd, M. R.; Matsunaga, S.; Fusetani, N.; Fuchs, P. L. *Bioorg. Med. Chem. Lett.* **1999**, *9*, 2587.
- (44) (a) Kim, S.; Fuchs, P. L. *Tetrahedron Lett.* **1994**, *35*, 7163. (b) Kim, S.; Sutton, S. C.; Fuchs, P. L. *Tetrahedron Lett.* **1995**, *36*, 2427. (c) Kim, S.; Sutton, S. C.; Guo, C.; LaCour, T. G.; Fuchs, P. L. *J. Am. Chem. Soc.* **1999**, *121*, 2056.
- (45) Gao, Y.; Sharpless, K. B. *J. Am. Chem. Soc.* **1988**, *110*, 7538.
- (46) Reich, H. J.; Peake, S. L. *J. Am. Chem. Soc.* **1978**, *100*, 4888.
- (47) Cox, G. G.; Miller, D. J.; Moody, C. J.; Sie, E. R. H. B. *Tetrahedron* **1994**, *50*, 3195.
- (48) Barton, D. H. R.; McCombie, S. W. *J. Chem. Soc., Perkin Trans. 1* **1975**, 1574.
- (49) Jeong, J. U.; Fuchs, P. L. *Tetrahedron Lett.* **1995**, *36*, 2431.
- (50) Dauben, W. G.; Fonken, G. *J. Am. Chem. Soc.* **1954**, *76*, 4618.
- (51) Heusler, K.; Wieland, P.; Meystre, C. H. *Org. Synth.* **1965**, *45*, 57.
- (52) Phillips, S. T.; Shair, M. D. *J. Am. Chem. Soc.* **2007**, *129*, 6589.
- (53) Lee, S.; Fuchs, P. L. *Org. Lett.* **2002**, *4*, 317.
- (54) Betancor, C.; Freire, R.; Perez-Martin, I.; Prange, T.; Suárez, E. *Org. Lett.* **2002**, *4*, 1295.
- (55) Lee, J. S.; Fuchs, P. L. *Org. Lett.* **2003**, *5*, 2247.
- (56) Lee, J. S.; Cao, H.; Fuchs, P. L. *J. Org. Chem.* **2007**, *72*, 5820.
- (57) LaCour, T. G.; Guo, C.; Boyd, M. R.; Fuchs, P. L. *Org. Lett.* **2000**, *2*, 33.
- (58) Fukuzawa, S.; Matsunaga, S.; Fusetani, N. *J. Org. Chem.* **1994**, *59*, 6164.
- (59) Reetz, M. T. *Angew. Chem., Int. Ed. Engl.* **1972**, *11*, 129.
- (60) Lee, J. S.; Fuchs, P. L. *J. Am. Chem. Soc.* **2005**, *127*, 13122.
- (61) Li, W.; Fuchs, P. L. *Org. Lett.* **2003**, *5*, 4061.
- (62) Li, W.; Fuchs, P. L. *Org. Lett.* **2003**, *5*, 2849.
- (63) Li, W.; Fuchs, P. L. *Org. Lett.* **2003**, *5*, 2853.
- (64) Lee, J. S.; Fuchs, P. L. *Org. Lett.* **2003**, *5*, 3619.
- (65) Fell, J. D.; Heathcock, C. H. *J. Org. Chem.* **2002**, *67*, 4742.
- (66) (a) Taber, D. F.; Joerger, J.-M. *J. Org. Chem.* **2008**, *73*, 4155. (b) Taber, D. F.; Joerger, J.-M. *J. Org. Chem.* **2007**, *72*, 3454. (c) Taber, D. F.; Taluskie, K. V. *J. Org. Chem.* **2006**, *71*, 2797.
- (67) Tsuzuki, S.; Honda, K.; Uchimaru, T.; Mikami, M.; Tanabe, K. *J. Am. Chem. Soc.* **2000**, *122*, 11450.
- (68) LaCour, T. G. Ph.D. Thesis, Purdue University, 2001.
- (69) Zhou, Y.; Garcia-Prieto, C.; Carney, D.; Xu, R.; Pelicano, H.; Kang, Y.; Yu, W.; Lou, C.; Kondo, S.; Liu, J.; Harris, D.; Estrov, Z.; Keating, M. J.; Jin, Z.; Huang, P. *J. Natl. Cancer Inst.* **2005**, *97*, 1781.
- (70) (a) Deng, L.; Wu, H.; Ty, B.; Jiang, M.; Wu, J. *Bioorg. Med. Chem. Lett.* **2004**, *14*, 2781. (b) Morzycki, A.; Wihtiekiewicz, A.; Wolczynski, S. *Bioorg. Med. Chem. Lett.* **2004**, *14*, 3323.
- (71) Rudy, A.; López-Antón, N.; Dirsch, V. M. *J. Nat. Prod.* **2008**, *71*, 482.
- (72) Deslongchamps, P. R. *Stereoelectronics in Organic Chemistry*; Oxford—Pergamon Press: Elmsford, NY, 1985; p 53.

- (73) Moore, H. W. *Science* **1977**, 527.
- (74) Pietruszka, J. *Angew. Chem., Int. Ed. Engl.* **1998**, 37, 2629.
- (75) Burres, N. S.; Premachandran, U.; Frigo, A.; Swanson, S. J.; Mollison, K. W.; Fey, T. A.; Krause, R. A.; Thomas, V. A.; Lane, B.; Miller, L. N.; McAlpine, J. B. *J. Antibiot.* **1991**, 44, 1331.
- (76) Bell, W.; Block, M. H.; Grant, A.; Timms, D. *J. Chem. Soc., Perkin Trans. 1* **1997**, 2789.
- (77) Hart, J.; B.; Blunt, J. W.; Munro, M. H. *J. Org. Chem.* **1996**, 61, 2888.
- (78) Sasaki, K.; Wright, J. L. C.; Yasumoto, T. *J. Org. Chem.* **1998**, 63, 2475.
- (79) Wang, M.; Young-Sciame, R.; Chung, F.-L.; Hecht, S. S. *Chem. Res. Toxicol.* **1995**, 8, 617.
- (80) Meyers, A. G.; Plowright, A. T. *J. Am. Chem. Soc.* **2001**, 123, 5114.
- (81) Lee, S.; LaCour, T. G.; Lantrip, D.; Fuchs, P. L. *Org. Lett.* **2002**, 4, 313.

CR800365M